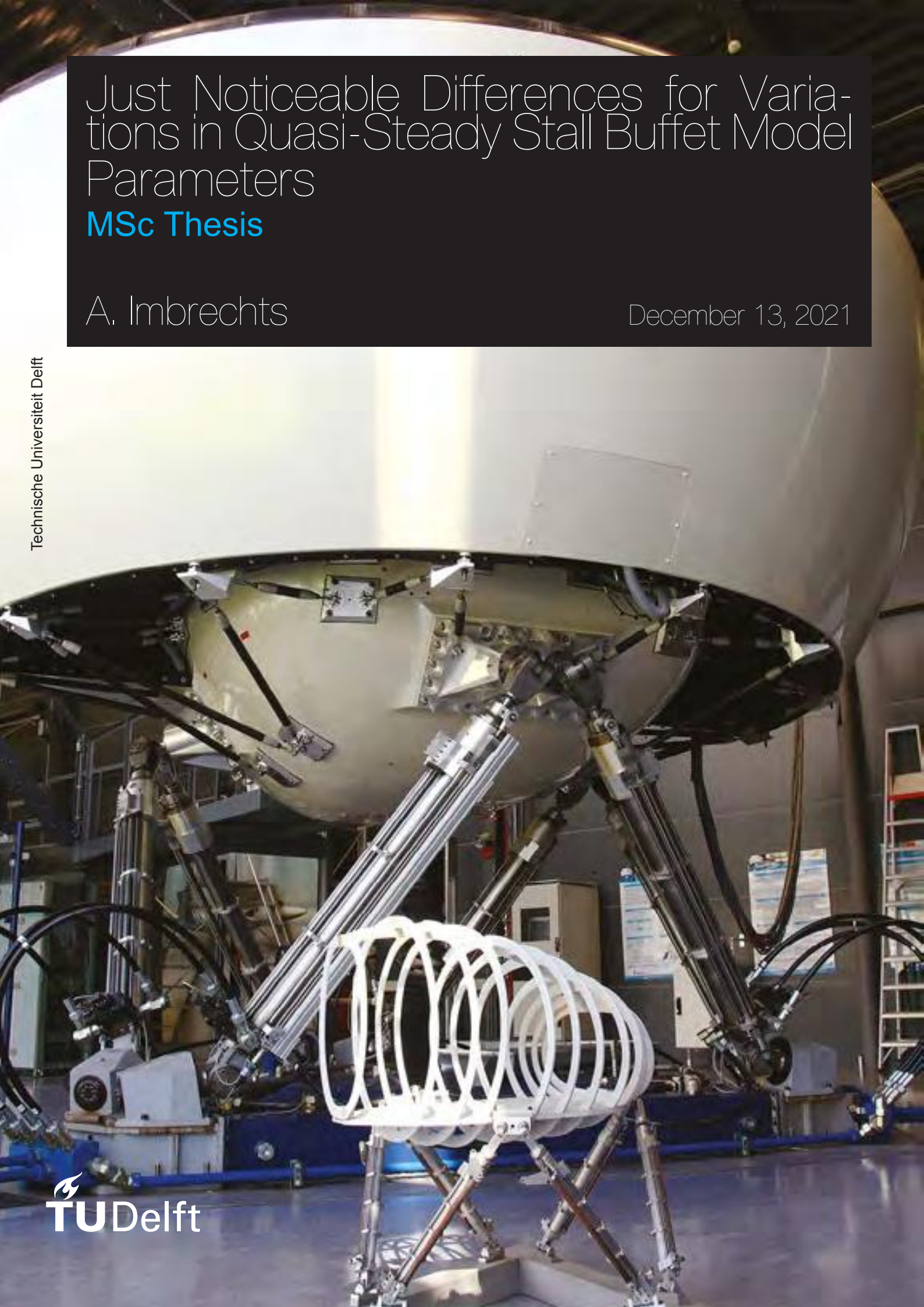


Just Noticeable Differences for Variations in Quasi-Steady Stall Buffet Model Parameters

MSc Thesis

A. Imbrechts

December 13, 2021



Just Noticeable Differences for Variations in Quasi-Steady Stall Buffet Model Parameters

MSc Thesis

by

A. Imbrechts

to obtain the degree of Master of Science
at the Delft University of Technology,
to be defended publicly on Thursday December 23, 2021 at 13:00.

Student number: 4359283
Project duration: April 1, 2020 – December 23, 2021
Thesis committee: Prof. dr. ir. M. Mulder, TU Delft, AE, Control & Simulation
Dr. ir. D.M. Pool, TU Delft, AE, Control & Simulation
Dr. ir. C.C. de Visser, TU Delft, AE, Control & Simulation
Dr. ir J.C.F. de Winter, TU Delft, 3mE, Human-Robot Interaction

An electronic version of this thesis is available at <http://repository.tudelft.nl/>.

Preface

Dear reader,

This Master thesis report details my research on the required level of stall buffet accuracy/fidelity for realistic stall simulations and effective stall training in flight simulators. After working more than a year on this research, I proudly look back on the process and am pleased to present the results and findings. It was certainly a challenging road to the finish, especially during these strange Covid-19 pandemic times, but I was able to acquire a lot of knowledge and could master myself in some specific fields related to stall buffet modelling and flight simulation.

I started looking for an interesting research topic within flight simulation at the beginning of the year 2020, which brought me to Daan Pool and Coen de Visser, who are both supervising the stall task-force group at the TU Delft. This group has as final goal to develop accurate stall modelling techniques and fidelity requirements for stall simulation training programs by using stall flight test data gathered with the Cessna Citation II laboratory aircraft that is jointly operated by the NLR and TU Delft. Daan Pool and Coen de Visser proposed a topic related to investigating required stall buffet model fidelity through a human-in-the-loop simulator experiment. I do not regret the choice for this topic, since I loved developing the experiment in DUECA and supervising the experiments from the control room of the SIMONA Research Simulator.

I do need to mention that I could not have realised this research on my own. Therefore I would like to thank several people. First of all, I would like to thank my daily supervisor Daan Pool for the lots of feedback and support that he gave me. I always liked the encouragement during the meetings. I would also like to thank Coen de Visser, who is also highly involved in the stall related research and was always available for questions and feedback. Both Daan and Coen helped a lot in publishing the research to the AIAA SciTech Forum 2022, which will be a first time for me experiencing an aerospace conference. I should also not forget the other master students and researchers involved in the two-weekly stall group meetings for sharing knowledge on stall modelling research and supporting each other. I also have to thank Max Mulder. Although very busy, he was always available for feedback and showed a lot of interest in the research progress. Olaf Stroosma and René van Paassen, I would like to thank you both for the support on coding the experiment in DUECA and supervising me when performing some experiment sessions in the SIMONA Research Simulator. Not to forget all the pilots that participated voluntary in my experiment. They provided me with relevant data to formulate my conclusions. Lastly, I would like to thank family and friends for the support and motivation during these pandemic times.

To finalise this preface, the structure of this report is as follows. The report has four parts. Firstly, there is a scientific paper that summarises the research and results in a scientific way. This paper is written using the AIAA style template, but has a slightly different content than the officially published version. Next, is the part containing the preliminary thesis work, which presents the literature review and the experiment set-up. The final two parts are appendices that respectively correspond to the preliminary thesis report and final report.

*A. Imbrechts
Delft, December 13, 2021*

Contents

Preface	iii
List of Figures	vii
List of Tables	ix
Nomenclature	xi
I Scientific Paper	1
II Preliminary Thesis Report	21
1 Introduction	23
2 Literature Review and Stall Buffet Simulation Model Requirements	27
2.1 Aircraft Stall Theory	27
2.1.1 Aerodynamic Stall	27
2.1.2 Stall Buffet	29
2.2 FAA Regulations for Stall and Buffet Models in FSTDs.	30
2.3 Simulator Fidelity	32
2.4 Current Stall Recovery Training in FSTDs	34
2.4.1 ICAO Qualification Levels for FSTDs	34
2.4.2 Stall Simulation Limitations in Common Hexapod Mounted Simulators	37
2.5 TU Delft Stall Model	38
2.5.1 Kirchhoff's Theory of Flow Separation.	38
2.5.2 Baseline Aerodynamic Stall Model	39
2.5.3 Stall Buffet Model.	40
2.6 Conclusion	42
3 Preliminary Sensitivity Analysis and Results	43
3.1 Stall Autopilot	43
3.2 Vertical Stall Buffet Model Sensitivity Analysis	45
3.2.1 Spectral Analysis	45
3.2.2 Time Domain Analysis	46
3.3 Conclusion	54
4 Experiment Setup	55
4.1 Just Noticeable Difference (JND) Thresholds	55
4.2 Experiment Variables and Design	57
4.2.1 Independent Variables	57
4.2.2 Dependent Variables	58
4.2.3 Control Variables	58
4.2.4 Participants and Condition Sequence	58
4.3 Experiment Hypotheses	59
4.4 Experiment Procedures	59
4.4.1 Procedures Experienced by the Participants	59
4.4.2 Background Procedures	60
5 Conclusion and Outlook	63
III Appendix to Preliminary Thesis Report	71
A Vertical Stall Buffet Model Time Domain Sensitivity Analysis Results	73

IV	Appendix to Final Report	77
B	Experiment Briefing and Consent Form	79
C	Individual Experiment Results	83

List of Figures

2.1	Typical sketch of a lift coefficient curve. The linear increase in lift with the angle of attack is shown as well as the non-linear stall where flow separates from the wing. Adopted from [21]	28
2.2	Typical buffet onset curve and flow separation mechanism at different flight regimes, adopted from [31]	29
2.3	Effect of changing wing geometry on the buffet onset curve, adopted from [31]	29
2.4	Fatalities per occurrence category from commercial aviation accident statistics from 2010 to 2019, adopted from [39]	31
2.5	Fatal general aviation accident statistics from 2011-2015 per aircraft upset event type and per flight phase, adopted from [40]	32
2.6	Overview of the total simulator motion cueing fidelity (in terms of aircraft simulation model and simulator motion system fidelity) that defines the level of realism of the physical motion cues provided to the pilot during flight simulation	33
2.7	Optimisation of the heave motion filter parameters for the Simona research simulator using the tuning approach by Schroeder [46] and three different aircraft simulation model runs. Adopted from [48]	34
2.8	Percentage wise distribution of UPRT training tasks per FSTD type level, adopted from [51]	36
2.9	Simulators used during the SUPRA research project	38
2.10	Visualisation of the flow separation variable X around the wing's airfoil. Adapted from [64]	38
2.11	Measured and modelled PSDs and buffet model Bode diagrams for buffet accelerations in vertical and lateral directions from Ref. [14].	41
2.12	Schematic overview of the vertical stall buffet model proposed in Ref. [14].	41
3.1	Stall auto-pilot flow chart showing the steps taken in the upset and recovery phases, adopted from [17]	44
3.2	Stall autopilot validation process, all the stall model parameters are set to their respective baseline value from table 2.4, adopted from [17]	45
3.3	Bode analysis of the second-order band pass buffet model filter ($H(j\omega)$) under variation of the filter parameters (H_0 , ω_0 , Q_0) individually	47
3.4	Example symmetrical quasi-steady vertical stall buffet model simulation results showing the PSD of a_z under variation of the buffet model parameters	48
3.5	Vertical buffet model acceleration during a 90 seconds steady symmetric stall simulation of the Cessna Citation II stall Simulink model developed at the TU Delft	49
3.6	Vertical buffet model acceleration during a 90 seconds steady symmetric stall simulation of the Cessna Citation II stall Simulink model developed at the TU Delft, detailed view on the stalled portion of the flight simulation	49
3.7	VAF of the vertical buffet acceleration $a_z(t)$ for varying buffet model parameters with respect to baseline, using a single constant noise realisation (Standard Matlab/Simulink noise seed: 23341) as the buffet model input	50
3.8	VAF of the vertical buffet acceleration $a_z(t)$ for varying buffet model parameters with respect to baseline, averaged over a constant range of 50 different noise realisations used as the buffet model input	50
3.9	VAF of the vertical buffet acceleration $a_z(t)$ for varying the ω_0 model parameter with respect to the baseline, results are shown for a range of parameter values that roughly span from -30% to +30% offset with respect to the baseline value (75.92 rad/s) shown in red	51

3.10	VAF of the vertical buffet acceleration $a_z(t)$ for varying the Q_0 model parameter with respect to baseline, results are shown for a range of 50 different noise realisations showing the average in black and min/max spread in red	52
3.11	VAF of the vertical buffet acceleration $a_z(t)$ for varying the ω_0 model parameter with respect to baseline, results are shown for a range of 50 different noise realisations showing the average in black and min/max spread in red	52
3.12	VAF of the vertical buffet acceleration $a_z(t)$ for varying the X_{thres} model parameter with respect to baseline, results are shown for a range of 50 different noise realisations showing the average in black and min/max spread in red	53
3.13	Quasi-steady stall simulation results of the Cessna Citation II stall model with baseline settings (Angle of Attack α and Flow Separation Point X) showing the current buffet onset point ($X = 0.89$) as well the limits for simulator qualification set by the FAA on buffet onset threshold in red.	53
4.1	The experiment setup in the SIMONA Research Simulator (SRS) used for the human sensitivity experiment	56
4.2	Example staircase procedure data for a_1 from Ref. [17]. Note that the performed staircase also includes 'null' measurements that were used to verify participant consistency	56
4.3	Experiment procedure for one JND threshold condition, adopted from [17]	60
A.1	Example symmetrical quasi-steady vertical stall buffet model simulation results showing A_z in the time domain under variation of the buffet model parameters, zoomed in on the stalled portion of the 90 seconds Cessna Citation II model simulations	74
A.2	Example symmetrical quasi-steady vertical stall buffet model simulation results showing A_z in the time domain under variation of the buffet model parameters, zoomed in on a smaller portion of the stalled parts of the 90 seconds Cessna Citation II model simulations showing more details on the effect of the variations in buffet model parameters	75
C.1	Staircase- and Cumulative Density Function plots of participant 1.	84
C.2	Staircase- and Cumulative Density Function plots of participant 2.	85
C.3	Staircase- and Cumulative Density Function plots of participant 3.	86
C.4	Staircase- and Cumulative Density Function plots of participant 4.	87
C.5	Staircase- and Cumulative Density Function plots of participant 5.	88
C.6	Staircase- and Cumulative Density Function plots of participant 6.	89
C.7	Staircase- and Cumulative Density Function plots of participant 7.	90
C.8	Staircase- and Cumulative Density Function plots of participant 8.	91
C.9	Staircase- and Cumulative Density Function plots of participant 9.	92
C.10	Staircase- and Cumulative Density Function plots of participant 10.	93
C.11	Staircase- and Cumulative Density Function plots of participant 11.	94
C.12	Staircase- and Cumulative Density Function plots of participant 12.	95
C.13	Staircase- and Cumulative Density Function plots of participant 13.	96
C.14	Staircase- and Cumulative Density Function plots of participant 14.	97
C.15	Staircase- and Cumulative Density Function plots of participant 15.	98
C.16	Staircase- and Cumulative Density Function plots of participant C1.	99
C.17	Staircase- and Cumulative Density Function plots of participant C2.	100
C.18	Staircase- and Cumulative Density Function plots of participant C3.	101
C.19	Staircase- and Cumulative Density Function plots of participant C4.	102
C.20	Staircase- and Cumulative Density Function plots of participant C5.	103
C.21	Staircase- and Cumulative Density Function plots of participant C6.	104

List of Tables

2.1	Qualification levels of Flight Simulation Training Devices (FSTDs) according to ICAO [49], elaborated by [50]	35
2.2	SRS geometric characteristics, adopted from [55]	37
2.3	SRS motion space in all six degrees of freedom, adopted from [54]	37
2.4	Baseline parameter values of the TU Delft stall aerodynamic model retrieved from [15]	40
2.5	Baseline parameter values of the vertical buffet model reported in Ref. [14]	40
3.1	Vertical buffet model parameter values for the sensitivity analysis	46
3.2	VAF values of the vertical acceleration $a_z(t)$ for varying model parameters with respect to baseline, using a single constant noise realisation (Standard Matlab/Simulink noise seed: 23341) as the buffet model input	50
3.3	VAF values of the vertical acceleration $a_z(t)$ for varying model parameters with respect to baseline, averaged over a constant range of 50 different noise realisations used as the buffet model input	50
4.1	Participant latin-square condition sequence for the experiment	59

Nomenclature

Abbreviations

2AFC	Two-Alternative-Forced-Choice
AoA	Angle of Attack
DASMAT	Delft University Aircraft Simulation Model and Analysis Tool
DUECA	Delft University Environment for Communication and Activation
FAA	Federal Aviation Administration
FFS	Full Flight Simulator
FFT	Fast Fourier Transform
FSTD	Flight Simulating Training Device
ICAO	International Civil Aviation Organization
ICATEE	International Committee for Aviation Training in Extended Envelopes
JND	Just Noticeable Differences
LOC-I	Loss Of Control In-flight
PSD	Power Spectral Density
SME	Subject Matter Expert
SRS	SIMONA Research Simulator
SUPRA	Simulation of Upset Recovery in Aviation
UPRT	Upset Prevention and Recovery Training
VAF	Variance Accounted For

Greek Symbols

α	Angle of attack	[°/rad]
α^*	Angle of attack for which $X = 0.5$	[rad]
α_{crit}	Critical angle of attack	[°/rad]
$\dot{\alpha}$	Rate of change of AoA	[rad/s]
ω_0	Resonance frequency of the buffet filter	[rad/s]
τ_1	Lag time constant of flow separation point X	[s]
τ_2	Hysteresis time constant of flow separation point X	[s]
θ	Pitch angle of the aircraft	[°/rad]

Latin Symbols

a_1	Shape parameter of flow separation point X	[-]
-------	--	-----

a_y	Lateral acceleration of the aircraft in the body axis system	$[m/s^2]$
a_z	Vertical/Normal acceleration of the aircraft in the body axis system	$[m/s^2]$
C_L	Lift coefficient of the aircraft's wing	[-]
C_l	Lift coefficient of an airfoil	[-]
H_0	Gain of the buffet filter	[-]
K_z	Extra compensating gain of the buffet model	[-]
Q_0	Quality factor of the buffet filter that is related to damping	[-]
V_{TAS}	True airspeed of the aircraft	$[m/s \text{ or } kts]$
X	Flow separation point	[-]
X_{thres}	Threshold on the flow separation point X to trigger the buffet model	[-]



Scientific Paper

Just Noticeable Differences for Variations in Quasi-Steady Stall Buffet Model Parameters

A. Imbrechts*

Delft University of Technology, Delft, The Netherlands

Supervisors: C.C. de Visser[†] and D.M. Pool[‡]

Delft University of Technology, Delft, The Netherlands

To gain more insight into human sensitivity to variations in simulated stall buffets, Just Noticeable Difference (JND) thresholds were estimated using a passive human-in-the-loop flight simulator experiment. Using an in-house developed flow separation-based stall and buffet model of the Cessna Citation II, JND thresholds were determined for the buffet characteristic frequency parameter ω_0 and the buffet onset threshold parameter X_{thres} for the most significant buffet direction, i.e., the vertical stall buffet only. With a subjective yes/no 1-up/1-down staircase procedure that uses repeated pairwise comparisons of quasi-steady symmetric stall simulations (where one is a stall with the baseline buffet model and the other one has an offset in buffet parameters), upper and lower JND thresholds were measured from 21 active pilots. Results show that at comparably similar percentage-wise offsets for X_{thres} and ω_0 with respect to the baseline parameter value, pilots noticed the differences in simulated buffet dynamics. The maximum observed JND thresholds did not exceed 30-35% across all experiment conditions, indicating that pilots are sensitive to small offsets in the key stall buffet model parameters, which should be accounted for when determining stall buffet models for flight simulating training devices. Furthermore, the estimated thresholds for ω_0 are in agreement with the ± 2 Hz tolerance currently set in stall buffet simulation qualification standards. However, for X_{thres} , results show that pilots already notice differences in stall buffet onset characteristics well before the maximum tolerance ($\pm 2.0^\circ$ angle of attack) is reached, which suggests that simulated buffet onset requirements for quasi-steady symmetric stall models may require stricter limits to support effective stall training in simulators.

Nomenclature

Roman Symbols

a_1	Stall abruptness parameter, -
a_y	Lateral stall buffet acceleration, m/s^2
a_z	Vertical stall buffet acceleration, m/s^2
C_L	Lift coefficient, -
H_0	Buffet shaping filter gain, -
$K_{\{q,x,z\}}$	Motion filter gain in pitch, surge and heave, -
Q_0	Buffet shaping filter quality factor, -
X	Flow separation point, -
X_{thres}	Buffet onset threshold on X , -

Greek Symbols

α	Angle of attack, rad or deg
α^*	Angle of attack for which $X = 0.5$, rad
$\zeta_{\{q,x,z\}}$	Motion filter damping coefficient in pitch, surge and heave, -
τ_1	Lag time constant of flow separation point X , s
τ_2	Hysteresis time constant of flow separation point X , s
ω_0	Buffet shaping filter natural frequency, rad/s
$\omega_{b_{\{q,x,z\}}}$	Motion filter break frequency in pitch, surge and heave, rad/s
$\omega_{n_{\{q,x,z\}}}$	Motion filter natural frequency in pitch, surge and heave, rad/s

*M.Sc. student, Control and Simulation Division, Faculty of Aerospace Engineering, P.O. Box 5058, 2600GB Delft, The Netherlands; a.imbrechts@student.tudelft.nl.

[†]Assistant Professor, Control and Simulation Division, Faculty of Aerospace Engineering, P.O. Box 5058, 2600GB Delft, The Netherlands; c.c.devisser@tudelft.nl. Member AIAA.

[‡]Assistant Professor, Control and Simulation Division, Faculty of Aerospace Engineering, P.O. Box 5058, 2600GB Delft, The Netherlands; d.m.pool@tudelft.nl. Senior Member AIAA.

I. Introduction

Aerodynamic stall is an intense dynamic, nonlinear and unsteady condition that may lead to unrecoverable airplane upset conditions if not corrected in time. Stalls are an important contributor to fatal accidents in civil aviation and are the primary cause of fatal accidents in general aviation [1–3]. Until recently, training simulators were not required to provide high-accuracy stall simulation [4–6]. However, this has changed with the mandatory requirement for all airline crew to receive flight simulator-based stall prevention and recovery training that is effective since 2019 [7–9]. As a result, there is a strong need for accurate and cost-effective stall and post-stall dynamic models for use in flight simulators.

A key characteristic of a stall is the buffet, as buffeting is an initial cue for pilots that indicates entering of the unsafe part of the flight envelope. The stall buffet, which occurs at high angles of attack, is the aerodynamic excitation due to flow separation causing pressure fluctuations over the wing [10–12]. A common remaining deficiency in current Flight Simulating Training Devices (FSTDs) is the insufficient haptic and physical vibratory feedback of buffeting felt by pilots in simulated stalled conditions [6, 13]. While this can partly be attributed to practical considerations, as limiting buffeting vibrations positively benefits the required FSTD maintenance and downtime, a major second reason is that it is, in fact, unknown what level of stall buffet accuracy or fidelity is actually required for realistic stall simulations and effective stall training. Available regulatory standards for stall buffet simulation [7] reflect this persisting uncertainty with quite lenient tolerances on buffet responses, e.g., *“the flight simulator results should exhibit the overall appearance and trends of the airplane plots, with at least some of the frequency ‘spikes’ being present within 2 Hz of the airplane data”* [7].

The goal of this paper is to provide additional quantitative guidance on the required accuracy for replicating stall buffets in flight simulators. It presents the results of a human-in-the-loop experiment in the SIMONA Research Simulator at TU Delft that was performed to measure Just Noticeable Difference (JND) thresholds for key parameters that characterize the frequency content and buffet onset threshold of simulated stall buffet vibrations. The experiment was performed by 6 Citation II pilots and 15 other pilots. It utilized a Cessna Citation II stall model identified in earlier research [14, 15]. For measuring the JND thresholds, use is made of the same experimental paradigm as described in Ref. 16, where participating pilots experienced simulated symmetrical quasi-steady stall maneuvers at an altitude of 5,500 m (18,000 ft), induced with a 1 kt/s deceleration into the stall, as a passive observer. Through a subjective staircase procedure, consisting of repeated pairwise comparisons of the stall with our baseline buffet model and a stall with adjustments to the buffet model parameters, the JND thresholds for these parameter variations were determined. Furthermore, the measured JND thresholds were objectively compared to tolerances that apply to simulated stall buffet characteristics from current regulatory standards [7, 17].

This paper is structured as follows. Section II provides a background on stall buffet model requirements for FSTDs. Furthermore, the Citation II buffet model used in this research is presented in the same section, as well as an offline sensitivity analysis of the buffet’s responses to changes in the model parameters. Section III describes the human-in-the-loop experiment and methods used to estimate the JND thresholds of key stall buffet model parameters. The results of the experiment are presented in Section IV, which is followed by a discussion and conclusions towards the end of the paper.

II. Stall Buffet Modeling

A. FAA Requirements for Stall Buffet Models in FSTDs

In an effort to reduce the occurrences of loss of control in-flight related incidents, the Federal Aviation Administration (FAA) introduced the binding requirement for airline flight crew to receive simulator-based stall prevention and recovery training. This mandatory stall training is effective since 2019 and reflects the need for accurate stall simulation models for flight simulators [9, 17, 18]. A key characteristic of stalled flight is the buffet, which serves as an initial cue to pilots upon entering of the unsafe part of the flight envelope. Current qualification standards that relate to the simulation of these stall buffets are the following:

- *“Buffet onset threshold of perception should be based on 0.03g peak to peak normal acceleration above the background noise with a tolerance of $\pm 2.0^\circ$ angle of attack”* [7, p. 95].
- *“Correct trend of growth of buffet amplitude from initial buffet to stall speed for normal and lateral acceleration will have to be demonstrated”* [7, p. 95].
- *“FSTD manufacturers may limit maximum buffeting based on motion platform capability/limitations or other simulator system limitations”* [7, p. 95].
- *“The overall trend of the PSD plot should be considered while focusing on the dominant frequencies”* [7, p. 131].

- “The appearance and trend of the buffet’s power spectra should match flight data with at least three of the predominant frequency spikes being within ± 2 Hz of the flight data frequency spikes” [7, p. 105].
- “Conduct an approach-to-stall with engines at idle and a deceleration of 1 knot/second. Check that the motion cues of the simulated buffet, including the level of buffet increase with decreasing speed, are representative of the actual airplane” [7, p. 182/183].
- “Tolerances on stall buffet are not applicable in case the first indication of the stall is the activation of the stall warning system (i.e. stick shaker/pusher, stall horn, ...)” [7, p. 96].

However, a common remaining deficiency in FSTDs is the insufficient modeling of such buffet responses. While this can partly be attributed to practical considerations, as limiting buffeting vibrations positively benefits the required FSTD maintenance and downtime, a major second reason is that it is largely uncertain what level of stall buffet model fidelity is required for accurate stall simulations [6, 13]. This uncertainty is reflected by regulatory standards with seemingly lenient tolerances on simulated buffet responses, see the bold tolerances above. These buffet characteristic tolerances have not been validated before from a pilot sensitivity point of view, something which the research in this paper focuses on.

B. Stall Buffet Model

In this paper, a limited-envelope aerodynamic stall model of the Cessna Citation II developed at TU Delft was used [14, 15, 19]. This model was identified from flight test data collected with the Cessna Citation II research aircraft (jointly operated by NLR and TU Delft) and includes the quasi-steady stall aerodynamics and buffet dynamics based on Kirchhoff’s theory of flow separation [20–22]. The model explicitly accounts for the flow separation point X , which ranges from 0 to 1, where 1 represents a fully attached flow and 0 means fully separated flow. The dynamics of X are modeled by a first-order differential equation:

$$\tau_1 \frac{dX}{dt} + X = \frac{1}{2} (1 - \tanh [a_1 (\alpha - \tau_2 \dot{\alpha} - \alpha^*)]) \quad (1)$$

The Kirchhoff model has four parameters for characterizing the stall dynamics, i.e., τ_1 , τ_2 , a_1 and α^* . The time constant τ_1 characterizes the effects of flow inertia, i.e., the time the air flow needs to readjust to a new condition. τ_2 models the effects of hysteresis during flow re-attachment. a_1 is a stall abruptness parameter and α^* equals the stall angle of attack where the flow separation point X is 0.5. The effects of varying the Kirchhoff model parameters on C_L and X have been investigated and are presented in past research [14, 16, 22]. In our stall buffet model, as described by Van Horssen et al. [14], also the temporal variations in stall buffet intensity are directly linked to the flow separation state X .

The stall buffet model proposed in Ref. 14 was derived from buffet vibrations measured during flight tests with the Cessna Citation II. The Power Spectral Densities (PSDs) of measured vertical and lateral accelerations during quasi-steady stall maneuvers were used to model the stall buffet frequency spectrum, see Fig. 1. Fig. 1 also shows the dominant frequencies of the buffet vibrations. In the vertical direction there is only one dominant frequency peak at around 12 Hz, while in lateral direction two main peaks are observed, at 6 Hz and 10 Hz. The longitudinal accelerations are not shown as stall buffet accelerations were found to be negligible in this direction [14]. Fig. 1 also shows that, as expected, the PSD of the vertical buffets is approximately 10 times larger in magnitude than the lateral buffets. Hence, in this paper we focus on measuring how noticeable variations in the vertical stall buffet are for human pilots.

The vertical stall buffet model proposed by Van Horssen et al. [14], see Fig. 2, passes unity-variance white noise through a second-order shaping filter $H(s)$ given by Eq. (2) that accounts for the average frequency spectrum of the buffet vibrations (see Fig. 1). The resonance frequency ω_0 of the second-order filter is used to create a band-pass filter replicating the 12 Hz (75 rad/s) frequency spike which dominates the vertical buffet characteristics of the Citation II.

$$H(s) = \frac{H_0 \omega_0^2}{s^2 + \frac{\omega_0}{Q_0} s + \omega_0^2} \quad (2)$$

The parameters in the buffet model of Eq. (2) were estimated by fitting the PSD of the filter output to the PSD of the raw buffet flight data, see Fig. 1. The baseline parameter values of $H(s)$ reported in Ref. 14 were a gain H_0 of 0.125, a resonance frequency ω_0 of 75.92 rad/s (12.08 Hz), and a quality factor Q_0 of 8.28 ($\zeta_0 = 0.06$, the quality factor is related to the inverse of the damping ratio $Q = \frac{1}{2\zeta}$). As shown in Fig. 2, the shaping filter output is further multiplied with a factor $1 - X$ to account for buffet intensity variations with the level of separated flow along the wing. Finally, the

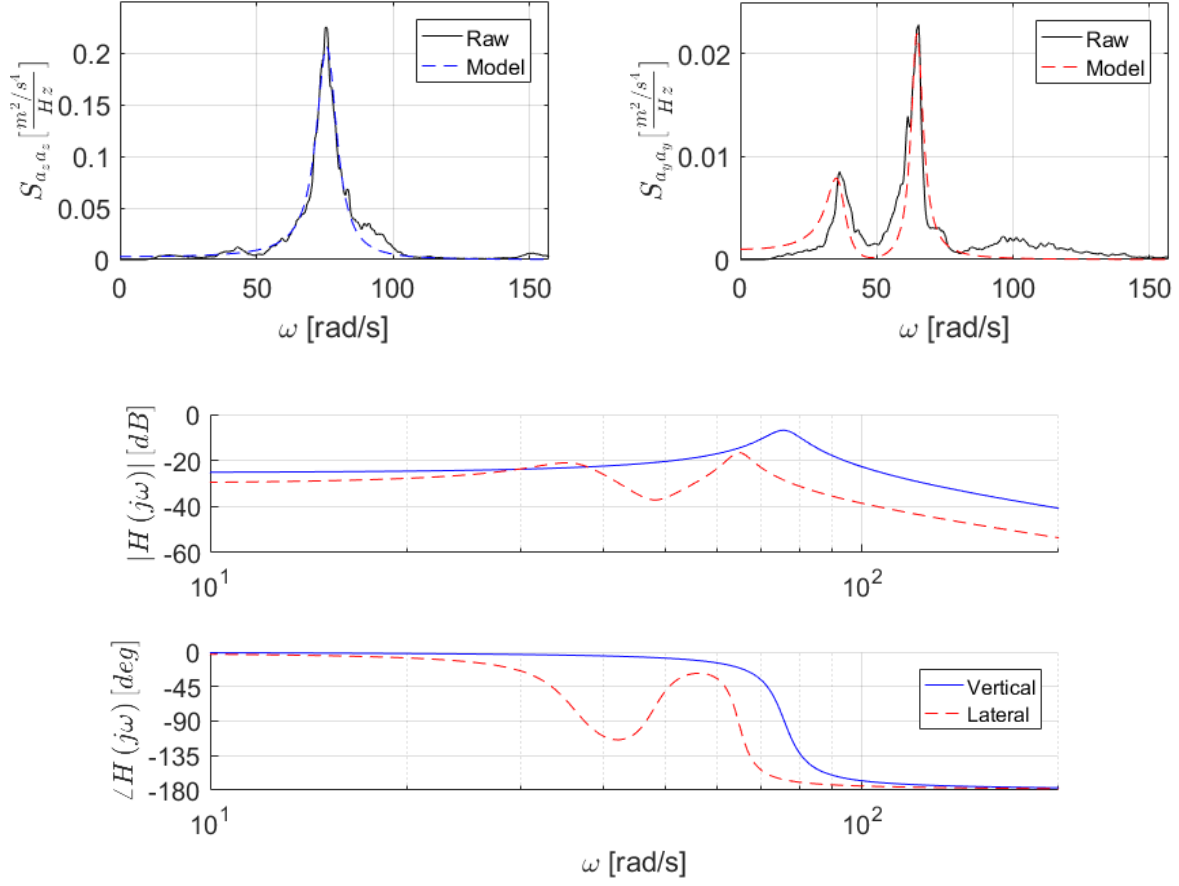


Fig. 1 Measured and modeled PSDs and buffet model Bode diagrams for buffet accelerations in vertical and lateral directions from Ref. 14.

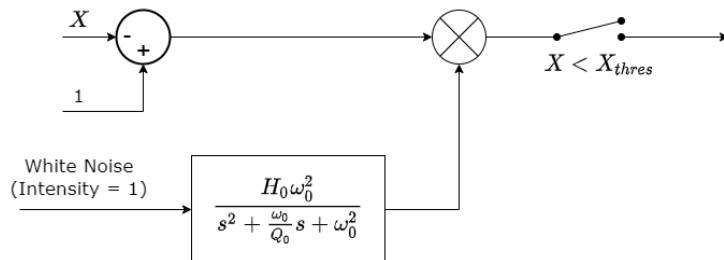


Fig. 2 Schematic overview of the vertical stall buffet model proposed in Ref. 14.

stall buffet model uses a threshold on X , i.e., X_{thres} , to trigger the buffet model: only when $X < X_{thres}$ (here 0.89) the stall buffet model becomes active and adds vibrations to the aircraft vertical acceleration.

C. Quasi-Steady Stall Buffet Simulations

For the buffet model simulations, the Cessna Citation II stall dynamics model from Ref. 15 that includes the buffet model from Ref. 14 has been implemented in Matlab/Simulink. A simulated “stall autopilot” developed for the earlier experiment of Ref. 16 was implemented to consistently perform 1 kt/s deceleration and the quasi-steady stall maneuver. Using this model, the effects of varying the buffet model parameters (H_0 , ω_0 , Q_0 and X_{thres}) were evaluated. Fig. 3 shows example symmetric quasi-steady 90 seconds vertical stall buffet simulation results in the frequency domain (PSD of a_z) for variations of -66%, -33%, 0%, +33% and +66% in all buffet model parameters individually with respect to their baseline values. The PSD plots were calculated experimentally using the time simulation results from the buffet model and the Fast Fourier Transform (FFT) algorithm in Matlab. To get a smoother estimate of the PSD, the results from 50 different white noise realizations with fixed intensity have been averaged.

In addition to the PSD sensitivities shown in Fig. 3, the sensitivity of the buffet model in the time domain was analysed, see Fig. 4. This was done by calculating the Variance Accounted For (VAF) values between the baseline buffet time response (a_z) and the buffet model output with offsets in the model parameters (\hat{a}_z) according to Eq. (3) and using a fixed seed for the white noise realization used as the buffet model input. The VAF value was calculated individually for 50 different white noise realizations and then averaged to find the results shown in Fig. 4 for each offset in the model parameters. The VAF quantifies the amount of variance that is common between two time signals. The closer it is to 100 percent, the more identical the two signals are.

$$\text{VAF} = \left(1 - \frac{\sum_{i=1}^N (a_z(t_i) - \hat{a}_z(t_i))^2}{\sum_{i=1}^N a_z(t_i)^2} \right) \cdot 100\% \quad (3)$$

As shown in Fig. 3, the characteristic frequency parameter ω_0 has the biggest influence on which frequency components are present in the simulated buffet. It directly parameterizes the frequency at which the dominant spike in the buffet spectrum occurs. According to regulatory standards from the FAA for qualification of stall dynamic models in FSTDs, the predominant frequency spikes of the simulated buffet should be within a tolerance of ± 2 Hz from airplane data [7]. This FAA tolerance compares to a 17% offset with respect to the baseline $\omega_0 = 75.92$ rad/s (12 Hz). The VAF value for such an offset in ω_0 already drops below the 0% mark, which indicates significant variances exists at the tolerance limits with respect to the baseline model time response.

Another parameter closely related to FSTD stall buffet requirements is X_{thres} that models the buffet onset point. Lowering the threshold value would delay buffet onset in the model as well as increase the initial buffet amplitude. According to FAA qualification standards, the buffet threshold of perception should be based on 0.03g peak to peak initial normal acceleration with a tolerance of ± 2.0 degrees in angle of attack [7]. In the specific case of quasi-steady stall simulations of the Cessna Citation II model, this translates to the limits shown in Fig. 5. Fig. 5 shows a considerable time frame of around 26 seconds that falls within the ± 2.0 degrees angle of attack range around the nominal buffet onset threshold point ($X = 0.89$). When increasing the X_{thres} parameter, the VAF value remains approximately 100% (see the asymmetry of the VAF plot around the baseline value for X_{thres} in Fig. 4), which indicates that there are almost no differences between the tuned and baseline buffet model responses when the X_{thres} parameter is increased. Therefore, an upper JND threshold for X_{thres} parameter was not measured during the experiment because it was concluded that upper variations in this parameter would not be noticeable to pilots.

As is clear from Fig. 3 and Fig. 4, parameters H_0 and Q_0 have similar effects on the simulated buffet model output. They both lift the buffet power spectra up and down around the peak, changing the intensity. No clear requirement is set on this stall buffet characteristic from regulatory standards. Ideally, this peak should match as close as possible the power spectra of the measured flight data and these model parameters can thus be identified accordingly by matching the peak heights. Hence, the parameters H_0 and Q_0 were not further investigated in this research.

In conclusion, based on analysis of the sensitivity of the buffet model responses to variations in H_0 , ω_0 , Q_0 and X_{thres} as shown in Fig. 3 and Fig. 4, the experiment only measured the JND thresholds for two key parameters that characterize the frequency content and temporal amplitude variations in the stall buffet vibrations: ω_0 and X_{thres} , respectively. The other parameters remained fixed at their baseline values as determined in Ref. 14 during the experiment.

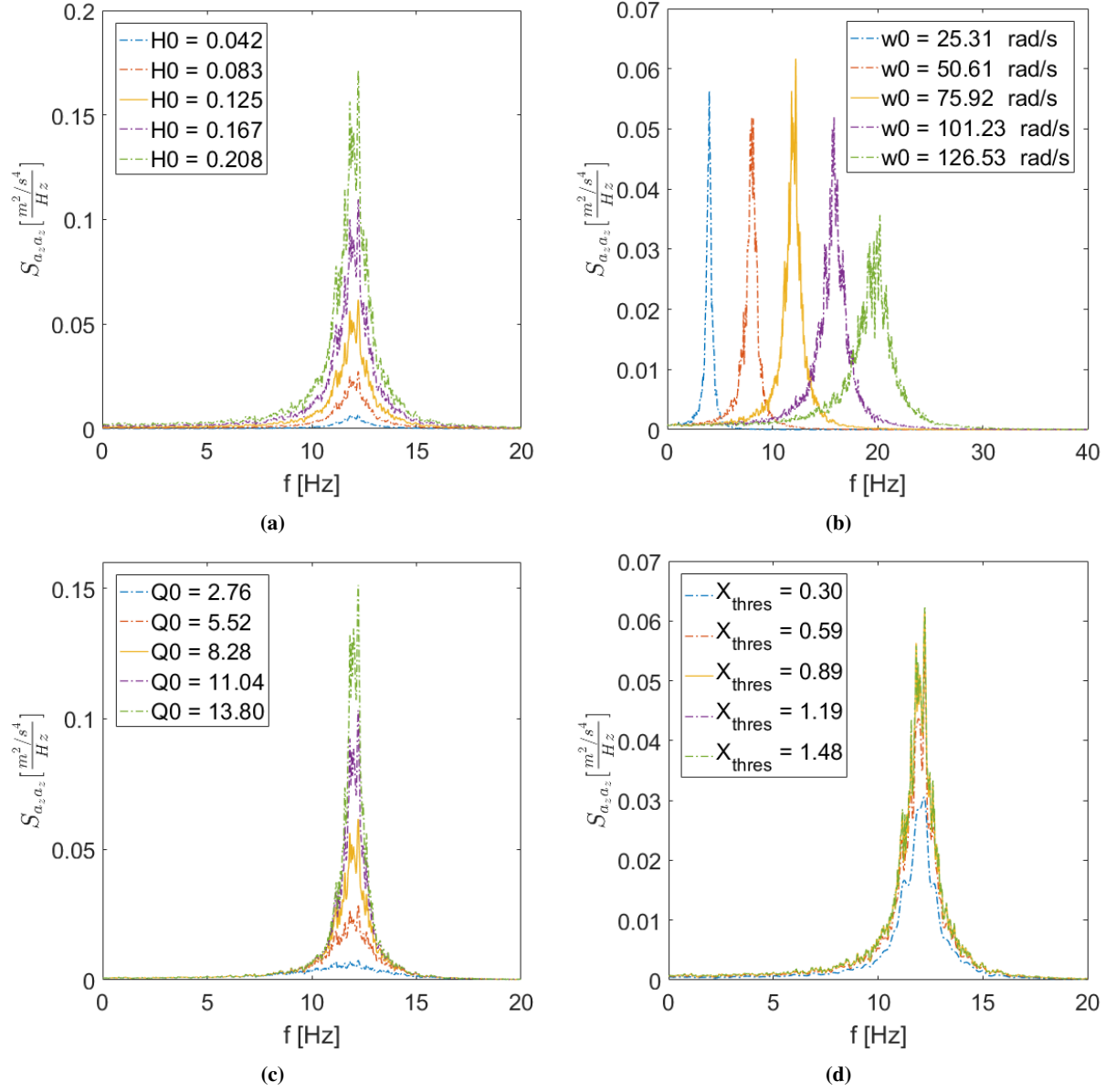


Fig. 3 Example symmetrical quasi-steady vertical stall buffet model simulation results showing the PSD of a_z under variation of the buffet model parameters.

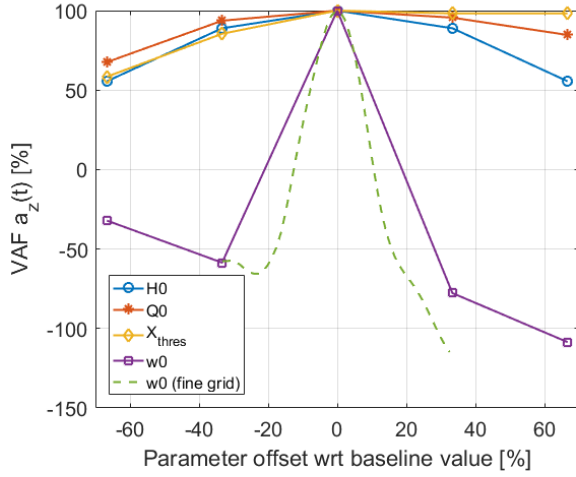


Fig. 4 VAF of the vertical buffet model output (a_z) presented as a function of model parameter offsets.

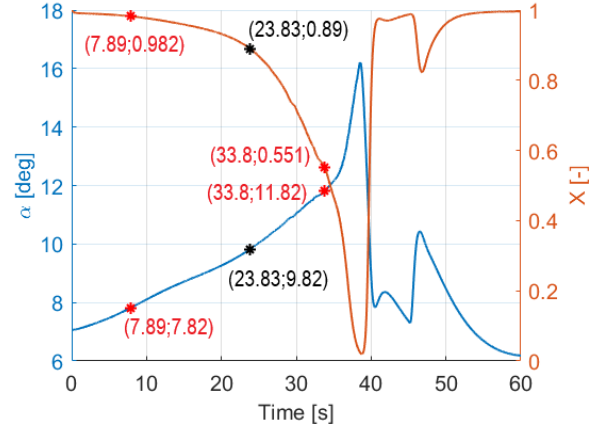


Fig. 5 Quasi-steady stall simulation results of the Cessna Citation II stall model with baseline settings (Angle of Attack α and Flow Separation Point X can be seen) showing the current buffet onset point ($X = 0.89$) in black as well as the limits for simulator qualification set by the FAA on buffet onset threshold in red.

D. JND Threshold Hypotheses

Two hypotheses for the human-in-the-loop experiment described in Section III about the JND thresholds for ω_0 and X_{thres} were formulated based on the results from the buffet model sensitivity analysis (see Section II.C). Furthermore, the JND thresholds were also compared to the tolerances set by the FAA on simulated buffet responses, see Section II.A.

H1 The JND threshold with respect to the baseline value for changes in ω_0 is lower than for X_{thres} . Based on the sensitivity analysis in the time domain (see Fig. 4), a similar percentage-wise offset in X_{thres} and ω_0 results in stronger VAF changes for ω_0 . Hence, it is expected that the JND threshold for changes in ω_0 is lower than for X_{thres} .

H2 The upper and lower JND thresholds for ω_0 are symmetric with respect to the baseline value. The green dashed line in Fig. 4 shows a symmetric variation of the VAF around the baseline value for ω_0 until an offset of about 20%. The JND thresholds are expected to be within this symmetric portion of the figure because the FAA tolerance of ± 2 Hz on buffet characteristic frequency suggests a maximum allowable variation of about 17% offset with respect to the baseline value of $\omega_0 = 75.92$ rad/s (12 Hz). Hence, the JND threshold results are expected to be symmetric around the baseline value for ω_0 .

III. Methods and Experiment Setup

The goal of the human-in-the-loop experiment was to determine threshold values on the allowable variation in ω_0 and X_{thres} parameters before the parameter changes became noticeable to pilots. To measure these JNDs from different pilots, the same experimental paradigm also applied by Smets et al. [16] was used. Here participants experience (as passive observers, i.e., the stall autopilot flew the maneuver) different sets of two sequential quasi-steady stalls, of which one represented the baseline parameter settings and the other a modified buffet parameter (ω_0 or X_{thres}) setting. Using a subjective staircase measurement procedure that also includes “null measurements” (i.e., baseline to baseline comparisons) to estimate the reliability of pilots’ responses [16], JND thresholds were estimated for 21 active pilots.

A. Apparatus

The SIMONA Research Simulator (SRS) at TU Delft was used to perform the experiment (see Fig. 6). The existing Cessna Citation II simulation environment available in the SRS was used, with our custom stall dynamics model implemented [14, 15, 19]. Participants were seated in the left pilot seat inside the SRS cockpit (see Fig. 6b) and wore a noise canceling headset to mask any noise coming from the simulator motion system hardware.



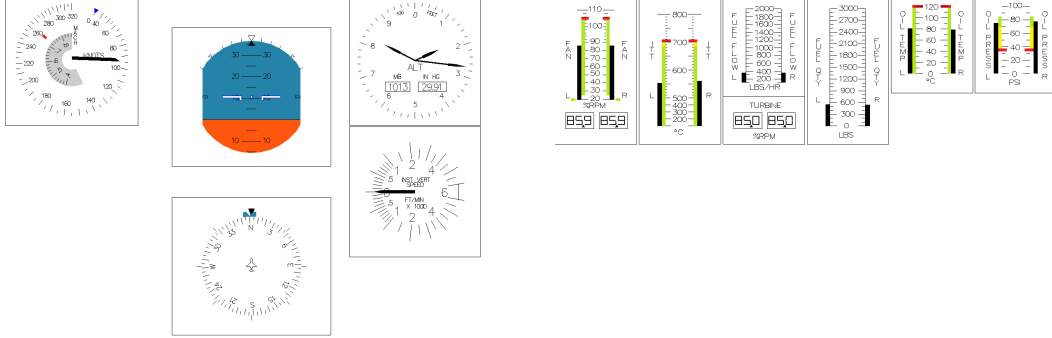
(a) Outside



(b) Inside

Fig. 6 The experiment setup in the SIMONA simulator used for the experiment.

During the experiment, participants were given outside visual cues generated using a FlightGear database and projected onto the 180x40 deg collimated screen of the SRS with an update rate of 60 Hz [23]. Next to the outside visual, also head-down visual cues were provided using the primary and secondary flight displays available in the SRS. Those displays showed in-house developed primary flight instruments and engine parameters, see Fig. 7.



(a) Primary flight display

(b) Secondary flight display

Fig. 7 The primary and secondary flight displays, showing conventional flight instruments and engine information, used during the experiment.

The SRS's motion system consists out of a six degree-of-freedom (DOF) hydraulic hexapod configuration, which can provide motion feedback at low latency and high accuracy [23, 24]. The experiment focused on symmetrical quasi-steady stall simulations. Hence, the asymmetric DOFs (i.e., roll, yaw and sway) were not used. The symmetric DOFs (i.e., pitch, surge and heave) were cued using a classical washout filter algorithm [25]. The used motion filter settings that remained constant during the experiment are listed in Table 1. Pitch (q) and surge (x) settings are set to typical reference values, identical to the ones used in Ref. 16. The heave settings, i.e., K_z and ω_{n_z} , were optimized using a ‘‘Gouverneur’’ analysis [26], as can be seen in Fig. 8. In this figure, each dot represents a filter configuration with K_z varying from 0.1 to 1 horizontally and ω_{n_z} from 0.1 to 4 rad/s vertically. The colored lines separate the feasible configurations (left and above the boundaries) from the ones where the simulator would hit its limits. The different colored boundaries represent stall simulations with different stall buffet model parameter settings, i.e., the most extreme experiment conditions possible and the baseline settings.

Ideally, a heave motion setting is chosen above and to the left of the colored lines, but as close to the right bottom corner as possible. That would result in the highest possible fidelity of the motion filter according to the Sinacori fidelity criterion [27, 28]. Three different settings were analysed during testing of the experiment, shown by blue/red markings in Fig. 8. They correspond to a constant gain K_z of 0.5 and ω_{n_z} equaling 3.0, 2.0 and 1.2 rad/s respectively. 3.0 rad/s is

the original safe setting from Ref. 16. It was investigated if a more optimal setting closer to the boundaries was possible. 1.2 rad/s was investigated as this gave heave settings identical to the surge ones. However, 2.0 rad/s was selected as the final heave motion setting for ω_{n_z} (red marker) because 1.2 rad/s was found to give too intense motion cues during stall recovery and reset of the simulator in between stall runs.

Table 1 Motion filter parameters used for the experiment.

High-pass filters						Low-pass filters	
ω_{n_q}	1.0 rad/s	ω_{n_z}	2.0 rad/s	ω_{n_x}	1.2 rad/s	ω_{n_x}	2.4 rad/s
ζ_q	0.5	ζ_z	0.7	ζ_x	0.7	ζ_x	0.7
ω_{b_q}	0.0 rad/s	ω_{b_z}	0.3 rad/s	ω_{b_x}	0.0 rad/s		
K_q	0.5	K_z	0.5	K_x	0.5		

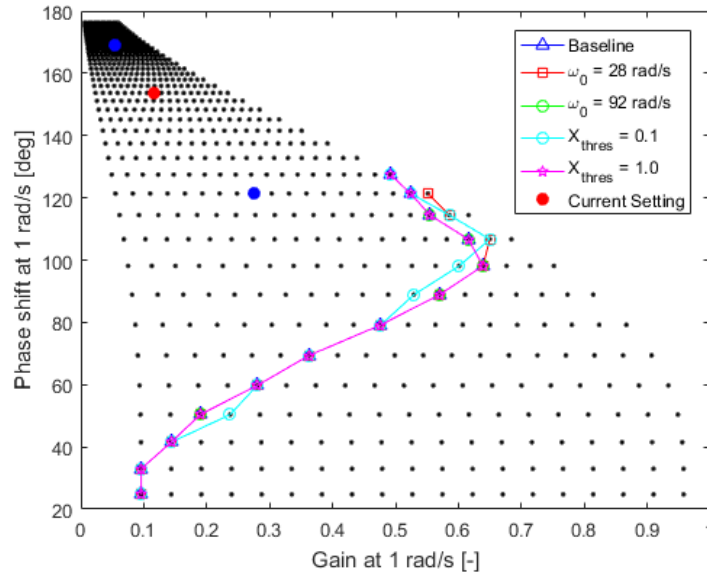


Fig. 8 Heave Gouverneur analysis [26] results for the baseline simulation settings and four extreme experiment condition settings. Configurations above and to the left of the colored lines ensure that the simulator remains within its motion limits.

B. Experiment Procedures and Conditions

The experiment measured an upper and a lower threshold for ω_0 and a lower threshold for X_{thres} . Upper thresholds are identified with a + superscript (ω_0^+), while lower thresholds are identified using a - superscript (ω_0^- and X_{thres}^-). This resulted in an experiment with three different conditions. The three experiment conditions (i.e., X_{thres}^- , ω_0^+ and ω_0^-) were performed by the participants in a randomized order using a Latin square design.

Every condition resulted in staircase data using a yes/no procedure (see Fig. 9) identical to the one used in a similar JND threshold experiment of Ref. 16. Every trial consisted of a comparison between two sequential quasi-steady stalls of around 15 seconds each, which ran from stall onset up until recovery was initiated. One of the two stalls represented the baseline buffet settings, while the other one had an offset in either ω_0 or X_{thres} , depending on the experiment condition. The order in which the baseline and offset parameter stall were presented varied randomly across trials.

At the end of the second stall, participants were asked to verbally answer the yes/no question: “Did you notice a difference?”. The given answer of the participants then determined the next parameter offset value. A “yes” answer would update the parameter closer to the baseline value, while a “no” answer would update further away. From the second reversal (i.e., a “yes” answer after a “no” or the other way around) onward, the step size reduced by 50% at

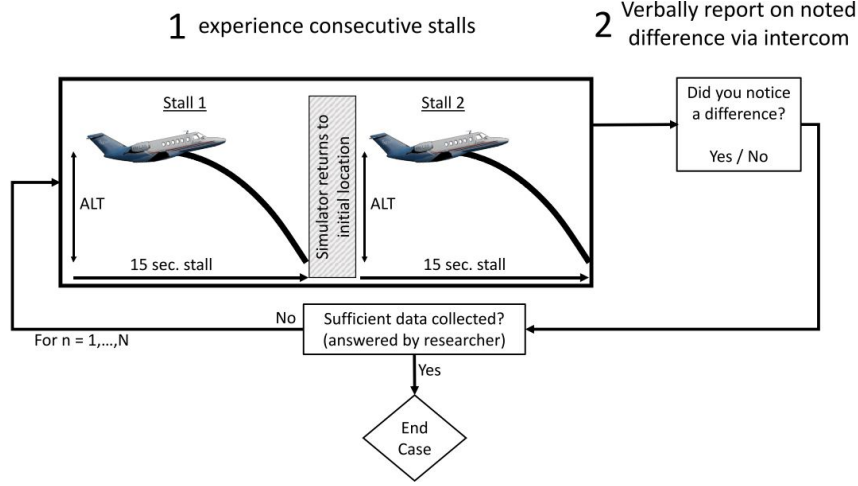


Fig. 9 Graphical representation of the experiment procedure and repeated consecutive simulated stalls, adopted from Ref. 16.

every reversal in the answers. If four consecutive answers were identical, the step-size doubled to converge faster to the threshold. Such an approach is referred to as an adaptive 1-up/1-down staircase method, which results in a 50% level of correctness JND threshold [29]. The researcher ended the staircase procedure, see Fig. 9, either when the participant’s staircase had converged (i.e., the step size was reduced to a value lower than 1/32th of the initial step size) or when a total of 30 comparisons was performed.

The initial starting position of the staircase for each experiment condition was chosen relatively far away from the baseline, such that the initial parameter offset was obvious to all participants. The initial step size was chosen accordingly to ensure convergence within a reasonable amount of trials. The initial parameter values and step sizes for each experiment condition are listed in Table 2. To mitigate the risk of participants following identical paths through the staircase procedure and increase the variety in the collected staircase data, small random parameter variations were added at every parameter update. The amplitude of the added white noise variations was set to 90% of the smallest allowed step size, making the noise more dominant close to the threshold value.

Table 2 Initial staircase values for each experiment condition.

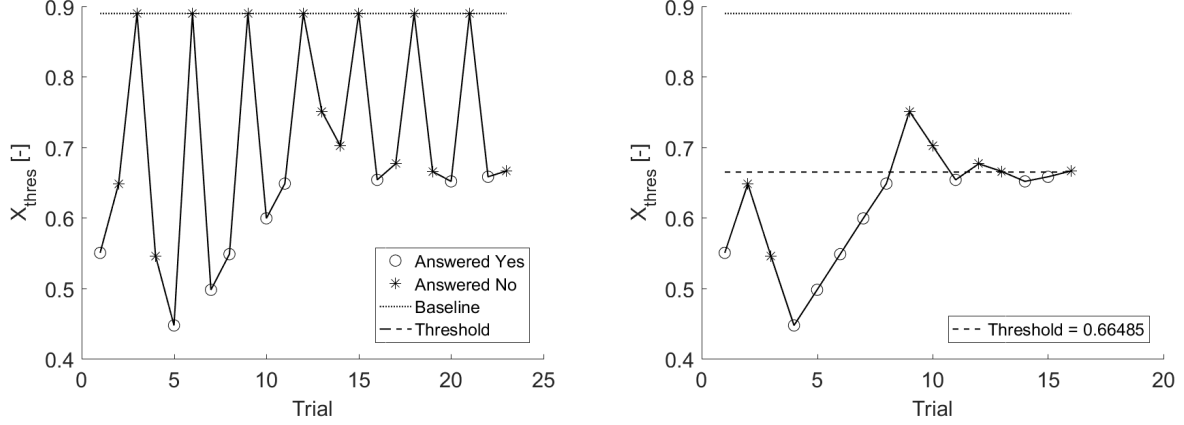
	X_{thres}^-	ω_0^+	ω_0^-
Initial value	0.55	92 rad/s	28 rad/s
Initial step	0.1	-5 rad/s	15 rad/s

Prior to the start of the experiment, participants were briefed on the safety and experiment procedures. They were instructed to only answer verbally on the yes/no question: “*Did you notice a difference?*” at the end of two consecutive quasi-steady stalls, and that no further explanation was required. No information about the goal of the experiment, the tested conditions or the data analysis was provided. Participants were trained for about 15 minutes, where they could practice detecting the differences between the two stalls using example runs of the different experiment conditions. Sufficient breaks were provided between the different test conditions to limit fatigue artifacts in the data.

C. Data Analysis

The threshold values for X_{thres}^- , ω_0^+ and ω_0^- were determined for each participant individually from the staircase data sets collected using the experiment procedure shown in Fig. 9. Such yes/no-staircase procedures are prone to biases [29, 30]. In order to mitigate these biases from the data, additional “null measurements” were performed at every third trial, see Fig. 10a. A null measurement was a comparison of a stall with baseline buffet model settings with itself, i.e., no differences were to be detected between the two stalls. The answers that participants gave to the null measurements were only used to assess the consistency and reliability of participants and had no influence on the

staircase procedure. The final threshold participants converged to was calculated after removing the null measurements and taking the average of the last three reversals in the staircase data, see Fig. 10b for an example of X_{thres}^- .



(a) Staircase example with null measures for X_{thres}^- lower. (b) Staircase example without null measures for X_{thres}^- lower.

Fig. 10 Example staircase data for X_{thres}^- . Note that the performed staircase also includes “null measurements” (see (a)) that were used to verify participant’s consistency.

D. Experiment Participants

A total of 21 active pilots (1 female and 20 males) participated in the experiment. The participants were from different age categories and they were subdivided into two groups to investigate differences between the measured JND thresholds. One group (n=15) consisted of a combination of glider, private and commercial pilots. The other group (n=6) were pilots that specifically hold a Cessna Citation II type rating (the simulated aircraft during the experiment). All participants were given a consent form to fill out and sign before starting the experiment. The study was approved by TU Delft’s Human Research Ethics Committee (HREC) under application number 1741.

IV. Results

A. Participants Reliability

The consistency and reliability of participants’ responses was based on the answers given to the added null measurements, i.e., the comparisons of two identical stall simulations with baseline buffet model settings. Fig. 11 shows the percentage of correctly answered null measures (i.e., participants provided a “no” answer on the null measurements) for all 21 pilots. Separate colored bars indicate the individual results for the different experiment conditions and a colored marker combines them into a total consistency percentage for each participant. The threshold to determine if participants’ staircase data were reliable or not was based on the lower bound of the 95% confidence interval on the average total consistency. This resulted in a boundary of 72.15% for the general pilot group (see Fig. 11a) and 59.68% for the group of Citation II pilots (see Fig. 11b). The dashed black lines in Fig. 11 indicate these boundaries. Fig. 11 shows a total of four general pilots (participants 3, 5, 13 and 14) and one Citation II pilot (participant C3) to have a total consistency that is below the boundary. Hence, these participants were concluded to be unreliable and inconsistent in answering and their data were not considered for further analysis. It was also investigated what the threshold boundary would become if the two pilot groups were combined. This resulted in a boundary of 71.98% (see the red dashed lines in Fig. 11). With this overall reliability limit, the same participants were to be excluded from the data analysis.

B. JND Thresholds for Stall Buffet Model Parameters

The experiment procedure explained in Section III.B was used to gather staircase data of every participant for each of the three experiment conditions, i.e., X_{thres}^- , ω_0^+ and ω_0^- . Average thresholds (across all participants) were estimated

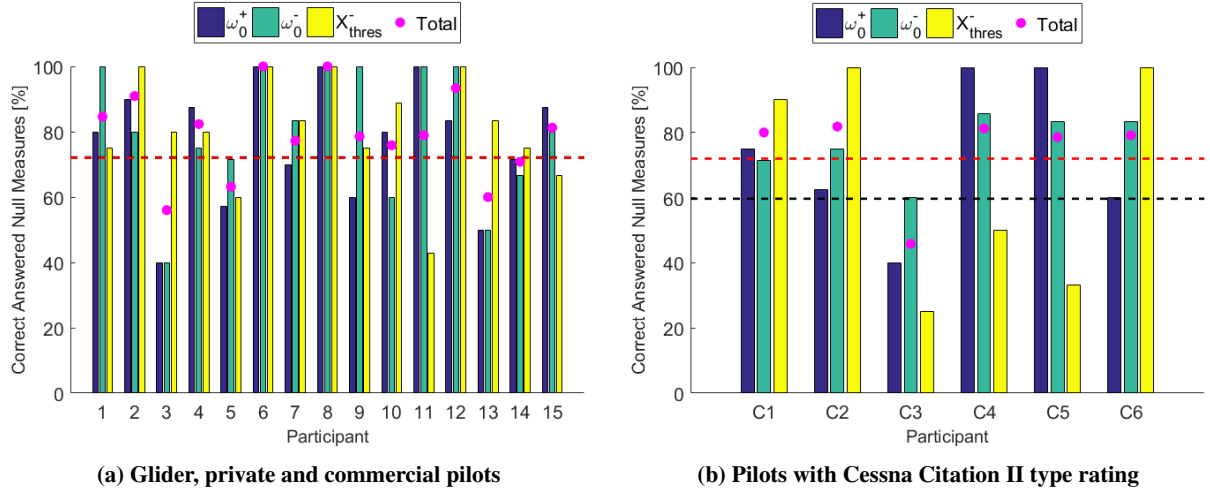


Fig. 11 Percentage of correctly answered null measurements (baseline comparisons) for two groups of experiment participants.

by fitting a Gaussian Cumulative Density Function (CDF) through all staircase data [31]. Fig. 12 shows the fitted CDFs for all three experiment conditions, where a “yes” answer was presented as 1 (100%) and a “no” answer as 0 (0%). The CDFs show 50% level of correctness thresholds that are unreliably close to the baseline values for a JND, especially in the case for ω_0 , see Fig. 12b and Fig. 12c. This is caused by some individual thresholds of participants being very close or even on the baseline value for ω_0 (see Fig. 13b). Such inconsistent results and limited data points at extreme values further away from the baseline made the CDF fits too unreliable for use. Therefore, the JND thresholds estimated from averaging the last three reversals in the staircase data are considered as the experiment results and are shown as a boxplot representation in Fig. 13 for all three experiment conditions. Note that the results shown in Fig. 13 are only based on the consistent participants, see Fig. 11.

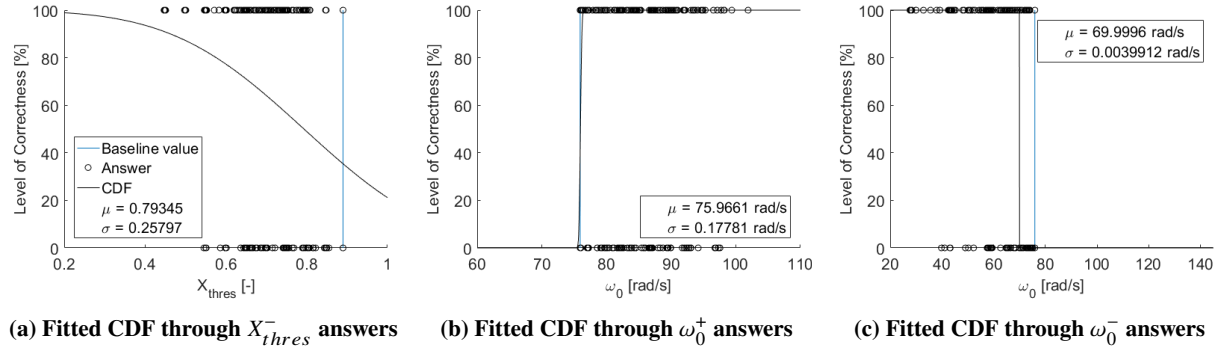


Fig. 12 Cumulative Density Function fits through all consistent experiment data for all three estimated thresholds.

Fig. 13 shows the threshold results for the general pilots and Citation II pilots separately as well as combined. The left vertical axis indicates the absolute values of the thresholds, while the right vertical axis shows them as Weber fractions, i.e., as percentage-wise difference with respect to the baseline value. Note that no significant differences are found between the results of the general pilots and Citation II pilots. This was expected since the experiment focus is on relative differences in simulated stall buffet accelerations, not on absolute comparisons with in-flight experiences. As a result, the data of the general and Citation II pilots were combined together to formulate conclusions.

Furthermore, Fig. 13a shows that for X_{thres}^- , which has a baseline value of 0.89, the lower average parameter threshold, expressed as the 95% confidence interval on the mean, across all pilots equals $X_{thres}^- = 0.72 \pm 0.037$ (-0.1896 \pm 0.0412 Weber fraction). For ω_0 , with a baseline value equal to 75.92 rad/s, Fig. 13b shows estimated upper and lower

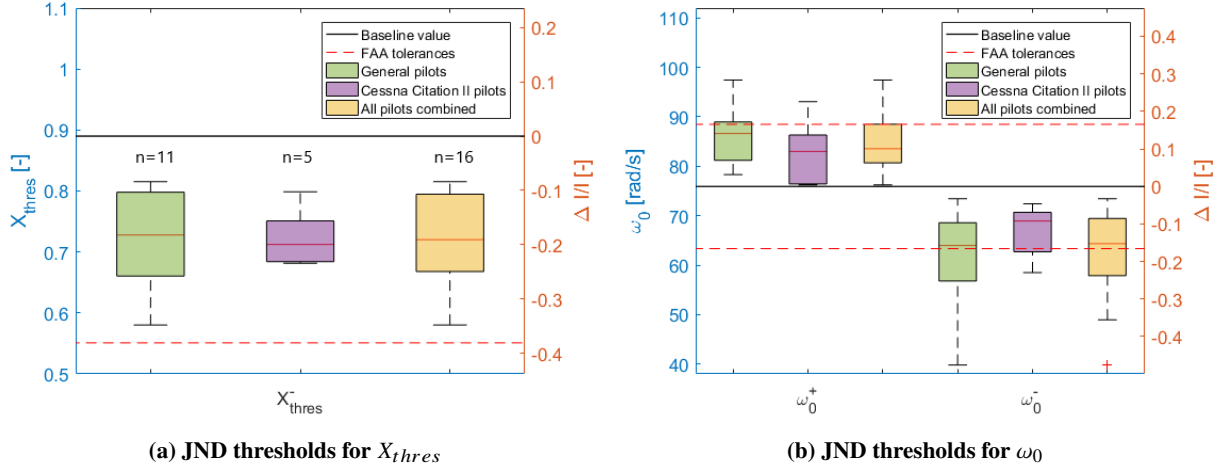


Fig. 13 Upper and Lower threshold values for X_{thres} and ω_0 estimated from the staircase experiment data.

average thresholds that are, respectively, $\omega_0^+ = 84.87 \pm 3.295$ rad/s (0.1179 ± 0.0434 Weber fraction) and $\omega_0^- = 63.04 \pm 4.813$ rad/s (-0.1696 ± 0.0634 Weber fraction). A statistical comparison test was performed between the upper and lower JND threshold data samples for ω_0 . A paired t-test was chosen because a Lilliefors test confirmed that the data sets are approximately normally distributed. The paired t-test resulted in the acceptance of the null hypotheses ($p = 0.1607 > 0.05$) that the JND threshold data for ω_0^+ and ω_0^- are statistically comparable.

The response of the stall buffet model for an offset in X_{thres} and ω_0 parameters, according to the estimated average JND thresholds that resulted from the experiment, is presented in Fig. 14 with comparison to the baseline buffet model time responses. Note that only the stalled time portion of the 90 seconds quasi-steady stall simulation of the Cessna Citation II model is shown. Outside this stalled portion, the buffet model is inactive and not modeling any stall vibrations. Fig. 14a and Fig. 14d clearly show the delay in buffet onset when the X_{thres} parameter is lowered with respect to the baseline. The tuned model starts about 6 seconds later with simulating the buffet vibrations as compared to the baseline buffet model response. Also note the more intense buffet amplitude at onset for the tuned model response. Fig. 14b and Fig. 14e show the increase in the buffet frequency ω_0 , while Fig. 14c and Fig. 14f show the decrease in buffet frequency. Note that the offset in frequency ω_0 with respect to the baseline is very small and difficult to see, only 12% and 17% offset respectively for the average upper and lower JND threshold for ω_0 . An increase in the ω_0 parameter also shows a slightly more intense amplitude of the buffet at the time instance of maximum flow separation, i.e. around 37 seconds (see Fig. 14b).

Finally, the JND threshold results were compared to the the FAA tolerances (see Section II.A) set on simulated buffet responses, see the red dashed lines in Fig. 13. For the buffet frequency ω_0 , the JND thresholds closely match with the ± 2 Hz tolerance set by the FAA. On the other hand, the average JND threshold for X_{thres}^- (0.72) is well above the tolerance ($\pm 2.0^\circ$ angle of attack) that the FAA justifies on buffet onset ($X = 0.551$), indicating that pilots already notice the differences in buffet onset during quasi-steady symmetric stall simulations well before the tolerance value is reached.

V. Discussion

This paper aimed at providing quantitative guidance on the minimum required accuracy of simulated stall buffets. For this we measured JND thresholds for two key stall buffet model parameters, the buffet shaping filter's characteristic frequency ω_0 and the flow separation threshold parameter X_{thres} that parameterizes the buffet onset point. These two parameters are most closely related to current FSTD stall buffet requirements as described by the FAA. During the experiment, participants experienced, as passive observers, consecutive quasi-steady symmetric stalls (one with baseline settings and one with the modified buffet) simulated with the TU Delft stall dynamics model of the Cessna Citation II aircraft. Through a subjective staircase procedure, JND thresholds for ω_0 and X_{thres} variations were determined.

The sensitivity analysis results of quasi-steady stall buffet simulations showed almost no differences in the buffet model responses upon increase of the X_{thres} parameter, so it was expected that an upper JND threshold would not be noticeable to human pilots. Looking at the buffet model lay-out (see Fig. 2), the shaping filter's output gets multiplied

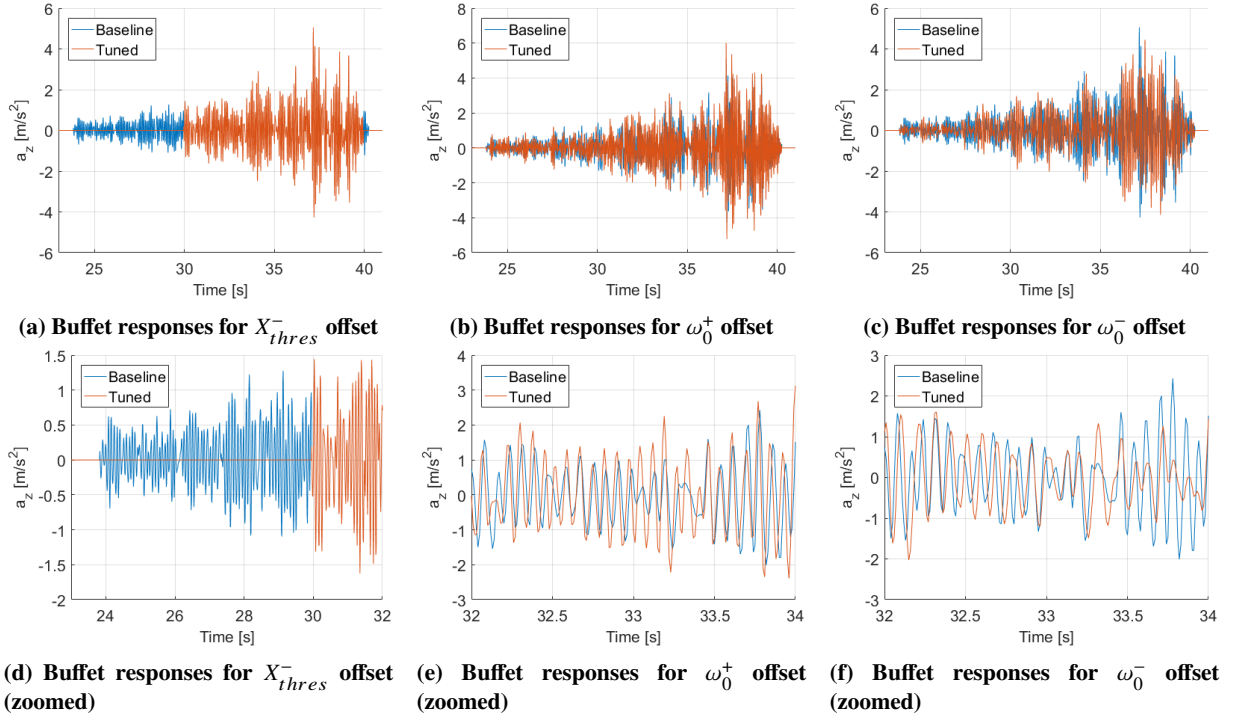


Fig. 14 Stall buffet model time responses showing results for the baseline model settings and tuned offsets in X_{thres} and ω_0 according to the estimated average JND thresholds found during the experiment. The time traces (see (a), (b) and (c)) only show the stalled portion of a 90 seconds quasi-steady symmetric stall simulation of the Cessna Citation II model. The subfigures (d), (e) and (f) present a zoomed in version on the details that are different between the baseline and tuned buffet model time responses.

with a 1- X factor. Hence, at baseline settings ($X_{thres} = 0.89$) the simulated buffet starts at about 10% of its maximum amplitude that is reached at full flow separation. Increasing the threshold value to the maximum possible value of 1 (X physically only varies between 0 and 1), would only make the buffet start with that 10% lower amplitude. Testing of the experiment confirmed the expectations that an upper threshold on X_{thres} was unnoticeable due to these small differences in amplitude at onset as compared to the baseline. As a result, the experiment only analysed three conditions, i.e., X_{thres}^- , ω_0^+ and ω_0^- .

Two hypotheses were formulated based upon the buffet model sensitivity results. First, it was expected that the JND thresholds for changes in ω_0 would be lower than those for X_{thres} (Hypothesis **H1**) because simulated buffet time responses showed much greater deviations from the baseline model response when ω_0 was varied with similar parameter offsets with respect to the baseline value. The collected experiment data reject this hypothesis, as the average JND threshold for X_{thres} was found to be much lower than expected and comparatively similar to the average upper and lower thresholds for ω_0 . All three average thresholds were between 10 and 20% offset with respect to the baseline values.

The sensitivity analysis further showed that for a similar percentage-wise increase or decrease in ω_0 up until an offset of around 20%, the VAF of the offset buffet model output compared to the baseline seemed to be symmetric. Hence, for ω_0 the upper and lower absolute JND thresholds were expected to be symmetric with respect to the baseline (Hypothesis **H2**). The experiment data showed that the upper JND threshold values were, on average, slightly closer to the baseline value than the lower threshold values for ω_0 . However, a paired t-test resulted in the upper and lower JND threshold values for ω_0 to be statistically equal, meaning that **H2** is confirmed. Although, a possible explanation for the estimated upper threshold values being slightly closer to the baseline for ω_0 could possibly be found in the installed Mode Control Panel (MCP) in the SRS. When the frequency of the simulated buffet was increased, this MCP soon started to vibrate heavily to the extent that it became visually noticeable to some of the participants (participants were wearing noise canceling headsets, so the heavy vibrations were not audible). Although a few participants indicated this aspect during debrief of the experiment, it is not considered as an artifact in the experiment data because vibrations in instruments are likely also to occur during real stall flights, which makes it difficult for pilots to read and control flight instruments during stall maneuvers. However, it might be different flight instruments suffering from vibrations during stall flights in the Cessna Citation II cockpit as compared to the more general instrument layout in the SRS. Therefore, future JND experiments could involve the use of virtual reality glasses to replicate the Cessna Citation II cockpit inside the SRS to investigate if the estimated upper JND thresholds for ω_0 remain similar or not.

Furthermore, the estimated JND thresholds were compared to current standards on stall buffet simulation qualification requirements. The thresholds for ω_0 were found to be in support of the ± 2 Hz tolerance defined on buffet characteristic peak frequency. However, the lower JND thresholds for X_{thres} showed results that are closer to the baseline value than the maximum tolerance of $\pm 2.0^\circ$ angle of attack set by the FAA on buffet onset threshold of perception. This indicates that pilots already notice the difference in buffet onset characteristics well before the X_{thres} parameter offset reaches the maximum tolerance, which suggests that the buffet onset requirements for quasi-steady stall training models may require stricter tolerances.

The current experiment attempted to measure the JND thresholds for variation in two key stall buffet model parameters by simulating quasi-steady symmetric stall dynamics of a Cessna Citation II aircraft. This is due to the current stall dynamics model only being validated for the quasi-steady symmetric flight envelope at an altitude of 5,500m (18,000ft). Current research at TU Delft focuses on the asymmetric stall dynamics as well as investigations on altitude variations to increase the validation region of the Cessna Citation II stall model. Future experiments should then focus on extending the JND measurements towards accelerated and more sudden stall maneuvers.

The used 1-up/1-down staircase procedure only allows for estimating 50% level of correctness JND thresholds. With the insight gained on the JND thresholds for key stall buffet model parameters from the current experiment, follow-up experiments should consider more accurate staircase procedures that would result in a higher level of correctness JND threshold (e.g., 70.7% for 1-up/2-down method). Finally, future work should also focus on determining the JND thresholds through an experiment where participants are actively flying the stall maneuver, as it is uncertain if the current estimated thresholds are also applicable in case pilots are in active control of the aircraft and thus occupied. While this would add valuable information for the research on required stall model fidelity for effective simulator-based stall training, it also implies a challenging experiment setup because pilots would be required to consistently fly a certain stall maneuver with varying buffet dynamics.

VI. Conclusions

This paper investigated the JND thresholds for two key stall buffet model parameters (X_{thres} and ω_0) to measure pilot sensitivity to differences in the simulated stall buffets. A buffet model sensitivity analysis and a human-in-the-loop experiment with 21 pilots in a flight simulator were used to provide improved quantitative guidance on the minimum required accuracy of simulated stall buffets. The experiment used a subjective staircase procedure where pilots experienced, as passive observers, sets of two consecutive quasi-steady symmetric stalls to compare (one of which was the baseline settings and the other one featured a modified buffet). The staircase procedure resulted in an upper and a lower JND threshold for ω_0 . For X_{thres} only a lower threshold was estimated because an increase in X_{thres} parameter (0.89 to 1.0) was found to hardly affect buffet model outputs and thus be unnoticeable to human pilots. The current findings indicate that the estimated JND thresholds for all three conditions closely match each other (average thresholds between 10-20% offset), with the highest individual JND thresholds not exceeding 30-35% offset with respect to the baseline value. This indicates that human pilots notice the differences in individual stall buffet model parameters already at comparatively small offsets. Furthermore, the upper and lower JND thresholds for ω_0 are found to support the ± 2 Hz tolerances that the FAA defines for the characteristic simulated buffet frequencies. However, all lower thresholds found for X_{thres} were found to be well above the tolerance of $\pm 2.0^\circ$ angle of attack set by the FAA on buffet onset threshold of perception. This indicates that human pilots already noticed the differences in buffet onset with respect to the baseline well before the parameter offset reached the maximum tolerance, which suggests that the buffet onset requirements for quasi-steady symmetric stall models may require stricter limits to support effective simulator-based stall training.

References

- [1] Boeing, “Statistical Summary of Commercial Jet Airplane Accidents, Worldwide Operations | 1959 – 2020,” , 2021.
- [2] Lambregts, A. A., Nesemeier, G., Wilborn, J. E., and Newman, R. L., “Airplane Upsets: Old Problem, New Issues,” *Proceedings of the AIAA Modeling and Simulation Technologies Conference and Exhibit, Honolulu (HI)*, 2008. <https://doi.org/10.2514/6.2008-6867>.
- [3] Crider, D. A., “Accident Lessons for Stall Upset Recovery Training,” *Proceedings of the AIAA Guidance, Navigation, and Control Conference, Toronto, Canada*, 2010. <https://doi.org/10.2514/6.2010-8003>.
- [4] J. V. Foster and K. Cunningham and C. M. Fremaux and G. H. Shah and E. C. Stewart and R. A. Rivers and J. E. Wilborn and W. Gato, “Dynamics Modeling and Simulation of Large Transport Airplanes in Upset Conditions,” *AIAA Guidance, Navigation, and Control Conference and Exhibit*, American Institute of Aeronautics and Astronautics (AIAA), San Francisco, CA, USA, 2005. <https://doi.org/10.2514/6.2005-5933>.
- [5] Advani, S. K., Schroeder, J. A., and Burks, B., “What Really Can Be Done in Simulation to Improve Upset Training?” *Proceedings of the AIAA Modeling and Simulation Technologies Conference, 2-5 August 2010, Toronto, Canada*, 2010. <https://doi.org/10.2514/6.2010-7791>.
- [6] Advani, S. K., and Field, J., “Upset Prevention and Recovery Training in Flight Simulators,” *Proceedings of the AIAA Modeling and Simulation Technologies Conference, Portland (OR)*, 2011. <https://doi.org/10.2514/6.2011-6698>.
- [7] Federal Aviation Administration, “Code of Federal Regulations, Title 14, Part 60: Flight Simulation Training Device Initial and Continuing Qualification and Use,” , 2016.
- [8] Anonymous, “Stall and Stick Pusher Training,” Advisory Circular 120-109, U.S. Department of Transportation, Federal Aviation Administration, Aug. 2012.
- [9] Advani, S. K., and Schroeder, J. A., “Global Implementation of Upset Prevention & Recovery Training,” *Proceedings of the AIAA Modeling and Simulation Technologies Conference, San Diego (CA)*, 2016. <https://doi.org/10.2514/6.2016-1430>.
- [10] Lemley, C. and Mullans, R., *Buffeting pressures on a swept wing in transonic flight - Comparison of model and full scale measurements*, Structures, Structural Dynamics, and Materials and Co-located Conferences, American Institute of Aeronautics and Astronautics (AIAA), 1973. <https://doi.org/10.2514/6.1973-311>.
- [11] Caruana, D., Mignosi, A., Corrège, M., Le Pourhiet, A. & Rodde, A. M., “Buffet and buffeting control in transonic flow,” *Aerospace Science and Technology*, Vol. 9, No. 7, 2005, pp. 605–616. <https://doi.org/10.1016/j.ast.2004.12.005>.
- [12] Marschalk, S., Luteijn, P. C., van Os, D., Pool, D. M., and de Visser, C. C., “Stall Buffet Modeling using Swept Wing Flight Test Data,” *AIAA Scitech 2021 Forum*, American Institute of Aeronautics and Astronautics Inc, AIAA, 2021. <https://doi.org/10.2514/6.2021-0286>.

- [13] J. A. Schroeder and J. Bürki-Cohen and D. A. Shikany and D. R. Gingras and P. Desrochers, "An Evaluation of Several Stall Models for Commercial Transport Training," *AIAA Modeling and Simulation Technologies Conference*, American Institute of Aeronautics and Astronautics (AIAA), National Harbor, MD, USA, 2014. <https://doi.org/10.2514/6.2014-1002>.
- [14] Van Horssen, L. J., de Visser, C. C., and Pool, D. M., "Aerodynamic Stall and Buffet Modeling for the Cessna Citation II Based on Flight Test Data," *Proceedings of the AIAA Modeling and Simulation Technologies Conference, Kissimmee (FL)*, 2018. <https://doi.org/10.2514/6.2018-1167>.
- [15] van Ingen, J. B., de Visser, C. C., and Pool, D. M., "Stall Model Identification of a Cessna Citation II from Flight Test Data Using Orthogonal Model Structure Selection," *Proceedings of the AIAA Modeling and Simulation Technologies Conference, Nashville (TN)*, 2021. <https://doi.org/10.2514/6.2021-1725>.
- [16] Smets, S. C., de Visser, C. C., and Pool, D. M., "Subjective Noticeability of Variations in Quasi-Steady Aerodynamic Stall Dynamics," *Proceedings of the AIAA Modeling and Simulation Technologies conference, San Diego (CA)*, 2019. <https://doi.org/10.2514/6.2019-1485>.
- [17] Schroeder, J. A., "Research and Technology in Support of Upset Prevention and Recovery Training," *Proceedings of the AIAA Modeling and Simulation Technologies Conference 2012, Minneapolis (MN)*, 2012. <https://doi.org/10.2514/6.2012-4567>.
- [18] Federal Aviation Administration, "Advisory Circular - Subject: Upset Prevention and Recovery Training (AC 120-111)," Tech. rep., 2017.
- [19] van den Hoek, M. A., de Visser, C. C., and Pool, D. M., "Identification of a Cessna Citation II Model Based on Flight Test Data," *Proceedings of the 4th CEAS Specialist Conference on Guidance, Navigation & Control, Warsaw, Poland*, 2017.
- [20] Goman, M., and Khrabrov, A., "State-Space Representation of Aerodynamic Characteristics of an Aircraft at High Angles of Attack," *Proceedings of the AIAA Astrodynamics Conference, Hilton Head (SC)*, 1992. <https://doi.org/10.2514/6.1992-4651>.
- [21] Fischenberg, D., and Jategaonkar, R. V., "Identification of Aircraft Stall Behavior from Flight Test Data," *Proceedings of the RTO SCI Symposium on System Identification for Integrated Aircraft Development and Flight Testing, Madrid, Spain*, 1998, pp. 17-1-17-8.
- [22] Dias, J. N., "Unsteady and Post-Stall Model Identification Using Dynamic Stall Maneuvers," *Proceedings of the AIAA Atmospheric Flight Mechanics Conference, Dallas (TX)*, 2015. <https://doi.org/10.2514/6.2015-2705>.
- [23] Stroosma, O., van Paassen, M. M., and Mulder, M., "Using the SIMONA Research Simulator for Human-machine Interaction Research," *AIAA Modeling and Simulation Technologies Conference and Exhibit*, American Institute of Aeronautics and Astronautics (AIAA), 2003. <https://doi.org/10.2514/6.2003-5525>.
- [24] Berkouwer, W. R., Stroosma, O., van Paassen, M. M., Mulder, M., and Mulder, J. A., "Measuring the Performance of the SIMONA Research Simulator's Motion System," *AIAA Modeling and Simulation Technologies Conference and Exhibit*, American Institute of Aeronautics and Astronautics, San Francisco, California, 2005. <https://doi.org/10.2514/6.2005-6504>.
- [25] Reid, L. D., and Nahon, M. A., "Flight Simulation Motion-Base Drive Algorithms: Part 1 - Developing and Testing The Equations," Tech. rep., University of Toronto, Institute for Aerospace Studies, 1985. UTIAS 296.
- [26] Gouverneur, B., van Paassen, M. M., Mulder, J. A., Stroosma, O., and Field, E. J., "Optimisation of the SIMONA Research Simulator's Motion Filter Settings for Handling Qualities Experiments," *Proceedings of the AIAA Modeling and Simulation Technologies Conference and Exhibit*, AIAA, Austin, Texas, 2003. <https://doi.org/10.2514/6.2003-5679>.
- [27] Sinacori, J. B., "The determination of some requirements for a helicopter flight research simulation facility," Tech. rep., NASA, 1977. NASA CR 152066.
- [28] Schroeder, J. A., "Helicopter Flight Simulation Motion Platform Requirements," Tech. rep., NASA, 1999. NASA/TP-1999-208766.
- [29] Kingdom, F., and Prins, N., *Psychophysics: A Practical Introduction*, Academic Press, 2016.
- [30] Jerald, J. J., "Scene-Motion-and Latency-Perception Thresholds for Head-Mounted Displays," Ph.D. thesis, University of North Carolina, Chapel Hill, 2010.
- [31] Beckers, N. W. M., Pool, D. M., Valente Pais, A. R., van Paassen, M. M., and Mulder, M., "Perception and Behavioral Phase Coherence Zones in Passive and Active Control Tasks in Yaw," *Proceedings of the AIAA Modeling and Simulation Technologies Conference 2012, Minneapolis (MN)*, 2012. <https://doi.org/10.2514/6.2012-4794>.



Preliminary Thesis Report

Already graded for AE4020

Introduction

Aerodynamic stall is an intense dynamic, nonlinear and unsteady condition that may lead to unrecoverable airplane upset conditions if not corrected in time. Stalls are an important contributor to fatal accidents in civil aviation and are the primary cause of fatal accidents in general aviation [1–3]. Until recently, training simulators were not required to provide high-accuracy stall simulation [4–6]. However, this has changed with the mandatory requirement for all airline crew to receive flight simulator-based stall prevention and recovery training that is effective since 2019 [7–9]. As a result, there is a strong need for accurate and cost-effective stall and post-stall dynamic models for use in flight simulators.

A key characteristic of a stall is the buffet, as buffeting is an initial cue for pilots which indicates entering of the unsafe part of the flight envelope. The stall buffet, which occurs at high angles of attack, is the aerodynamic excitation due to flow separation causing pressure fluctuations over the wing [10–12]. A common deficiency that remains in current Flight Simulating Training Devices (FSTDs) is the insufficient haptic and physical vibratory feedback of buffeting felt by pilots in simulated stalled conditions [6, 13]. While this can partly be attributed to practical considerations, as limiting buffeting vibrations positively benefits the required FSTD maintenance and downtime, a major second reason is that it is, in fact, unknown what level of stall buffet accuracy or fidelity is actually required for realistic stall simulations and effective simulator-based stall training. Available regulatory standards for stall buffet simulation [7] reflect this persisting uncertainty with quite lenient tolerances on buffet responses in flight simulators, e.g., “*The flight simulator results should exhibit the overall appearance and trends of the aeroplane plots, with at least some of the frequency ‘spikes’ being present within 1 or 2 Hz of the aeroplane data*” [7].

Therefore, the goal of this thesis research is to provide additional quantitative guidance on the required accuracy for replicating stall buffets in flight simulators. This research will involve a human-in-the-loop experiment in the SIMONA Research Simulator (SRS) at the TU Delft to measure Just Noticeable Difference (JND) thresholds for key parameters that characterise the frequency content and temporal amplitude variations of stall buffet vibrations. The experiment will utilise a Cessna Citation II stall model identified in our earlier research [14–16]. For measuring the JNDs, use will be made of the same experimental paradigm as described in [17], where participating pilots (aim: 10-20 pilots) will experience simulated symmetrical quasi-steady stall manoeuvres at an altitude of 5,500 m (18,000 ft), induced with a 1 kts/s deceleration into the stall, as an observer. Through a subjective staircase procedure, consisting of repeated pairwise comparisons of the stall with our baseline buffet model and a stall with adjustments to the buffet model parameters, the JNDs for these parameter variations will be determined. Furthermore, the measured JNDs will be objectively compared to tolerances on stall buffet characteristics from current regulatory standards [7, 18].

Research Objective

The main research objective of this thesis is to:

“Determine the required accuracy with which stall buffet models, used for replicating stall buffet vibrations in flight simulator training devices, have to be identified by measuring the

pilot's sensitivity to changes in the stall buffet model dynamics during a human-in-the-loop simulator experiment where pilots are observers.”

This main research objective can be split into sub-goals needed to achieve the main objective. These sub-goals will form the work packages of the research project and can be used to structure the research. The different sub-goals are the following:

- Look into different buffet modelling methodologies developed at the TU Delft and decide which one will be implemented into the stall model for further research.
- Perform a sensitivity analysis of the buffet model output with respect to variations in the buffet model parameters to identify the key buffet model parameters.
- Define the experimental set-up and method used to measure the JND thresholds of pilots for key buffet model parameters.
- Integrate the DASMAT Simulink stall and buffet model into Delft University Environment for Communication and Activation (DUECA) such that it can run on the SIMONA simulator and implement a user interface for the JND measuring method.
- Perform the human-in-the-loop simulator experiment.
- Analyse the experiment results and answer the research questions.
- Compare resulting JND thresholds to regulatory standards for simulator qualification.

Research Question

The main research question of this thesis is stated as follows:

How far can the key stall buffet model parameters deviate from their baseline value before the difference in buffet dynamics becomes noticeable to a human pilot in a flight simulating training device?

The main research question can be split into smaller sub-questions:

- *How sensitive is the stall buffet model output to variations in the individual buffet model parameters?*
- *Is there a difference in magnitude of the absolute JND thresholds of individual buffet model parameters?*
- *Are the JND thresholds of the key buffet model parameters symmetrically distributed around the baseline values or not?*
- *Do the JND thresholds of key buffet model parameters compare to the regulatory standards for simulator qualification or not?*

Answering the research questions will ensure that the research objective is completed.

Methodology & Report Structure

To answer the main research question and complete the research objective for this thesis, different steps will be required in a chronological order that also structure the project outline:

Step 1 Literature Study: The first step of the thesis is to get familiar with the research topic by performing a literature study. It is an important step to prepare methods that can be useful to find answers to the research questions. The literature review can be found in chapter 2.

Step 2 Sensitivity Analysis: With the stall and buffet model implemented into Matlab/Simulink a preliminary sensitivity analysis was executed. Chapter 3 shows the impact of varying the buffet model

parameters on the simulated buffet vibrations. From this analysis, the key model parameters are identified for further research.

Step 3 Define Experimental Set-up: Now that the key buffet model parameters are identified, the next step is to define a method to determine the JND thresholds for those important model parameters. The experiment procedures are elaborated in chapter 4.

All the next steps are not covered in this preliminary thesis report, but will be discussed in detail in the paper that will be published for this thesis research.

Step 4 SIMONA Software Integration: The software integration in the SRS is a big step. Here the stall and buffet model of the Cessna Citation II are implemented to run on the simulator. The entire experiment procedures to measure JND thresholds for the key model parameters will be automated in the software with a simple user interface for the researcher to perform the experiments.

Step 5 Human-in-the-loop Experiment: The experiment step is the one where data is gathered about the JND thresholds for key parameters. At this step, external persons will be involved in the research as participants in the experiments.

Step 6 Result Processing: After the experiments in the simulator are finished, the results will be analysed and discussed in the conference paper. Answers will be given to the different research questions. Possible confounds in the experiment might raise recommendations that will also be shown in the final paper.

Literature Review and Stall Buffet Simulation Model Requirements

2.1. Aircraft Stall Theory

This section elaborates on the theory behind aircraft stall behaviour. It explains the theory of stall and the structural vibrations (known as stall buffet) that can be experienced during a stall.

2.1.1. Aerodynamic Stall

Aerodynamic stall is the phenomenon where airflow separates from the wings of the aircraft. This can occur at high angles of attack or at high Mach numbers. The consequences of a stalled condition are two sudden and precipitous effects, namely a decrease in the lift and an increase in (pressure) drag [19]. At low Mach numbers (subsonic flow regime), flow separation occurs when the aircraft exceeds its critical angle of attack (α_{crit}), which is also referred to as the stall angle of attack. Figure 2.1 shows a typical sketch of the lift coefficient of an airfoil. First, C_l increases linearly with increasing angle of attack (α) until a certain point (α_{crit}) where the relation becomes non-linear and a sudden drop in C_l is visible as a result of the flow separation. At high Mach numbers (transonic/supersonic flow regimes), flow separation occurs due to the presence of shock waves that result in high pressure gradients. This type of stall and flow separation behaviour is omitted from this research since the focus is on stall and buffet modelling of commercial transport aircraft. Those aircraft generally travel at speeds lower than Mach 1 (excluding The Concorde, which used to be one of only two supersonic aircraft flying commercially) [20].

In the subsonic airspeed region, flow separation may be categorised into three different types based on the airfoil thickness, camber and nose radius [21]:

1. **Trailing edge stall:** Trailing edge stall is characterised by flow separation starting at the trailing edge and gradually moves forward with increasing angle of attack. This type of flow separation is typical for thick airfoils with a large nose radius.
2. **Leading edge stall:** A leading edge stall is an abrupt stall starting at the leading edge and causes immediate flow separation over the entire wing. This type of stall is most common with moderate leading edge radius.
3. **Thin airfoil stall:** With a thin airfoil stall, first a long separation bubble develops over the airfoil with increasing angle of attack and then finally the flow separates over the entire airfoil.

Aircraft stall can be directly linked to the critical angle of attack of an aircraft and the speed at which this happens is the stall speed. At the stall speed, the aircraft is just able to maintain level flight. Continuing to maintain altitude at lower speeds will automatically result in a stall. Stalling speeds are not constant and are dependent on the aircraft's configuration and the flight conditions [19, 21]. For example, an aircraft is usually equipped with high-lift devices to temporarily change the geometry of the wing in order to lower the stall speed for landing purposes. Wing planform parameters such as

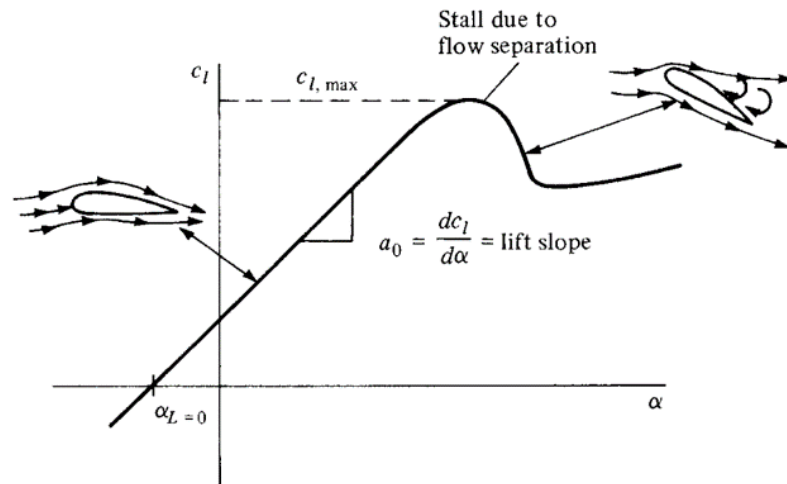


Figure 2.1: Typical sketch of a lift coefficient curve. The linear increase in lift with the angle of attack is shown as well as the non-linear stall where flow separates from the wing. Adopted from [21]

sweep angle also affect the aerodynamic stall properties of an aircraft. Sweep angles increase the lift coefficient over the outboard wing sections, which leads to stall at the wing tips first. As a result, roll control is lost and pitch-up tendencies further intensify the stalled condition [22]. Therefore, swept wing aircraft use, for example, taper ratios to move the lift inboard again or stall prevention systems like a stick pusher that forces the aircraft nose down in case it is getting dangerously close to a stalled condition [23].

Flight conditions can have a negative effect on the stall speed. During turning, bank angles result in lower lifting capabilities of the wing, hence a higher stall speed [19]. Turning stalls are also referred to as accelerated stalls. An angle of sideslip due to the flow field around the aircraft result in different stall properties for the left and right wing of an aircraft which can lead to dangerous spin situations in case one wing stalls before the other [24]. Although aircraft geometry and flight conditions are important aspects that greatly influence the stall behaviour of an aircraft during critical phases in flight, the main focus during this research is on quasi-steady symmetric stall flights with a clean wing configuration. This is due to the limiting flight envelope of the currently developed Cessna Citation II stall dynamic model of the TU Delft [14–16].

Weather can have a significant influence on the stall properties as well. External environment factors often play a role in the cause of Loss Of Control In-flight (LOC-I) accidents. NASA statistical analysis has shown that aircraft icing is a very common LOC-I causal factor. The different ways on how aircraft icing can lead up to LOC-I accidents are the following [25]:

- **Ice build-up causes aircraft performance to degrade.** Ice that contaminates the wings lead to increased drag, which slows the aircraft down and gets it closer to the stall speed. Additionally, a higher weight of the aircraft also results in an increase in stall speed and a reduction of the stall angle of attack, two dangerous factors that can result in unintentional stall upset.
- **Degraded take-off performance due to snow and ice build-up on the ground.** Snow and ice can accumulate quickly on the ground, preventing the aircraft from achieving sufficient flight speeds during take-off.
- **Ice accretion can cause flight control difficulties.** Degraded aerodynamics over the flight control surfaces lead to a lower control effectiveness.
- **LOC-I accident resulting from propulsion system failure.** Ice ingestion into the engine or carburetor ice can cause power losses and asymmetric thrust situations that can result in LOC-I.
- **Pitot or static pressure ports can get blocked by ice.** This can cause complete airdata system failure or false indication of airspeed and altitude. This can lead to pilot disorientation and LOC-I accidents.

Not only ice is dangerous, volcanic ashes can contaminate the wings of an aircraft as well. Both ice and volcanic ashes affect the flow field around the wings [26, 27]. This greatly influences the aerodynamics of the flow as well as the stall speed which can result in sudden and unexpected flow separation leading to aerodynamic stall. Although modelling the aerodynamics in case of ice or other environmental conditions is an interesting and challenging topic, it is outside the scope of this research topic.

The highly dynamic, non-stationary, unsteady, configuration-dependant and unpredictable nature of aerodynamic stall dynamics [28] make predicting and modelling of stall behaviour a very challenging task. Ralston et al. [29] recommends that the following stall specific properties should be implemented into simulator aerodynamic flight models in order to positively train pilots in stall prevention and recovery procedures using FSTDs:

- Degradation in lateral directional stability and control response
- Uncommanded roll off tendencies
- Pitch stability changes
- Stall hysteresis
- Mach number effects
- Stall buffet vibrations

2.1.2. Stall Buffet

A key characteristic feature of a stall is the buffet. The stall buffet, which occurs at high angles of attack or high Mach numbers, is the aerodynamic excitation of the aircraft's structure due to flow separation causing pressure fluctuations over the wing [10–12].

Airplane buffeting characteristics are important to aircraft designers and are already estimated early in the design process, as buffeting eventually limits the aircraft's flight envelope. Buffet onset and maximum buffeting characteristics determine aircraft structural limitations and induce structural fatigue. Therefore, the buffet characteristics and onset envelope are an important aspect during the structural design phase of an aircraft [30]. A typical graphical representation of the buffet onset envelope is shown in fig. 2.2. It is also referred to as the buffet onset boundary chart and visualises the onset point of the buffet as function of the Mach number and lift coefficient. Three different flight regime regions can be seen where the buffet is the result of either shock induced flow separation, leading edge flow separation or a mix of both [31].

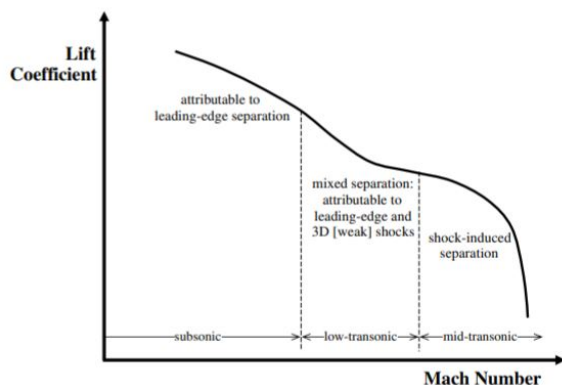


Figure 2.2: Typical buffet onset curve and flow separation mechanism at different flight regimes, adopted from [31]

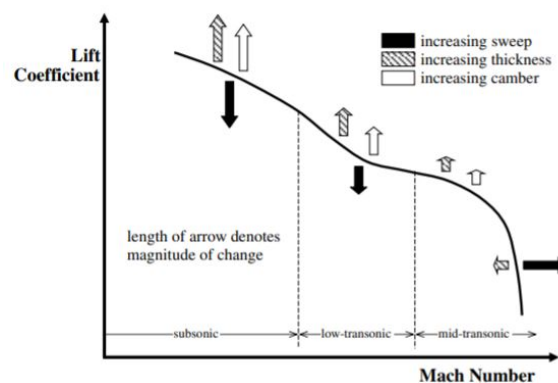


Figure 2.3: Effect of changing wing geometry on the buffet onset curve, adopted from [31]

Buffet characteristics can vary significantly between aircraft models based on differences in wing geometry, configuration and structural stiffness. As an example, the effect of changing sweep angle, thickness/chord ratio and camber of the wing's planform on the buffet onset curve can be seen in fig. 2.3. Mabey investigated thoroughly the effects of aircraft geometry on the buffeting characteristics

by performing several buffeting tests on a series of wings with varying sweep, camber, thickness/chord ratio, position of maximum thickness and aspect ratio. His conclusions resulted in the effects on the buffet onset curve when varying those parameters [32, 33]. Buffet onset point is not the only varying buffet characteristic with aircraft configuration. The buffet frequency and intensity also vary with aircraft wing geometry/configuration and airfoil design [34].

Besides limiting of the aircraft's flight envelope, buffeting also proves to be useful for pilots. It is an initial cue which indicates entering of the unsafe part of the flight envelope and can be very intense and deterrent for those who are unfamiliar with the concept [35]. Buffeting serves as a warning to pilots that a stall is pending and corrective action is required. For some aircraft types, stall warning systems are a combination of audible systems, pre-stall buffet, stick shaker/pusher (deep stall risk) and/or angle of attack sensors. However, in many aircraft, like the LOCKHEED C-130 and Cessna Citation II for example, the buffet provides the sole warning of the impending stall [36]. Therefore, buffeting is an important aspect of a stall that should be accurately represented in the stall dynamic models used for training purposes in simulators [37].

2.2. FAA Regulations for Stall and Buffet Models in FSTDs

Focusing on the statistics of commercial aviation accidents of the past decade (see fig. 2.4), it can be seen that LOC-I is the most common cause of fatalities in civil aviation. Hence, reducing the LOC-I related accidents is one of the global safety priorities defined by the International Civil Aviation Organization (ICAO) in their 2020 safety report [38]. LOC-I is usually a consequence of an aircraft entering an unsafe part of the flight envelope resulting from airplane upset conditions. Airplane upsets are defined as one of the following situations [8]:

- A pitch attitude larger than 25° nose up
- A pitch attitude of more than 10° nose down
- A bank angle of more than 45°
- Flying within the above mentioned limits, but at inappropriate airspeeds

The most common type of airplane upset is aerodynamic stall and airplane buffeting (see fig. 2.5). Recovery from an upset or stall is possible, given the pilots have the correct skills and knowledge to identify upsets or stalls and apply the correct recovery procedures. Failure to identify/prevent upsets and improper recovery strategies generally lead to fatal outcomes [2]. As a result to familiarise pilots with such unusual flight situations, the Federal Aviation Administration (FAA) has the binding requirement for flight simulator-based stall recovery training for all airline flight crew that is effective since 2019 [8, 9]. This means that each airline pilot will be obliged to follow Upset Prevention and Recovery Training (UPRT). Pilots will train in awareness, prevention and recovery of airplane upsets and stalls in particular.

Like most pilot training, stall training and UPRT will most likely take place in FSTDs due to cost and safety benefits. While training simulators were until recently not required to provide high-accuracy stall simulation [4–6], this has changed with the new regulations being effective since 2019 [8, 9, 18]. The FAA FSTD qualification requirements have been updated to include the following stall related requirements:

- The dynamic model used for training purposes in the flight simulator should be valid for flights with an angle of attack range until at least 10° above the critical angle of attack (stall angle of attack) [7, p. 229].
- Qualification of the FSTD is based on three types of stall manoeuvres. 1) wings-level (1g) stall entry, 2) stall entry during turning flight with a bank angle larger than 25 degrees (accelerated stall), and 3) a stall entry with power-on conditions (this requirement is only valid for propeller driven aircraft) [7, p. 59, 95].
- The evaluation for each of the three stall manoeuvres needs to be performed in at least one of the following flight conditions: 1) high-altitude cruise, close to the performance limit of the aircraft with clean conditions, 2) approach/landing configurations, with corresponding flap setting and

extended landing gear, and 3) second-stage climb, with another flap setting and landing gear configuration than the one used in condition 2 [7, p. 59, 95].

- For simulator qualification, the simulated time histories of aircraft states are subjected to numerical tolerances compared to flight data. These tolerances are valid up to but not beyond the stall angle of attack [7, p. 95].
- Beyond the stall angle of attack, simulated time histories must follow flight data in terms of magnitude and trend through the recovery phase [7, p. 95].
- FSTDs will undergo a subjectively rated validation process by a Subject Matter Expert (SME) . SMEs are legitimised by the FAA and are required to have sufficient experience in stalling the aircraft type of which the flight simulator has to be validated [7, p. 59]. Since human beings will be involved in the validation process of FSTDs, there is an interest in knowing how sensitive humans are to variations in the individual stall model parameters, as it can be linked to the required accuracy for stall model parameters.
- Specific requirements are defined for the stall buffet model, which will be discussed in more detail below.

Fatalities by CICTT Aviation Occurrence Categories

Fatal Accidents | Worldwide Commercial Jet Fleet | 2010 through 2019

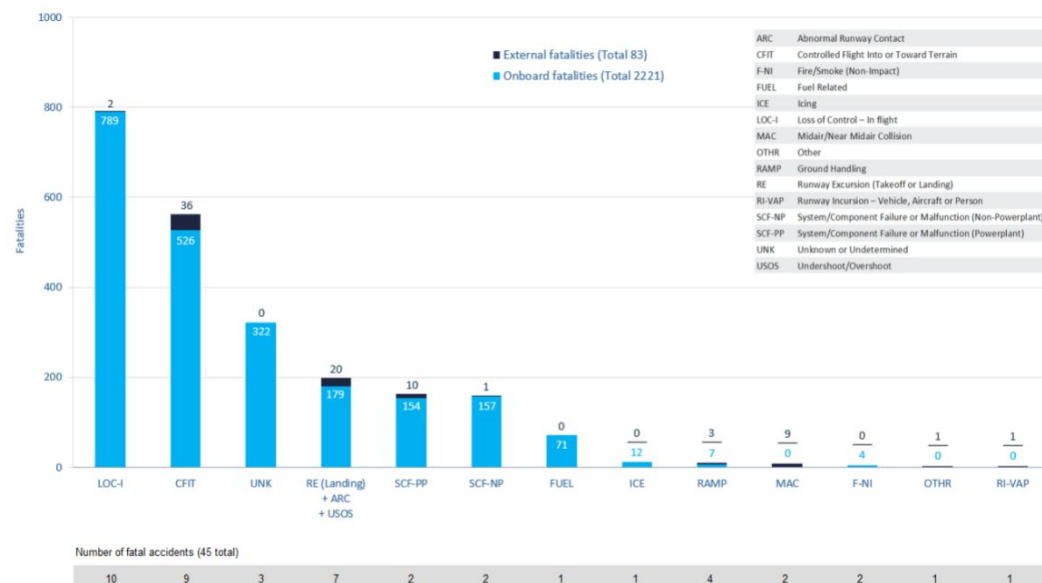


Figure 2.4: Fatalities per occurrence category from commercial aviation accident statistics from 2010 to 2019, adopted from [39]

A common remaining deficiency in current FSTDs is the insufficient haptic and physical vibratory feedback of buffeting felt by pilots in simulated stalled conditions [6, 13]. While this can partly be attributed to practical considerations, as limiting buffeting vibrations as part of a simulator's motion filtering/cueing positively benefits the required FSTD maintenance and downtime, a major second reason is that it is, in fact, unknown what level of stall buffet accuracy or fidelity is actually required for realistic stall simulations and effective stall training. Available regulatory standards, the FAA for example, reflect this persisting uncertainty with quite lenient tolerances and requirements on simulated buffet responses:

- Buffet threshold of perception should be based on 0.03g peak to peak normal acceleration above the background noise with a tolerance of 2.0° angle of attack [7, p. 95].
- Correct trend of growth of buffet amplitude from initial buffet to stall speed for normal and lateral acceleration will have to be demonstrated [7, p. 95].

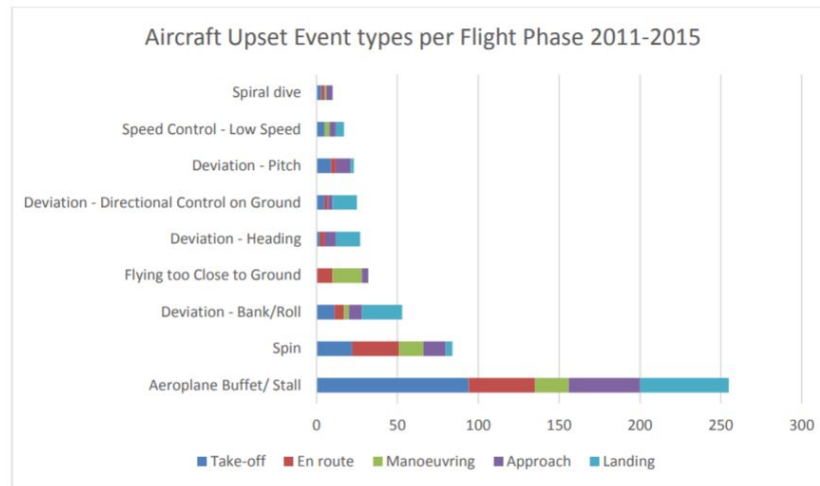


Figure 2.5: Fatal general aviation accident statistics from 2011-2015 per aircraft upset event type and per flight phase, adopted from [40]

- FSTD manufacturers may limit maximum buffeting based on motion platform capability/limitations or other simulator system limitations [7, p. 95].
- The overall trend of the Power Spectral Density (PSD) plot should be considered while focusing on the dominant frequencies [7, p. 131].
- The appearance and trend of the buffet's power spectra should match flight data with at least three of the predominant frequency spikes being within ± 2 Hz of the flight data frequency spikes [7, p. 105].
- Conduct an approach-to-stall with engines at idle and a deceleration of 1 knot/second. Check that the motion cues of the simulated buffet, including the level of buffet increase with decreasing speed, are representative of the actual airplane [7, p. 182/183].
- Tolerances on stall buffet are not applicable in case the first indication of the stall is the activation of the stall warning system (i.e. stick shaker/pusher, stall horn, ...) [7, p. 96].

2.3. Simulator Fidelity

As mentioned earlier, pilot training most likely takes place in ground-based FSTDs, because flight simulation is a flexible, safe, efficient and less costly alternative than compared to real flight. To provide positive transfer of training to pilots in a simulator, a realistic in-flight environment and experience needs to be replicated in the simulator. However, a one-to-one replication of the physical motion cues that are experienced during real flight in ground-based simulators is not feasible, because of technological, practical and financial limitations [41, 42]. Therefore, simulator fidelity is typically referred to as the extent to which a simulator is capable of replicating the corresponding in-flight environment and experience [43]. Achieving a high level of fidelity can be straightforward for some simulator subsystems. This is, for example, the case for replicating the aircraft cockpit environment. Replicas of real aircraft components and flight instruments can simply be installed in that case. Other subsystems like the out-of-the-window view and, most importantly, the motion system used to generate the aircraft motion cues in the simulator are not as straightforward to achieve high fidelity [43]. The simulator motion cueing fidelity, for example, is visualised in fig. 2.6 in terms of model fidelity and motion system fidelity.

The model fidelity in a simulator is related to the accuracy of the mathematical model used to simulate the aircraft responses for certain manoeuvres. Typically, this accuracy is high when simulating aircraft motion well within the flight envelope. However, some concern exists about the fidelity of current aircraft models used in flight simulation when simulating aircraft motion in extreme attitudes and during upset recovery [5, 6]. With the binding requirement for flight-simulator based stall and upset recovery training that is effective since 2019 [7, 8], there is a strong need for updated and more accurate mathematical models that simulate the aircraft responses during stall manoeuvres. An important

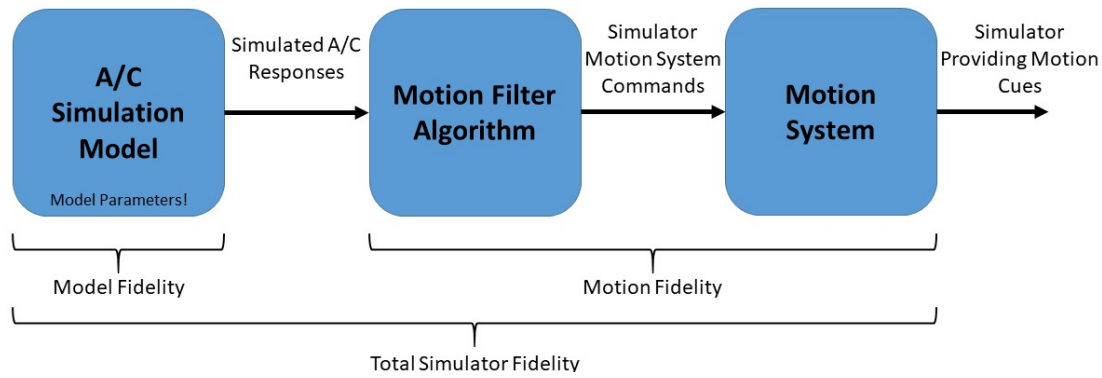


Figure 2.6: Overview of the total simulator motion cueing fidelity (in terms of aircraft simulation model and simulator motion system fidelity) that defines the level of realism of the physical motion cues provided to the pilot during flight simulation

note here is the level of stall buffet fidelity required for realistic stall simulations and positive transfer of training. Therefore, this research will focus on quantifying the required accuracy of stall buffet models from a pilot sensitivity point of view. A human-in-the-loop simulator experiment will be used to measure the JND thresholds on key buffet model parameters.

The second part that influences the quality of the generated motion cues in FSTDs is the motion system fidelity, a combination of system hardware dependencies and motion filter algorithms. System characteristics such as latency, bandwidth and smoothness of the actuator dynamics greatly influence motion cueing fidelity [44]. In addition to these effects of motion system hardware, there is also the filtering aspect. Motion filter algorithms are applied to the true aircraft translational and rotational motion to transform it into simulator motion that can be cued within the limited available motion space. A frequently applied filtering algorithm is the classical washout algorithm. It applies a combination of frequency-independent scaling and high-pass frequency filtering to the simulated aircraft responses [45]. Such an algorithm reduces the absolute magnitude and filters out low-frequency components that typically result in large displacements of the simulator motion platform and have the risk of hitting the limits of the simulator [42].

The impact of the motion filter algorithm on stall buffet simulations is usually limited to the scaling gains. Since buffet dynamics are high-frequency vibrations, they usually have no issue passing through the high-pass filters and are in fact well present in the simulator motion. However, the magnitude of the simulated buffet is impacted by the scaling gains. Simulator manufacturers like those gains low, as limiting buffeting vibrations positively benefits the required FSTD maintenance and downtime. Although, from a fidelity point of view, the scaling gains should be as close to one as possible, in combination with a low (close to zero) break-frequency for the high-pass filter. Nevertheless, this optimal combination of filter gain and break-frequency is infeasible due to the physically limited motion space of the simulator [42]. Therefore, an optimisation of the filter parameters is required to yield an acceptable fidelity level and staying within the physical limitations of the simulator. Such a tuning approach has been proposed by Schroeder [46], based upon the Sinacori fidelity criteria [47]. The developed method tunes the motion filter parameters and analyses the fidelity of the filter in terms of the gain and phase shift of the high-pass filter at 1 rad/s, see fig. 2.7.

In fig. 2.7, each dot represents a possible combination of gain and break-frequency for the high-pass filter. The three different characteristic aircraft simulation runs each create a boundary between the infeasible filter designs, i.e. reaching the physical limitations of the simulator actuators, and the possible ones. The dots below and to the right of the boundary are infeasible filter designs. The figure also shows the regions of low, medium and high fidelity in terms of the different filter designs. Thus, in order to achieve the best possible level of fidelity, a set of filter parameters should be selected as close as possible to the boundary (on the left-hand side).

A similar analysis, as depicted in fig. 2.7, will be executed prior to the simulator experiment of this research to determine the optimal motion filter parameters, while taking the different experiment conditions into account. This will yield the highest possible motion filter algorithm fidelity for performing the experiment. The research will then focus on investigating the required level of accuracy of the stall buffet simulation model. The combination of an accurate stall and buffet simulation model with a high

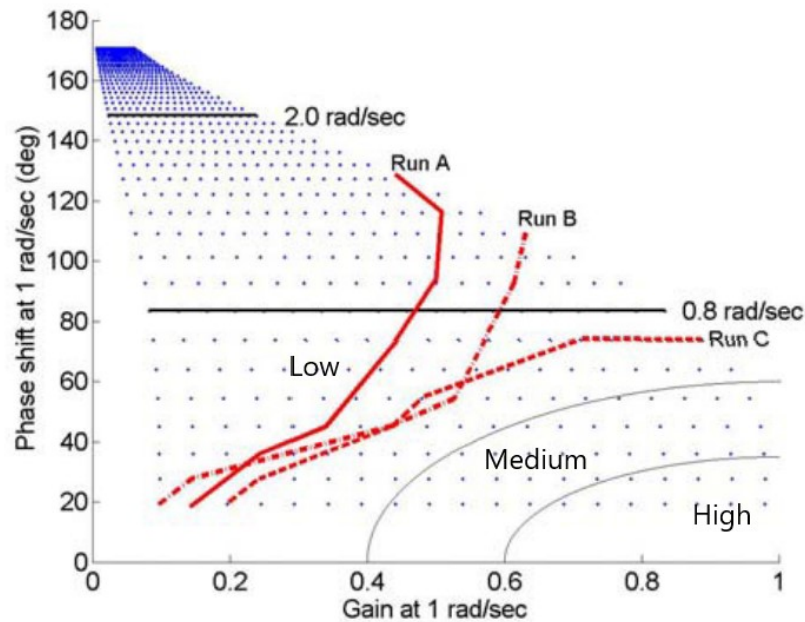


Figure 2.7: Optimisation of the heave motion filter parameters for the Simona research simulator using the tuning approach by Schroeder [46] and three different aircraft simulation model runs. Adopted from [48]

motion filter algorithm fidelity results in high fidelity stall simulation that can be used for training pilots in stall recovery procedures using ground-based simulators.

2.4. Current Stall Recovery Training in FSTDs

This section elaborates on the set-up of the current stall recovery training tasks in FSTDs. It highlights the training objectives of UPRT that can and cannot be performed in the existing levels of simulator training devices and emphasises the need for more updated and accurate, yet cost-effective stall and post-stall dynamics in flight simulator models.

2.4.1. ICAO Qualification Levels for FSTDs

ICAO DOC 9625 "Manual of Criteria for the Qualification of Flight Simulation Training Devices" [49] is the document that describes methods, procedures and testing standards for the qualification of FSTDs. It exists in two volumes, one for helicopter simulators and one for aeroplanes. ICAO defines seven types of FSTDs according to different levels of fidelity and characteristic requirements for qualification of the training devices. These seven levels can be found in table 2.1 alongside their respective characteristic requirements elaborated by KOBLEN and KOVÁOVÁ [50].

The International Committee for Aviation Training in Extended Envelopes (ICATEE), is an initiative of the Royal Aeronautical Society aimed at bringing together the world's flight training and simulation technology experts to develop guidelines for UPRT, with the main goal of the group to address LOC-I related accidents. The ICATEE training subcommittee developed a training matrix for a comprehensive UPRT training programme which includes 176 training objectives required for effective training in the awareness, prevention and recovery of aircraft upsets and stalls in particular [51].

The ICATEE Research & Technology team did an analysis where the training objectives from the training matrix were mapped onto the training device capabilities. Their analysis showed that some of the UPRT training tasks can be performed in existing flight simulator devices (Type III, V or VII devices). However, some tasks (like high altitude stall for example) require simulator fidelity levels greater than the highest ICAO level FSTD (Type VII) as well as improved motion cuing and the ability to generate sustained G forces [51].

Figure 2.8 shows the percentage wise distribution of UPRT training tasks per FSTD type level. It can be noted that ≈56% of all UPRT training tasks can be performed using existing ICAO approved FSTDs (Type III, V and VII) combined with ground training possibilities. The remaining (≈44%) of UPRT

Table 2.1: Qualification levels of Flight Simulation Training Devices (FSTDs) according to ICAO [49], elaborated by [50]

Type of FSTD	Characteristics of requirements
I	The first level would contain an enclosed or perceived cockpit/flight deck, excluding distraction, which will represent that of the aeroplane derived from, and appropriate to class, to support the approved use; lighting environment for panels and instruments should be sufficient for the operation being conducted; modelling of aerodynamics and engines (thrust, temperature, mass); aircraft systems; sound system; visual system. The ATC environment simulation is not required.
II	Meets the same requirements as the 1st level, but also contain the simulation of ATC environment such as messages, visual environment, operation on the airport, weather reporting and others.
III	Meets the previous requirements, but also contain for example the simulation of runway condition, including information on pavement condition (wet, dry). The ATC environment simulation is not required.
IV	This level meets the same requirements as previous levels. It is added for example on ATC environment simulation; sounds of outside environment (weather, meteoric water); voice control.
V	This level meets the same requirements as level IV but is added for example on runway conditions simulation (dry, wet, icings, water holes); aircraft systems simulation (communication, navigation, warning device); dynamic feeling of control; failure of brakes dynamics and tires; degradation of brakes efficiency.
VI	This level meets the same requirements as level V but is added for example on ATC extended environment simulation; the motion system includes the acceleration feeling, Buffet in the air due to flap and spoiler/speed brake extension; Buffet due to atmospheric disturbances, e.g. turbulence in three linear axes (isotropic), In-flight vibrations A motion system (force cueing) should produce cues at least equivalent to those of a 6 DOF platform motion system (i.e., pitch, roll, yaw, heave, sway, and surge). Weather environment contains e.g. simulation of turbulence.
VII	The highest approved level. It has to meet all previous requirements with their detail and authentic realisation as in the real aircraft.

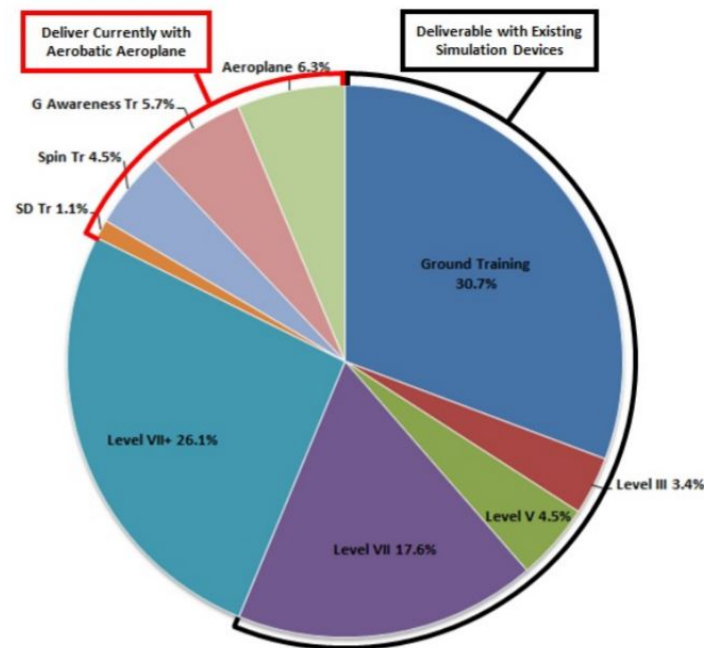


Figure 2.8: Percentage wise distribution of UPRT training tasks per FSTD type level, adopted from [51]

tasks will require an upgrade of, or addition to, a currently approved ICAO training device. About $\approx 18\%$ of these remaining tasks can reliably be delivered in light aerobatic aeroplanes. The other $\approx 26\%$ requires a higher level than ICAO type VII simulator training device. Therefore, the ICATEE defined five supplemental training devices that are currently not ICAO approved such that all of the UPRT training objectives can be met. The fidelity requirements of these training devices are summarised below [51] and emphasise the need for updated and more accurate (higher fidelity) simulator models for effective pilot UPRT and stall training.

1. **Type VII+ Training Devices** are not new devices but result from upgrading existing Type VII devices. Additional requirements were defined to enhance the following features:
 - flight models
 - flight control responses and control forces
 - motion cuing
 - environmental/weather capabilities
 - instructor operating stations
2. **Type GAD - G-Awareness Devices** are capable of generating sustained load factors to support G-awareness training.
3. **Type SPD - Spin Training Devices** constitute an upgrade of the Type VII FSTD beyond that required for a Type VII+ device, should spin training become a requirement and simulators be used for that purpose. These devices replicate the rapid attitude changes and sustained G forces experienced in a spin manoeuvre and are characterised by a flight model more sophisticated than those of Type VII+ devices.
4. **Type SDD - Spatial Disorientation Training Devices** support tasks where enhanced visual and motion cues and sensations cannot be replicated readily in a flight simulation training device.
5. **On-Aeroplane Training** is required for tasks where physiological and psychological effects can be experienced only in an all-attitude/all-envelope environment that cannot be replicated using current simulator technology.

2.4.2. Stall Simulation Limitations in Common Hexapod Mounted Simulators

The major part of commercial pilots are usually trained in Full-Flight Simulators (FFS) with a type-specific cockpit. The most advanced FFS approved for pilot training is classified as Level D by the FAA [7] or Type VII by ICAO [49] and requires a six degrees-of-freedom motion platform. The commonly used motion platform is a hexapod [43, 52]. A hexapod mounted motion system consists out of 6 linear actuators positioned in such a way that the motion platform with the cabin mounted on top has a total of 6 degrees-of-freedom. Such six actuators are limited in their velocity, acceleration and how much they can retract and extend. For example, the SRS at TU Delft [53] is a hexapod mounted simulator. These actuators have a length of 2.08 m retracted and 3.33 m extended. With some safety margin taken into account, the maximum stroke length of the actuators is 1.15 m [54]. Table 2.2 lists the geometric characteristics of the SRS, whereas the motion space for each degree of freedom independently is shown in table 2.3. However, the operational limits of the SRS during activation of the motion system might be reached before reaching the workspace of an individual degree of freedom. The operational limits of the SRS are set at ± 0.575 m actuator extension, 1 m/s actuator velocity and 10 m/s^2 actuator acceleration. More details on the hardware and software of the SRS can be found in [55].

Table 2.2: SRS geometric characteristics, adopted from [55]

Parameter	Length [mm]
Upper circle radius	1600
Lower circle radius	1650
Upper gimbal spacing	200
Lower gimbal spacing	600
Minimum actuator length	2081
Maximum actuator length	3331
Lower and upper buffer length	50
Operational actuator stroke	1150

Table 2.3: SRS motion space in all six degrees of freedom, adopted from [54]

DOF	Minimum	Maximum
Surge	-0.981 m	1.259 m
Sway	-1.031 m	1.031 m
Heave	-0.636 m	0.678 m
Roll	-25.9°	25.9°
Pitch	-23.7°	24.3°
Yaw	-41.6°	41.6°

To effectively train pilots in stall recovery, it is important that the simulator motion driving algorithm provides accurate and effective motion cues and that false cues are minimised during the stall simulation. However, standard hexapod mounted simulators are rather limited in acceleration, acceleration duration and motion space. As a result, they are unable to provide high accelerations, angular rates and sustained G-forces that are inherent to stalls and upsets in general [56]. Furthermore, current flight simulators are considered inaccurate for simulation of many upset conditions as the flight dynamics and aerodynamic models in general only apply to the normal flight regimes and aircraft behaviour can vary significantly outside this envelope during upsets and stalls. Therefore, the objective of the European research project, Simulation of Upset Recovery in Aviation (SUPRA) [56, 57], was to develop new engineering methods to extend the aerodynamic model to higher angles of attack as well as innovative motion cueing solutions, by using standard hexapod simulators and centrifuge-based simulators, see fig. 2.9.

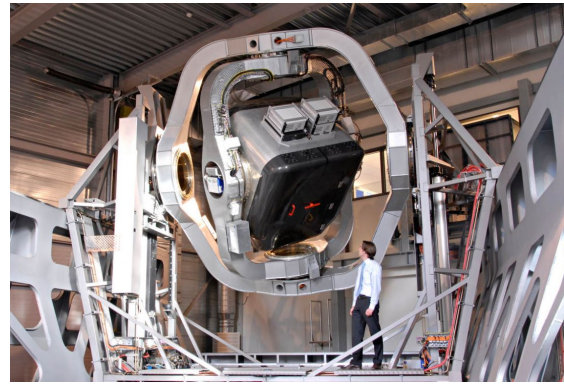
As part of the SUPRA project, research was performed on the GRACE simulator that used to be situated at the NLR in the past. This is a standard hexapod mounted simulator that was used to evaluate the newly updated aerodynamic models for their acceptability in simulating aircraft behaviour within and outside the normal flight envelope. This was done through piloted evaluation during upset and stall simulation. The research also included the investigation of optimising the classical hexapod motion cueing filters for the specific needs of UPRT. Two different approaches were taken: 1) Optimising the motion filters to maximally use the available workspace; 2) Optimising the motion filters based on motion perception knowledge [56].

Pilots can experience large variations in gravitational forces during stalls and aircraft upsets. Since these G-forces cannot be mimicked in hexapod mounted simulators, SUPRA also performed research in the DESDEMONA simulator at TNO to investigate the effects of G-forces during stall simulation. The DESDEMONA simulator integrates a fully gimballed cabin, i.e. can rotate indefinitely about all axes. It can move vertically along a heave axis and horizontally along a linear arm. The linear arm is allowed to rotate about its central vertical axis to generate centripetal forces inside the cabin. This way, DESDEMONA can simulate sustained G-loads of up to 3G [56].

The SUPRA project concluded [56] that classic hexapod mounted simulators are valuable training



(a) GRACE Simulator used to be installed at NLR in the past, picture adopted from [58]



(b) DESDEMONA Simulator at TNO, picture adopted from [59]

Figure 2.9: Simulators used during the SUPRA research project

devices for UPRT and stall recovery simulation, given that the aerodynamic flight simulator models are upgraded to also include outside normal flight envelope dynamics and the motion cuing solutions are optimised for a better use of the available workspace. Reproduction of G-forces in centrifuge-based simulators has been proven valuable for stall simulations and improves simulator fidelity, because pilots that are unfamiliar with high G-loads are more likely to perform recovery tasks less aggressively than required. However, the regulations about stall simulations do not require the implementation of high G-loads at this stage.

2.5. TU Delft Stall Model

Within TU Delft, a stall task force group researches methods of developing accurate aerodynamic stall and buffet models from flight test data to effectively train pilots in UPRT using FSTDs. For this purpose, the research group has access to both quasi-steady symmetric and accelerated stall flight test data gathered with the Cessna Citation II laboratory aircraft of the TU Delft. This section will explain details of the most advanced TU Delft stall model of the Cessna Citation II that includes quasi-steady symmetric stall aerodynamics and buffet dynamics identified in earlier research [14–16]. More recent research at the TU Delft is focusing on the lateral/asymmetric counterpart of the dynamics of an aircraft during stall [60]. The research in this thesis elaborates more on the buffet dynamics during stall and human noticeability of buffet parameter changes during stall simulation.

2.5.1. Kirchhoff's Theory of Flow Separation

The limited-envelope simulator model of the Cessna Citation II includes quasi-steady symmetric stall aerodynamics based on Kirchhoff's theory of flow separation [61–63]. Which is a relation (eq. (2.1)) between the angle of attack (AoA) and the lift of the wing's airfoil C_l that accounts for the portion of the wing where flow is separated due to stall. It includes an extra internal variable X , the flow separation point. X ranges from 0 to 1, where 1 means fully attached flow and 0 means fully separated flow (see fig. 2.10).

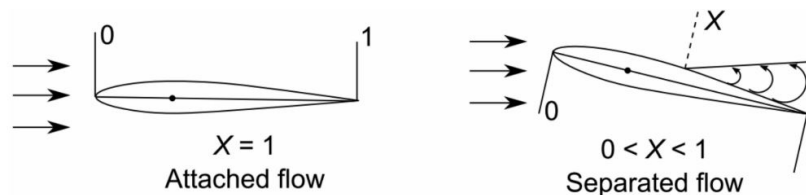


Figure 2.10: Visualisation of the flow separation variable X around the wing's airfoil. Adapted from [64]

$$C_L = C_{L\alpha} \left(\frac{1 + \sqrt{X}}{2} \right)^2 \alpha \quad (2.1)$$

The dynamics of X are modelled by a first-order ordinary differential equation (ODE) using four parameters (τ_1 , τ_2 , a_1 , α^*):

$$\tau_1 \frac{dX}{dt} + X = \frac{1}{2} (1 - \tanh[a_1 (\alpha - \tau_2 \dot{\alpha} - \alpha^*)]) \quad (2.2)$$

The four Kirchhoff parameters each characterise specific stall dynamics that are listed below:

- τ_1 : **Time required to readjust to a new condition.** Flow around an airfoil can be disturbed by external forces, i.e. gust or turbulence, and there will be a latency in the flow readjusting to such a new condition.
- τ_2 : **Characterises the effect of hysteresis.** The dependency of the flow separation point on the rate of change of angle of attack $\dot{\alpha}$.
- a_1 : **Stall abruptness parameter.** The larger this parameter is, the faster the flow separation point moves towards the leading edge with increasing angle of attack. The lift coefficient will also drop more aggressively during the stall.
- α^* : **Angle of attack in radians where the flow separation point X is equal to 0.5.** A change in α^* will lead to a similar change in the critical angle of attack.

The effects of varying the Kirchhoff model parameters on C_L and X have been investigated and visualised in past research [14, 63]. Smets et al. extended the research by also investigating the effect of variations in the Kirchhoff parameters on the aircraft symmetric states during stall simulations and how noticeable such variations are to human pilots [17].

2.5.2. Baseline Aerodynamic Stall Model

The current most advanced and relatively accurate TU Delft aerodynamic stall model of the Cessna Citation II was defined by Van Ingen et al. [15]. It is based on collected flight test data of quasi-steady and accelerated stalls at an altitude of $\approx 5,500\text{m}$. The aerodynamic force and moment model equations are given by eqs. (2.3) and (2.4) and their associated baseline parameter values can be found in table 2.4.

$$\begin{aligned} \hat{C}_L &= C_{L_0} + C_{L\alpha} \left(\frac{1 + \sqrt{X}}{2} \right)^2 \alpha + C_{L\alpha^2} (\alpha - 6^\circ)_+^2 \\ \hat{C}_D &= C_{D_0} + C_{D\alpha} \alpha + C_{D\delta_e} \delta_e + C_{DX} (1 - X) + C_{DC_T} C_T \\ \hat{C}_Y &= C_{Y_0} + C_{Y\beta} \beta + C_{Yp} \frac{pb}{2V} + C_{Yr} \frac{rb}{2V} + C_{Y\delta_a} \delta_a \\ \hat{C}_l &= C_{l_0} + C_{l\beta} \beta + C_{lp} \frac{pb}{2V} + C_{lr} \frac{rb}{2V} + C_{l\delta_a} \delta_a \\ \hat{C}_m &= C_{m_0} + C_{m\alpha} \alpha + C_{m\delta_e} \max\left(\frac{1}{2}, X\right) \delta_e + C_{mC_T} C_T \\ \hat{C}_n &= C_{n_0} + C_{n\beta} \beta + C_{nr} \frac{rb}{2V} + C_{n\delta_r} \delta_r \end{aligned} \quad (2.3)$$

$$(\alpha - 6^\circ)_+^2 = \begin{cases} (\alpha - 6^\circ)^2 & \text{when } \alpha \geq 6^\circ \\ 0 & \text{when } \alpha < 6^\circ \end{cases} \quad (2.4)$$

Table 2.4: Baseline parameter values of the TU Delft stall aerodynamic model retrieved from [15]

Name	Dim	Value	Name	Dim	Value	Name	Dim	Value
τ_1	[s]	0.2547	$C_{D(1-x)}$	[-]	0.0732	C_{l_r}	[-]	0.1412
τ_2	[s]	0.0176	$C_{D C_T}$	[-]	0.3788	$C_{l_{\delta a}}$	[-]	-0.0853
a_1	[-]	27.6711	C_{m_0}	[-]	0.0032	C_{l_0}	[-]	0.0183
α^*	[rad]	0.2084	C_{Y_β}	[-]	-0.5222	C_{m_α}	[-]	-0.5683
C_{L_0}	[-]	0.1758	C_{Y_p}	[-]	-0.5000	$C_{m_{\delta e x}}$	[-]	-1.0230
C_{L_α}	[-]	4.6605	C_{Y_r}	[-]	0.8971	$C_{m_{C_T}}$	[-]	0.1443
$C_{L_{\alpha^2}}$	[-]	10.7753	$C_{Y_{\delta a}}$	[-]	-0.2932	C_{n_0}	[-]	0.0013
C_{D_0}	[-]	0.0046	C_{l_0}	[-]	-0.0017	C_{n_β}	[-]	0.0804
C_{D_α}	[-]	0.2372	C_{l_β}	[-]	-0.0454	C_{n_r}	[-]	-0.0496
$C_{D_{\delta e}}$	[-]	-0.1857	C_{l_p}	[-]	-0.1340	$C_{n_{\delta e}}$	[-]	0.0492

2.5.3. Stall Buffet Model

The buffet model currently implemented into the Cessna Citation II stall model of the TU Delft was proposed by Van Horssen et al. and derived from buffet vibrations measured during flight tests with the TU Delft's laboratory aircraft [14]. The averaged PSDs of measured vertical and lateral accelerations during quasi-steady stall manoeuvres were used to model the stall buffet frequency spectrum, see fig. 2.11. Figure 2.11 also shows the dominant frequencies in the buffet spectra of the Cessna Citation II. The vertical direction only shows one dominant frequency peak at around 12 Hz, while in the lateral direction two main peaks are observed, at 6 Hz and 10 Hz. The longitudinal accelerations are not shown as stall buffet vibrations were found to be negligible in x-direction [14]. Figure 2.11 also shows, as expected, the PSD of the vertical buffets is approximately 10 times larger in magnitude than for a_y . Hence, in this research the focus will be predominantly on measuring how noticeable variations in the vertical stall buffet model are for human pilots.

The vertical stall buffet model proposed by Van Horssen et al. [14], see fig. 2.12, passes unity-variance white noise through a second-order shaping filter $H(j\omega)$ given by eq. (2.5) that accounts for the average frequency spectrum of the measured buffet vibrations (see fig. 2.11). The resonance frequency ω_0 of the second-order filter is used to create a band-pass filter focused on the 12 Hz frequency spike dominating the vertical buffet characteristics of the Cessna Citation II.

$$H(j\omega) = \frac{H_0 \omega_0^2}{(j\omega)^2 + \frac{\omega_0}{Q_0} j\omega + \omega_0^2} \quad (2.5)$$

The parameters in the buffet model of eq. (2.5) were estimated by fitting the PSD of the filter output to the PSD of the raw buffet flight data, see fig. 2.11. The baseline parameter values of $H(j\omega)$ reported in Ref. [14] can be found in table 2.5. As can be seen in fig. 2.12, the shaping filter output is further multiplied with a factor $1-X$ to account for buffet intensity variations with the level of separated flow along the wing. As on average this X-dependent scaling reduced the amplitude at maximum buffeting, an extra compensating gain (here $K_z = 2.5$) was applied again to match modelled buffet amplitude levels with the in-flight buffet data. Finally, the stall buffet model uses a threshold on X , i.e. X_{thres} , to trigger the buffet model: only when $X < X_{thres}$ (here 0.89) is the stall buffet model active and adding vibrations to the aircraft's vertical acceleration.

Table 2.5: Baseline parameter values of the vertical buffet model reported in Ref. [14]

	H_0 [-]	ω_0 [rad/s]	Q_0 [-]	K_z [-]	X_{thres} [-]
Value	0.05	75.92	8.28	2.5	0.89

Marschalk et al. [12] developed a different methodology to model stall buffet dynamics by using

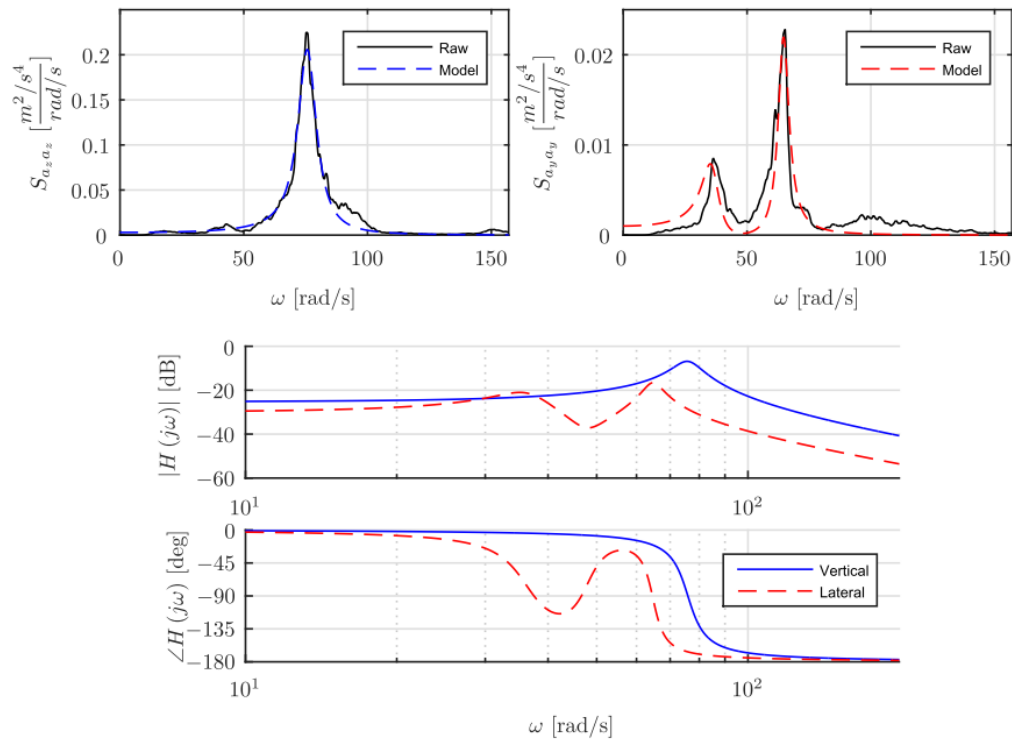


Figure 2.11: Measured and modelled PSDs and buffet model Bode diagrams for buffet accelerations in vertical and lateral directions from Ref. [14].

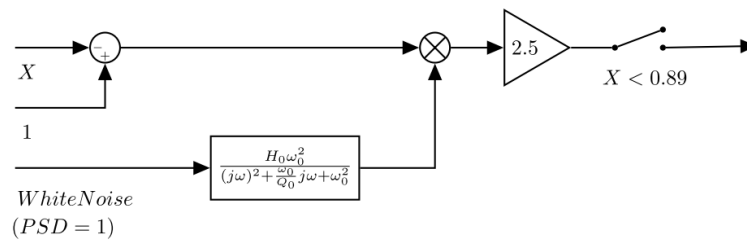


Figure 2.12: Schematic overview of the vertical stall buffet model proposed in Ref. [14].

extensive flight test data of the Fokker 100 transport aircraft. This methodology features the same frequency response fitting process as the model of Van Horssen et al. [14] where white noise with an intensity of 1 passes through a series of second-order band pass filters to replicate the peak frequencies as identified from the measured buffet power spectra. The differences between the two methodologies can be found in the buffet on- and offset modelling. Marschalk's method does not rely on the flow separation point X , instead it relies on exceeding the AoA at maximum lift coefficient. At this point during the simulation, the $C_L - \alpha$ curve will shift slope from positive to negative. The sign change is used as the activation trigger of the buffet. Calculation of the lift curve slope is done through a weighted moving average function where a window shifts over the time simulation data. Currently, the window uses both past and future data points making it unfit for real-time applications such as simulator training. The offset criteria is based on a change in sign of $\dot{\alpha}$ indicating that the AoA is increasing again and that the aircraft has recovered from the stall. Furthermore, the scaling in of the buffet from onset to maximum buffet is assumed to be quadratic [12] and fitted onto a fixed onset duration time which is the median from all recordings. Finally, a gain is multiplied with the frequency response output to ensure the correct maximum buffet intensity. This gain is the result of a multivariate polynomial where the parameters will require tuning using flight test data.

This methodology was predominantly based on Fokker 100 stall flight test data. Since this is a swept wing aircraft, it has considerable different stall properties than a straight wing aircraft like the Cessna Citation II. Nevertheless, the model was also validated using Cessna Citation II flight data and it showed acceptable results indicating a generic use of the buffet modelling methodology [12]. However, the complex model structure, different on- and offset criteria that require tuning and the fact that the model is currently unfit for real-time applications, resulted in the decision to keep the original buffet model of Van Horssen et al. [14] implemented in the Cessna Citation II stall model of the TU Delft for the purpose of this thesis research.

2.6. Conclusion

Since 2019, the FAA requires commercial pilots to receive training in the prevention and recovery of stall upsets in an effort to reduce the occurrences of LOC-I related accidents. For operational and financial benefits, a large part of this training will be performed using FSTDs. However, a study performed by the ICATEE concluded that a total of 26.1% of the required stall training tasks cannot be performed using the existing levels of FSTDs. As a result, there is a strong need for accurate, yet cost-effective solutions for including updated stall and post-stall dynamics in flight simulator models. The SUPRA project concluded that the classical hexapod mounted FSTDs are valuable stall training devices, especially with updated aerodynamic and buffet models.

A key characteristic of a stall is the buffet, as buffeting can be quite intense for certain aircraft types and be an important cue for pilots that they are entering an unsafe part of the flight envelope. A common remaining deficiency in FSTDs is the insufficient haptic and physical vibratory feedback of buffeting felt by the pilots in simulated stalled conditions. This can partly be attributed to practical considerations, as limiting buffeting vibrations positively benefits the simulator maintenance and downtime. However, a second major reason is that it is, in fact, unknown what level of stall buffet accuracy is actually required for realistic stall simulation and effective simulator-based training. This persisting uncertainty is also reflected by regulatory standards with quite lenient tolerances on buffet responses in flight simulators.

Therefore, the goal of this research is to provide quantitative guidance on the required accuracy/fidelity for replicating stall buffets in flight simulators. The research will involve a human-in-the-loop experiment in Simona at the TU Delft to measure JND thresholds for key stall buffet model parameters. Such human sensitivity thresholds can be linked to the required effort (accuracy) that is needed in defining specific stall buffet model parameters, in particular since simulator qualification is partly executed by a SME. The experiment will utilise a Cessna Citation II stall dynamic model identified from flight test data by the TU Delft stall task force group. It includes extensive modelling of stall and buffet dynamics during quasi-steady symmetric stall manoeuvres at an altitude of about 5500 m (18,000 ft), induced with a 1 kts/s deceleration into the stall. This research will mainly focus on the vertical stall buffet dynamics of the Cessna Citation II, since it was shown by previous analysis at the TU Delft that the lateral buffet PSD is about 10 times smaller than the vertical buffet.

Preliminary Sensitivity Analysis and Results

The Cessna Citation II stall dynamics model from Ref. [15] that includes the buffet model from Ref. [14] has been implemented in a Matlab/Simulink framework by master thesis students and professors from the TU Delft stall team [14–16], using the Delft University Aircraft Simulation Model and Analysis Tool (DASMAT) [65]. As mentioned in section 2.5, the focus for this research is on the vertical buffet model as this is the most dominant stall buffet direction for the Cessna Citation II, hence the most significant one for human pilot senses. The vertical buffet model relies on five parameters (H_0 , ω_0 , Q_0 , K_z , and X_{thres}). For the research on human sensitivity to detect variation in the buffet model parameters using motion-based flight simulators, only the effect of varying the vertical buffet model parameters will be analysed in detail. A preliminary sensitivity analysis similar to Smets et al. [17] is conducted to get a better insight into how the vertical buffet model behaves when varying the above mentioned parameters. The results of this preliminary sensitivity analysis are discussed in this chapter.

3.1. Stall Autopilot

It is desired to have the stall model input automated for all the simulation runs as well as during the human sensitivity experiment in the simulator. That way, the variation in the model states and buffet vibrations is only dependent on variation of the vertical buffet model parameters. Analysing the stall model with human participants flying the simulator could lead to a lot of inconsistencies and also decreases the focus of participants on detecting differences in the buffet dynamics. For example, varying deceleration during the approach to stall phase, different pitch/thrust controls during the stall recovery, etc. Such inconsistencies might trigger the participants in noticing differences that are unrelated to changes in the buffet dynamics that can result in unwanted bias in the results of the research. Therefore a simulated “stall autopilot” that was developed for a similar earlier experiment of Ref. [17] is implemented to consistently perform the 1 kts/s deceleration and the quasi-steady stall manoeuvre.

The autopilot used to generate the input to the stall model consists out of two phases, an upset phase which will lead the aircraft into the stall, and a recovery phase that will bring the aircraft out of the stalled condition. The outline of how these two phases work is visualised in fig. 3.1.

During the upset phase, both an altitude hold mode and bank angle controller are activated. The thrust setting is positioned such that a 1 kts/s deceleration of the aircraft is realised. The recovery phase of the autopilot is activated once the AoA reaches a value higher than or equal to 0.28 radians (≈ 16.05 degrees). In this phase the altitude hold mode is disabled and a pitch attitude controller is activated to control the pitch of the aircraft during recovery.

During the recovery phase, a reference pitch angle θ is set to -0.5° and no changes are done to the thrust yet. From that point on, the true airspeed V_{TAS} and the climb-rate are monitored. Both will act as a switch once a specific threshold is reached:

- **$V_{TAS} > 86$ m/s:** The reference pitch angle is changed from -0.5° to $+10^\circ$.
- **The aircraft loses less than 18 m/s in altitude:** Thrust will be set to the maximum.

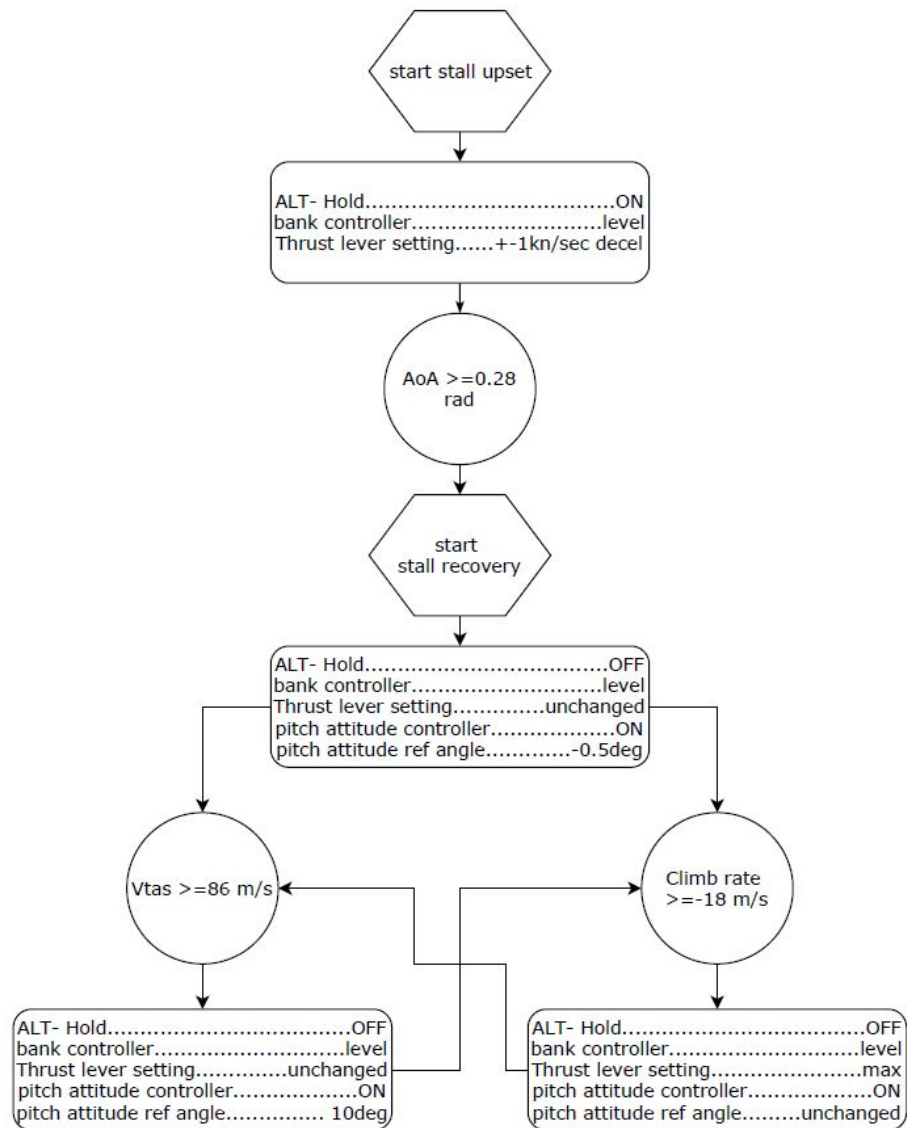


Figure 3.1: Stall auto-pilot flow chart showing the steps taken in the upset and recovery phases, adopted from [17]

The stall autopilot behaviour has been validated with respect to quasi-steady symmetric real stall flight test data of the Cessna Citation II and is displayed in fig. 3.2. The effect of the high frequency stall buffet vibrations on the aircraft states is clearly visible in the figures around the 40 seconds mark (the stalled portion of the flight data).

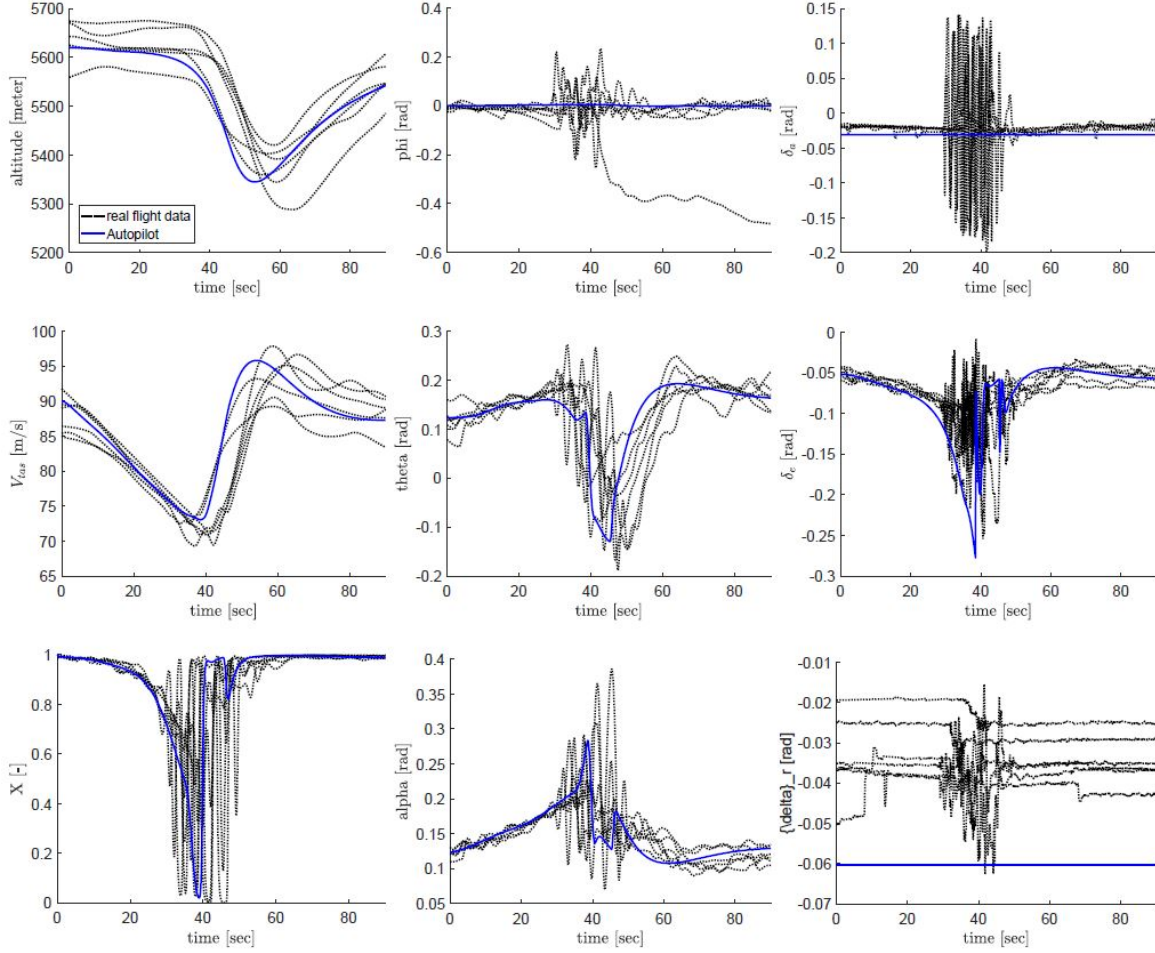


Figure 3.2: Stall autopilot validation process, all the stall model parameters are set to their respective baseline value from table 2.4, adopted from [17]

3.2. Vertical Stall Buffet Model Sensitivity Analysis

The sensitivity analysis of the buffet model features stall simulation flights performed in Matlab/Simulink over a time span of 90 seconds with the above described autopilot. Each stall simulation run started at the same initial conditions, only one vertical buffet model parameter, i.e. H_0 , ω_0 , Q_0 , K_z or X_{thres} , is varied individually per stall flight while keeping all other parameters fixed at their respective baseline settings (see tables 2.4 and 2.5). The individual variations in the buffet parameters are percentage-wise offsets with respect to the baseline settings, i.e., -66%, -33%, 0% (baseline setting), +33% and +66%. The exact values of the buffet parameters that are evaluated in the sensitivity analysis are stated in table 3.1. Note that the third run is in fact the baseline settings as described in Ref. [14].

3.2.1. Spectral Analysis

The spectral analysis shows the sensitivity of the buffet model in the frequency domain. The effects of varying model parameters on the frequency spectrum of the simulated buffet was evaluated. Figure 3.3 shows the Bode analysis of the second-order band pass filter $H(j\omega)$, see eq. (2.5). It can be noted from the magnitude plots that most frequencies are suppressed by this shaping filter except for the ones close to the peak. This results in the dominant frequency spikes visible in the PSDs of a_z from buffet

Table 3.1: Vertical buffet model parameter values for the sensitivity analysis

		H_0 [-]	ω_0 [rad/s]	Q_0 [-]	K_z [-]	X_{thres} [-]
run 1	-66.66 %	0.01667	25.3067	2.76	0.8333	0.2967
run2	-33.33 %	0.03333	50.6133	5.52	1.6667	0.5933
run 3	0 %	0.05	75.92	8.28	2.5	0.89
run 4	+33.33 %	0.06667	101.2267	11.04	3.3333	1.1867
run 5	+66.66 %	0.08333	126.5333	13.8	4.1667	1.4833

model simulations, see fig. 3.4. Figure 3.4 shows example symmetric quasi-steady vertical stall buffet simulation results in the frequency domain (PSD of a_z) for variations in all buffet model parameters (see table 3.1) individually with respect to their baseline values. The PSD plots are calculated experimentally using the time simulation results of the buffet model output $a_z(t)$ and the Fast Fourier Transform (FFT) algorithm in Matlab. In particular, they are periodograms which are the best possible estimates of the continuous PSD of a_z . In order to get smoother estimates of the PSDs, the results from 50 different random noise realisations (used as the approximation of the unity variance white noise input signal for the simulations) have been averaged.

As shown in figs. 3.3 and 3.4, the characteristic frequency parameter ω_0 of the buffet model has the biggest influence on which frequency components are active inside the simulated buffet. It directly parameterizes the frequency at which the dominant spike in the buffet spectrum occurs, ideally this is around 12 Hz according to the measured vertical buffet flight data from the Cessna Citation II. According to regulatory standards from the FAA for qualification of dynamic models in FSTDs, the predominant frequency spikes of the simulated buffet should be within a tolerance of ± 2 Hz from airplane data [7]. This tolerance will be subjectively verified from a pilot's sensitivity standpoint by comparing it to the measured JND thresholds on ω_0 .

As is clear from fig. 3.3 and fig. 3.4, the gains H_0 and K_z have exactly the same effect on the simulated buffet spectra and should for simplicity of the model in fact be combined into one gain, as expected. They both lift the buffet power spectra up and down, changing the intensity of the peak. No clear requirement is set on this stall buffet characteristic from regulatory standards [7, 66]. Ideally this peak should match as close as possible the power spectra of the measured flight data, such that model parameters like gains can be identified accordingly by matching the peak heights. This process results in pretty accurate gain parameters. The quality factor Q_0 acts as the inverse of a damping component and mainly affects the frequencies close to the resonance frequency of the filter, see fig. 3.3. Since the buffet spectrum itself is concentrated along that same resonance frequency, effects of Q_0 on the buffet model output are almost similar to those of the gains, with minor differences regarding the width of the peak (see fig. 3.4). Hence, all three parameters H_0 , K_z and Q_0 will not be further investigated during the human-in-the-loop experiment to measure pilot sensitivity on variations in the buffet model parameters, since those three parameters can accurately be identified by matching peak heights between simulated and measured buffet spectra. They are also less directly related to the requirements set by the FAA [7] on simulated buffet dynamics.

3.2.2. Time Domain Analysis

In addition to the spectral analysis, the sensitivity of the vertical buffet model is also analysed in the time domain. The baseline vertical buffet model time response is visualised in fig. 3.5, with a detailed view on the stalled portion of the flight simulation given by fig. 3.6. The results are shown for 90 seconds quasi-steady symmetric stall simulation flights of the Cessna Citation II stall Simulink model that was developed at the TU Delft and flown by the autopilot described in section 3.1. The figures clearly show the buffet onset and offset time instances as well as the initial amplitude at buffet onset and the gradual increase in buffet amplitude towards the fully developed stall. The sensitivity of the buffet model time responses for different offsets in the model parameters isn't included here, but can be found in appendix A. Due to the oscillatory nature of the buffet responses, it is hard to visually inspect any differences between the baseline and tuned model time responses. Instead, the Variance Accounted For (VAF) values for $a_z(t)$ are calculated between the baseline output (y) and the buffet model output with offsets in the model parameters (\hat{y}), i.e. -66.66%, -33.33%, +33.33% and +66.66% with respect to the baseline value, using eq. (3.1). The VAF value quantifies the amount of variance that is common

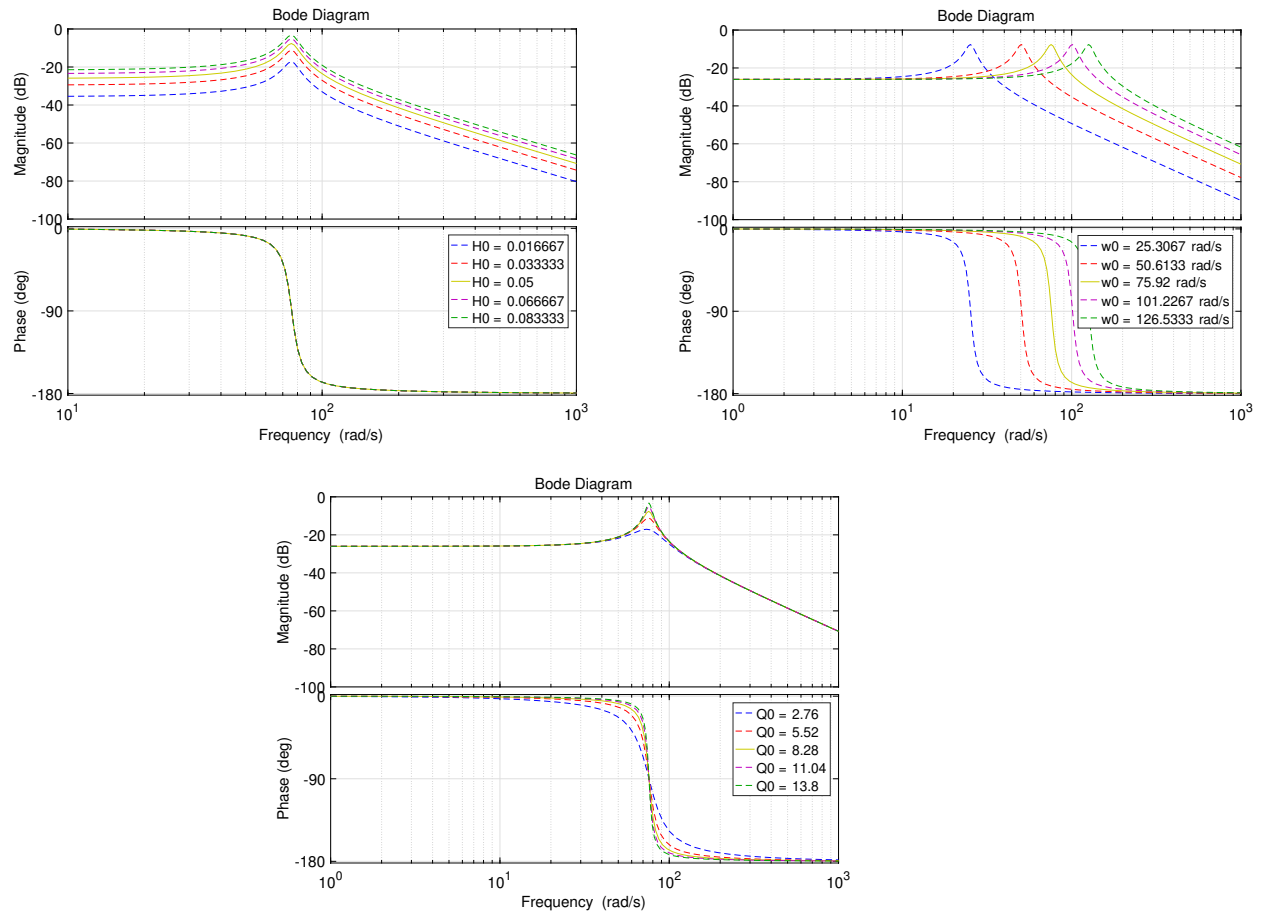


Figure 3.3: Bode analysis of the second-order band pass buffet model filter ($H(j\omega)$) under variation of the filter parameters (H_0 , ω_0 , Q_0) individually

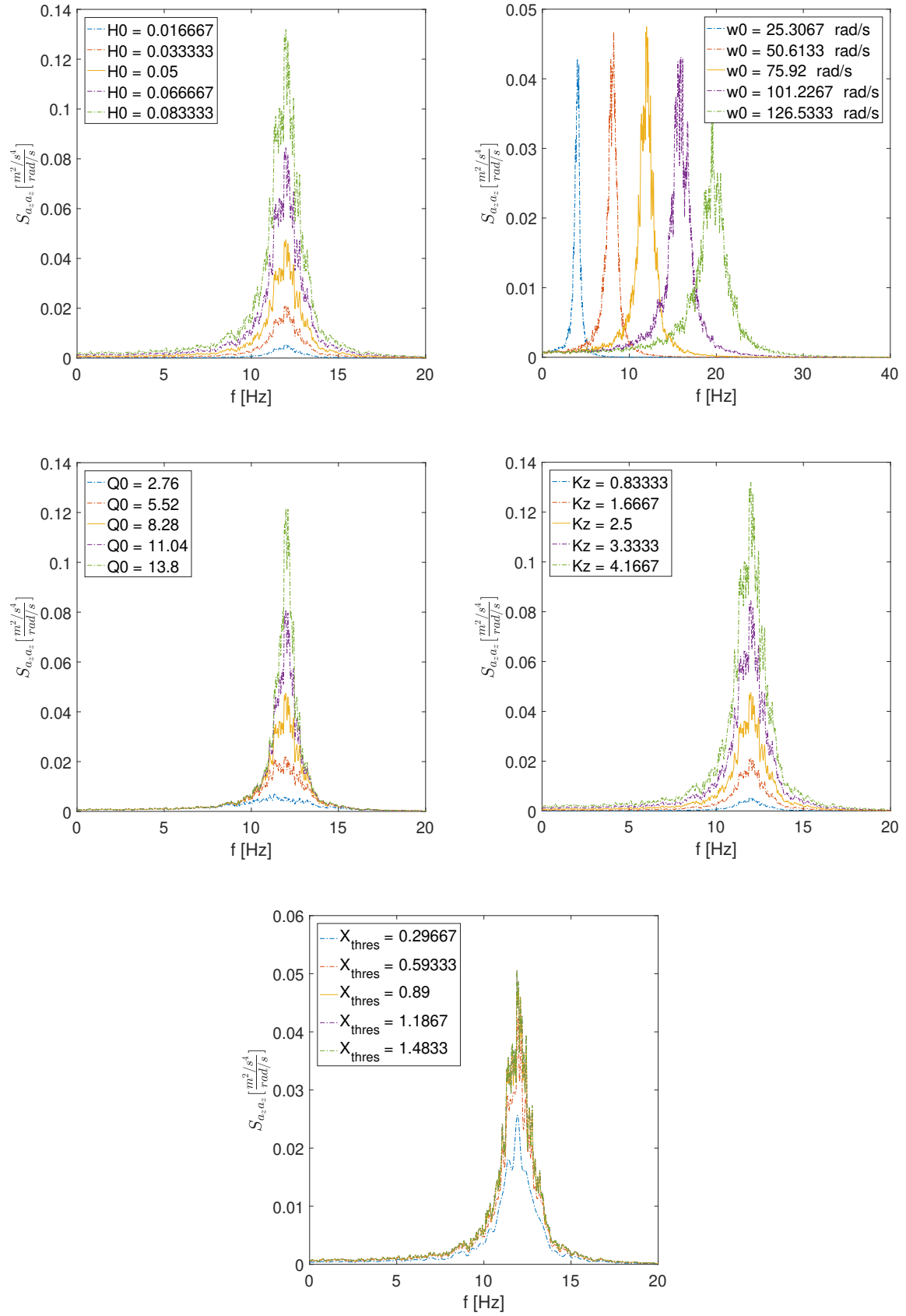


Figure 3.4: Example symmetrical quasi-steady vertical stall buffet model simulation results showing the PSD of a_z under variation of the buffet model parameters

between two time signals. The closer it is to 100 percent, the more identical the two time signals are.

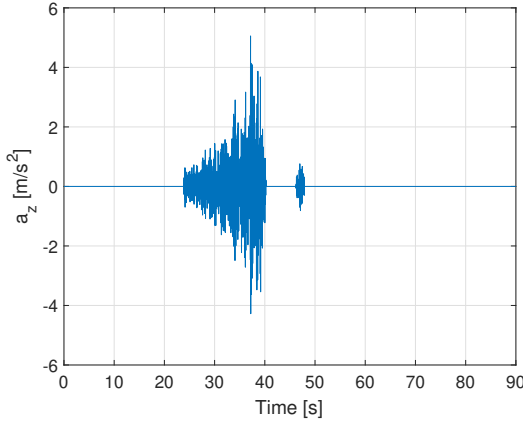


Figure 3.5: Vertical buffet model acceleration during a 90 seconds steady symmetric stall simulation of the Cessna Citation II stall Simulink model developed at the TU Delft

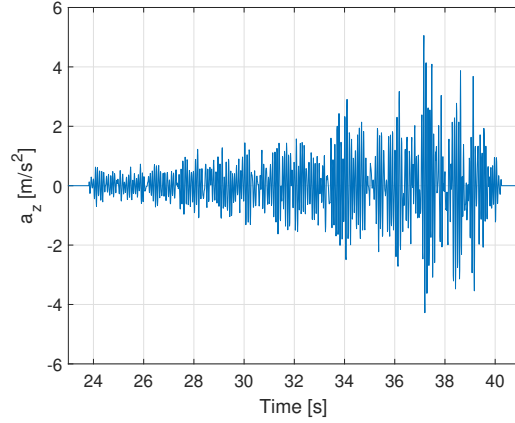


Figure 3.6: Vertical buffet model acceleration during a 90 seconds steady symmetric stall simulation of the Cessna Citation II stall Simulink model developed at the TU Delft, detailed view on the stalled portion of the flight simulation

$$\text{VAF} = \left(1 - \frac{\sum_{i=1}^N (y(t_i) - \hat{y}(t_i))^2}{\sum_{i=1}^N y(t_i)^2} \right) \cdot 100\% \quad (3.1)$$

Results of the VAF analysis are given in tables 3.2 and 3.3 and visualised in figs. 3.7 and 3.8. Table 3.2 and fig. 3.7 give the results of the VAFs under a single constant noise realisation for the buffet model input which is the standard noise seed used in Matlab/Simulink (23341). The results shown in table 3.3 and fig. 3.8 are averaged VAFs from a constant range of 50 different noise realisations. The sensitivity with respect to different noise realisations of the VAF of $a_z(t)$ for all the individual parameter offsets can be found in figs. 3.10 to 3.12. Both the average as well as the min/max spread is visible. Note that no results are shown for the 0% offset cases. Those cases reflect a tuned model that has the same parameters as the baseline model. Hence, no difference will be detected between the two outputs and the VAF will consequently be 100, independent of the specific noise realisation used. Also, no results are given for the gains H_0 and K_z . It was noted that the VAF values for both gains were insensitive to variation in the applied noise realisation. This can be explained by going back to the buffet spectra of fig. 3.4. Gains are lifting this spectra up and down with similar proportions across the entire frequency spectrum. Independent of which noise realisation is applied at the input, all frequency components in it will be varied with similar proportions resulting in the exact same VAF values for all noise realisations. The opposite is true for the other model parameters. Here the form of the spectra does change along the frequency axis with different proportions. Different noise realisations with certain frequencies being more dominant than others will be affected differently between the tuned and baseline model resulting in varying VAF values. The effect is stronger if there is more variation in the spectrum along the frequency axis. Therefore the spreading of the VAF values with respect to the average is the biggest for the characteristic frequency parameter ω_0 .

As is clear from figs. 3.7 and 3.8, both gains H_0 and K_z are inducing the same amount of variance into the simulated time responses when altered with respect to the baseline settings. This also indicates that both parameters have the exact same effect on the model output, something which was already found during the spectral analysis. For reasons discussed above (see section 3.2.1), H_0 , K_z and Q_0 are not further analysed in this thesis research. Q_0 also induces the least amount of variance of all parameters.

The most variance is induced by changing the frequency parameter ω_0 , see fig. 3.8. The buffet model output is thus very sensitive to small variations in this parameter. The VAF value is already negative at an offset of -33.33% and +33.33%, indicating a significant difference between the baseline and tuned buffet model time responses. To form a more reliable conclusion about the sensitivity of the model with respect to ω_0 parameter, a higher resolution for the VAF figure is applied. Figure 3.9

Table 3.2: VAF values of the vertical acceleration $a_z(t)$ for varying model parameters with respect to baseline, using a single constant noise realisation (Standard Matlab/Simulink noise seed: 23341) as the buffet model input

Offset	VAFs $A_z(t)$ [%]			
	-66.66%	-33.33%	+33.33%	+66.66%
H_0	55.56	88.89	88.89	55.56
ω_0	-35	-56.45	-114.40	-148.16
Q_0	68.14	93.60	96.55	87.60
K_z	55.56	88.89	88.89	55.56
X_{thres}	50.91	81.85	97.71	97.71

Table 3.3: VAF values of the vertical acceleration $a_z(t)$ for varying model parameters with respect to baseline, averaged over a constant range of 50 different noise realisations used as the buffet model input

Offset	VAFs $A_z(t)$ [%]			
	-66.66%	-33.33%	+33.33%	+66.66%
H_0	55.56	88.89	88.89	55.56
ω_0	-32.10	-58.57	-77.72	-108.57
Q_0	67.58	93.65	95.58	84.69
K_z	55.56	88.89	88.89	55.56
X_{thres}	58.43	85.42	98.24	98.24

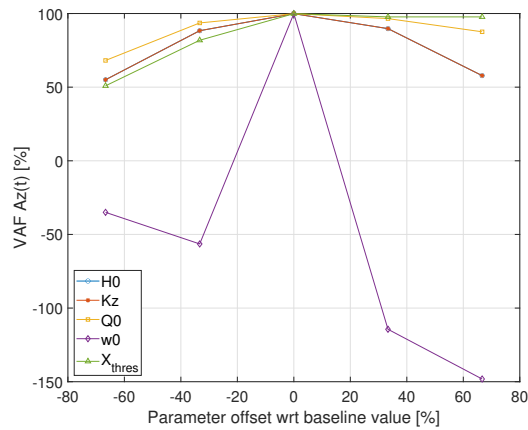


Figure 3.7: VAF of the vertical buffet acceleration $a_z(t)$ for varying buffet model parameters with respect to baseline, using a single constant noise realisation (Standard Matlab/Simulink noise seed: 23341) as the buffet model input

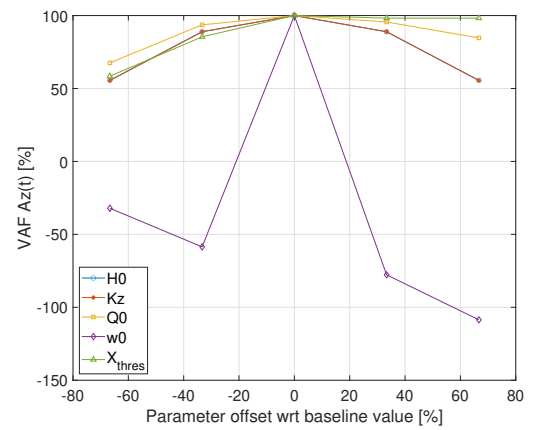


Figure 3.8: VAF of the vertical buffet acceleration $a_z(t)$ for varying buffet model parameters with respect to baseline, averaged over a constant range of 50 different noise realisations used as the buffet model input

shows the VAF value of $a_z(t)$ between the tuned and baseline model output when ω_0 is varied between 50 and 100 rad/s. This is a more in-depth analysis of the portion in between -33.33% and +33.33% offset from the baseline value ($\omega_0 = 75.92$ rad/s, shown by the red dot). It can be seen that the VAF quickly drops when ω_0 is changed from the baseline and that remains more or less symmetric around the baseline until an offset of about 20%. Not only are the VAF values very small indicating a significant difference in the time domain, they are also highly sensitive to different noise realisations used as the buffet model input, see fig. 3.11, making ω_0 an interesting parameter for further analysis. This buffet model parameter is also related to FSTD stall buffet requirements set by the FAA [7].

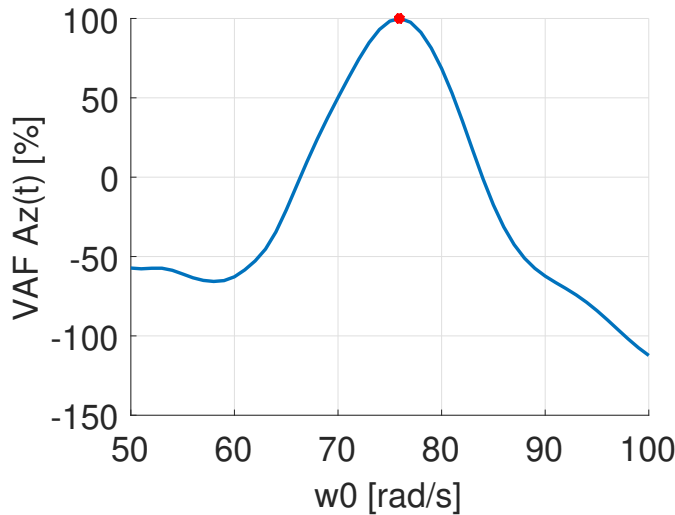


Figure 3.9: VAF of the vertical buffet acceleration $a_z(t)$ for varying the ω_0 model parameter with respect to the baseline, results are shown for a range of parameter values that roughly span from -30% to +30% offset with respect to the baseline value (75.92 rad/s) shown in red

Lastly, the X_{thres} parameter was analysed. This is another parameter closely related to FSTD stall buffet requirements set by the FAA [7]. The parameter induces similar variances as the gains in the model time responses when lowered with respect to its baseline value, see fig. 3.8. Lowering the threshold will delay buffet onset in the model as well as increase the initial buffet amplitude at onset. On the other hand, increasing the threshold will trigger the buffet sooner and with lower initial amplitude, but it hardly induces any variance with respect to the baseline model output in the time domain. This is because the nominal buffet onset point of 0.89 is already relatively high, since X can only vary between 0 and 1. Having a threshold setting above 1 doesn't make any sense, as it will lead to the same buffet model output every time and thus also the same VAF values. The multiplication inside the model with $1-X$ factor results in an already low initial amplitude with the nominal buffet onset point of $X = 0.89$. As a result, increasing the threshold does not add much vibrations extra to the output $a_z(t)$. That is why the VAF values are very close to 100 for an increase in the X_{thres} , see fig. 3.8. Not only are the VAF values close to 100, indicating almost no difference between baseline and tuned model output, also the sensitivity with respect to the noise realisation used as buffet model input is small, see fig. 3.12. This low induced amount of variance implies that there is a possibility that human pilots will not be able to detect differences when the X threshold parameter is increased. This will have to be checked during the testing of the human-in-the-loop experiment in Simona to determine if this condition should be analysed or not.

FAA qualification standards also state that the buffet threshold of perception should be based on 0.03g peak to peak initial normal acceleration with a tolerance of ± 2.0 degrees in AoA [7]. In the specific case of quasi-steady stall simulations of the Cessna Citation II model, this translates in the limits shown in fig. 3.13. Figure 3.13 shows a considerable time frame of around 26 seconds that falls within the ± 2.0 degrees AoA range around the nominal buffet onset threshold point ($X = 0.89$). Comparison with the measured JND thresholds on X_{thres} will verify the acceptability of this range of buffet onset thresholds.

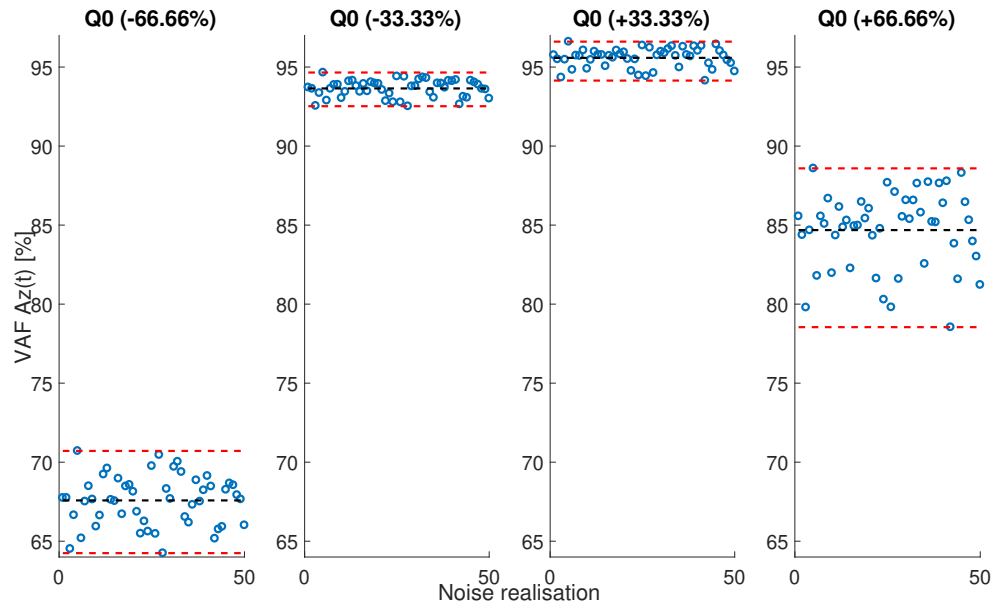


Figure 3.10: VAF of the vertical buffet acceleration $a_z(t)$ for varying the Q_0 model parameter with respect to baseline, results are shown for a range of 50 different noise realisations showing the average in black and min/max spread in red

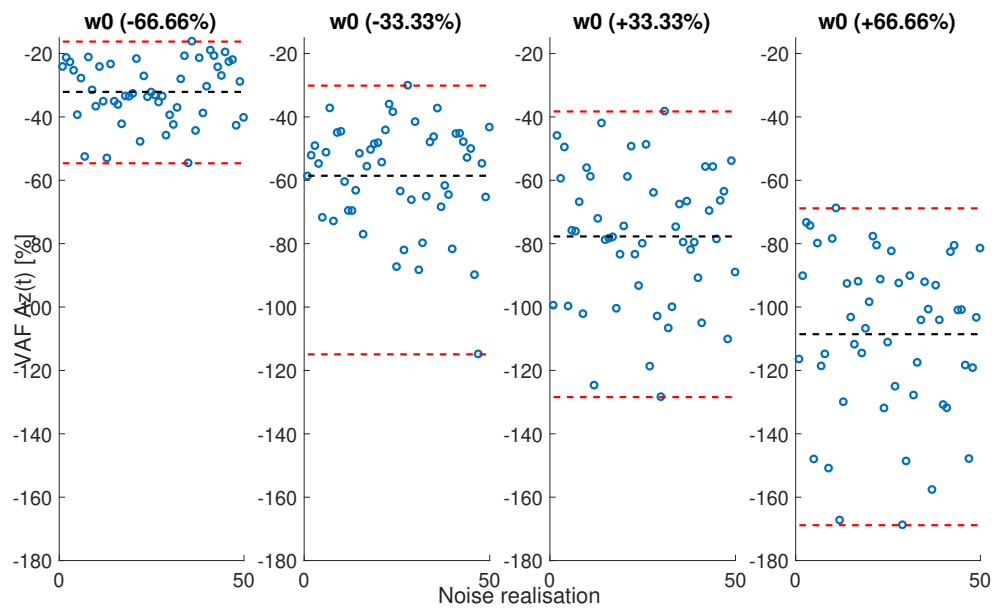


Figure 3.11: VAF of the vertical buffet acceleration $a_z(t)$ for varying the ω_0 model parameter with respect to baseline, results are shown for a range of 50 different noise realisations showing the average in black and min/max spread in red

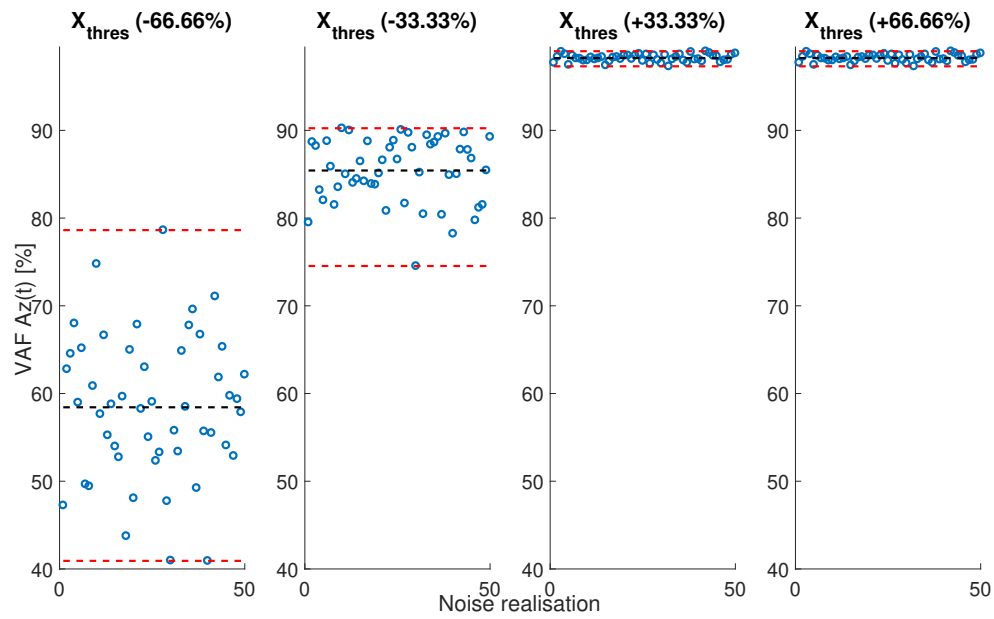


Figure 3.12: VAF of the vertical buffet acceleration $a_z(t)$ for varying the X_{thres} model parameter with respect to baseline, results are shown for a range of 50 different noise realisations showing the average in black and min/max spread in red

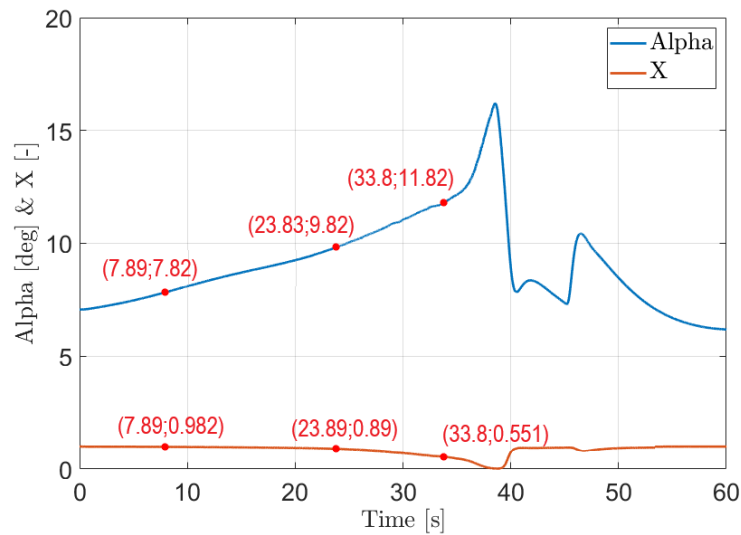


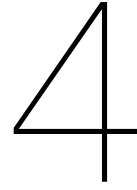
Figure 3.13: Quasi-steady stall simulation results of the Cessna Citation II stall model with baseline settings (Angle of Attack α and Flow Separation Point X) showing the current buffet onset point ($X = 0.89$) as well the limits for simulator qualification set by the FAA on buffet onset threshold in red.

3.3. Conclusion

Based on analysis of the sensitivity of the buffet model responses to variations in H_0 , ω_0 , Q_0 , K_z and X_{thres} on average over different white noise practical realisations as shown in table 3.3, fig. 3.4 and fig. 3.8, the human-in-the-loop experiment will only measure the JND thresholds for two key parameters that characterise the frequency content and temporal amplitude variations in the stall buffet vibrations: ω_0 and X_{thres} , respectively. These two parameters can be closely related to FSTD qualification requirements regarding stall and buffet simulations [7, 66]. The other parameters in the stall buffet model will remain fixed at their baseline values as determined in Ref. [14] during the experiment. Some hypotheses about the JND thresholds for ω_0 and X_{thres} can be formulated by analysing the sensitivity results. These will be tested during the human-in-the-loop experiment and either be retained or rejected.

1. **The upper JND threshold for X_{thres} is larger than the lower JND threshold for X_{thres} .** It can be seen in fig. 3.8 that for the same percentage-wise increase/decrease in X_{thres} with respect to the baseline, the buffet vibration is affected with different magnitude. When increasing the X_{thres} , almost no variance is observed with respect to the baseline settings. Therefore, the JND upper threshold will be larger than the JND lower threshold for X_{thres} .
2. **The upper JND threshold for X_{thres} is unnoticeable to human pilots.** There is a chance that the upper JND threshold for X_{thres} might not be noticeable to human pilots at all during the human-in-the-loop experiment, since the VAF stays $\approx 100\%$ when X_{thres} is increased (see fig. 3.8). This hypothesis will have to be checked during the testing phase of the experiment. In case it is true, this condition will be excluded from the experiment.
3. **The upper and lower JND thresholds for ω_0 are symmetric with respect to the baseline value.** Figure 3.9 shows a symmetric variation of the VAF value around the baseline value of ω_0 until an offset of about 20%. The JND thresholds are expected to be within this symmetric portion of the figure because the buffet model time response changes quickly when ω_0 is altered. Therefore, the JND threshold results are expected to be symmetric around the baseline value for ω_0 .

It was noted from figs. 3.10 to 3.12 that the vertical buffet model output is sensitive to the specific noise realisation which is the series of random numbers generated during the simulations as a practical implementation for the unity-variance white noise buffet model input. As a result, it is important to always make sure that the same set of random noise is used in all simulation runs during the experiment. That way no differences in the buffet dynamics are the result of different noise realisations that could possibly bias the measured JND results.



Experiment Setup

To measure the sensitivity of human pilots to variations in the two most relevant parameters of the stall buffet model, ω_0 and X_{thres} , a human-in-the-loop experiment will be performed in the SIMONA Research Simulator (SRS) at the TU Delft [54] (see fig. 4.1). For this, the realistic Cessna Citation II simulation environment available in the SRS will be used, with our custom stall dynamics model.

The goal of the experiment is to determine threshold values on the allowable variation in ω_0 and X_{thres} parameters before the parameter changes become noticeable to the human pilots participating in the experiment. To measure these JNDs from different pilots, the same experimental paradigm will be used that is also applied by Smets et al. [17]. Here participants experience (as observers) different sets of two sequential quasi-steady stalls, of which one will represent the baseline parameter settings and the other the modified stall buffet. Using a subjective staircase measurement procedure that also includes 'null' measurements to estimate the reliability of pilots' responses, see fig. 4.2, thresholds will be estimated for at least 12 participants with an active pilot license (min. PPL). Details of the proposed experiment can be found in this chapter.

4.1. Just Noticeable Difference (JND) Thresholds

Human senses are not perfect and can vary individually from person to person. Take for example two different bags. One bag weighs 10kg and the other 9.99kg. If a computer was used to measure differences, this 0.01 kg difference would be noticed. However, if a human being would be asked to spot any differences between the two bags, the difference would most likely go unnoticed. It is a different situation if one bag is 10 kg and the other 5 kg. In this case the human is capable of spotting the difference. This means that the sensory threshold for humans when comparing weights is somewhere between 0.01 kg and 5 kg. Such a sensory/perception threshold where a human being is on the verge of detecting a difference is also referred to as the JND threshold. JND thresholds are not only calculated when comparing weights of bags, but can also be determined for simulator dynamic model parameters as is the case in this thesis research.

A common way to determine the JND threshold of a human is by making use of a performance based procedure, like a staircase one. The Up/Down staircase method, initially developed by Dixon and Mood [67], is one of the methods that can be applied to detect JND thresholds. In this algorithm, the next trial set-up is determined by the answer to the previous trial. If for example a difference is detected between two cases, the difference is made smaller with a fixed step size until the difference isn't noticeable anymore. Then the difference is made larger again and so fourth until enough data is gathered to calculate the JND threshold. This 1 Up/1 Down method (settings of the compared cases are changed at every trial) with a fixed step size results in the 50% level of correctness at the threshold value.

In case a higher level of correctness at the JND threshold is required, a transformed or weighted Up/Down staircase method could be applied. In the transformed Up/Down method[68], the decreasing of the difference is based on the answers to the last few trials and not only the previous one (like is the case with the 1 Up/1 Down method). A 1 Up/2 Down method for example would result in 70.71 % level of correctness. The weighted Up/Down method [69] is a 1 Up/1 Down method where the step-up

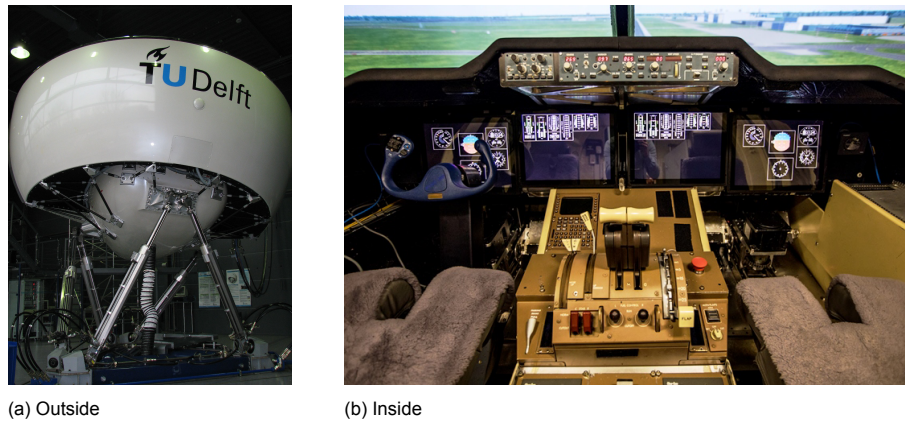


Figure 4.1: The experiment setup in the SIMONA Research Simulator (SRS) used for the human sensitivity experiment

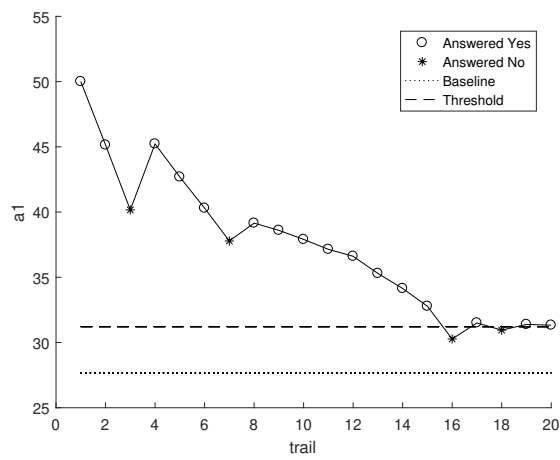


Figure 4.2: Example staircase procedure data for α_1 from Ref. [17]. Note that the performed staircase also includes 'null' measurements that were used to verify participant consistency

size is different from the step-down size. In case the step-up size is four times larger than the step-down size, a 80% level of correctness is stated. A combination of the two methods can also be used to increase the level of correctness [70]. While these methods do increase the level of correctness of the determined JND threshold, they also decrease the convergence rate of the staircase procedure towards the threshold. Hence, more trials will be needed and lengthier experiments will be the result. Long experiments are not ideal when working with human participants as fatigue will influence the obtained results. Therefore, a 1 Up/1 Down staircase method is preferred when determining JND thresholds for human participants to minimise the fatigue bias in the results.

When a staircase procedure is applied to measure the JND thresholds, participants will be asked to compare two situations to notice differences at every trial. The way the question is asked to the participants whether a difference is detected or not, is an important key variable in the experiment. There are two different ways to do it: The question can be asked as a yes/no problem (in case of the bag weight problem: "Is the weight of the 2 bags the same?"). It can also be asked as a two-alternative-forced-choice (2AFC) question. In this case the question is formulated as follows: "Which of the two bags is heavier?". Participants are then forced to give a quantitative answer and are less biased to a specific answer type. Whenever possible, a 2AFC method is preferred over a yes/no problem, because yes/no questions are prone to biases [71, 72]. Participants can be biased to predominantly answer either yes or no. It is also unaware to the researcher if participants are giving honest answers or not during the experiment. In case participants are aware of the underlying staircase procedure and a difference is to be found in every comparison situation, participants might be tempted to always answer yes. The result is a very sensitive human being with an infinitely small JND threshold, but practically useless result and a waste of the experiment potential for the particular participant. This is to be avoided at all times and extra measures will be required to minimise these possible biases.

Although yes/no methods are harder to implement correctly for measuring JND thresholds, it is not uncommon to use them. For example, Ref [73] used a yes/no method to determine coherent zones where both the visual cues and motion cues matched for yaw motion based on human perception. Smets et al. [17] used a modified yes/no method to measure JND thresholds on key stall aerodynamic model parameters. That same method will be applied in this research to measure JND thresholds on key stall buffet model parameters.

4.2. Experiment Variables and Design

This section will describe the variables that are going to be altered (independent), measured (dependent) and fixed (control) during the experiment. It also focuses on the participants and how experiment conditions are distributed over them for taking the measurements.

4.2.1. Independent Variables

Based on the results of the sensitivity analysis of the vertical buffet model (chapter 3), it was decided to only focus on two key buffet model parameters. Namely ω_0 and X_{thres} that respectively characterise the frequency content and temporal amplitude variations of the simulated buffet vibrations. Both variables are considered independent variables during the experiment and a lower and upper JND threshold will be defined for both parameters using a staircase procedure. Resulting in an experiment with four conditions to be analysed for the different participants:

- Lower JND threshold of ω_0 (ω_0^-)
- Upper JND threshold of ω_0 (ω_0^+)
- Lower JND threshold of X_{thres} (X_{thres}^-)
- Upper JND threshold of X_{thres} (X_{thres}^+)

When testing a condition for a participant to determine its individual threshold for either ω_0 or X_{thres} , only one of the two critical parameters will vary at a time. All other model parameters will be kept constant at their baseline settings from references [14, 15].

4.2.2. Dependent Variables

A subjective staircase procedure method is used to define the participant's individual JND threshold per condition. Here, the next comparison setting is based on the answer of the participant given to the question: "Did you notice a difference between stall buffet one and stall buffet two?". This answer can only be Yes/No. The answer given to the question can be considered as the dependant variable during the experiment.

4.2.3. Control Variables

Participants during the experiment will undergo two consecutive stalls simulated in the SRS. They will then be instructed to return a "Yes/No" answer to the question: "Did you notice a difference between stall buffet one and stall buffet two?". The answer to the question will then determine the comparison settings between the two stalls for the next iteration. Using a subjective staircase method the participants individual JND threshold per condition can then be determined.

In order to reduce the amount of external factors influencing the answers of the participants given, the following control variables will remain fixed throughout the experiment procedures:

- **Seated left-hand chair:** Results of the experiment might be biased as a result of key visual cues that are visible from either the left or right chair in the simulator. Therefore the chair used for all participants during the experiment will be fixed to the left chair. This is preferred over the right chair as private pilots flying usually sit in the left chair in reality as well.
- **Instrument panel:** The instrument panel will be a fixed layout for all participants showing the same information about the aircraft states.
- **Control task:** Participants will only be subjectively involved during the experiment. Their task will be fixed to comparing stall buffets and returning a "Yes/No" answer to the researcher.
- **Initial conditions:** At the start of each iteration of the staircase procedure, the simulator will be initialised with the same initial conditions for each stall simulation. This includes the location inside the simulation environment as well as trim conditions.
- **Stall autopilot:** The same stall autopilot will be used for all the flown simulations, such that the model input is always the same and not influencing the output.
- **White noise realisation:** The series of random numbers used as an approximation of the unity-variance white noise acting as the buffet model input is a fixed series for all simulations. The standard Matlab noise seed of 23341 will be used.
- **Simulator motion filter settings:** The motion filter settings of the SRS will remain fixed throughout the entire experiment. They will be optimised with respect to the experiment conditions.
- **Frequency of null measures:** The reliability of the participants' answers will be tested by performing null measures (two consecutive stalls performed with no difference in buffet dynamics) with a fixed frequency. The applied frequency will be set to three

4.2.4. Participants and Condition Sequence

It is decided to use participants with an active pilot license (min. PPL) for the experiment. Although the participants will not have to perform any piloting task (only subjective feedback is required), pilots are preferred since they have experience with stall and buffet dynamics from their careers. Pilots are also used to scanning instrument panels, so they can simultaneously keep their focus on the outside environment as well as scanning of the instruments.

The stall buffet dynamics being simulated are those of the Cessna Citation II. However, it is not required that participants are familiar with the Citation II aircraft. The goal of the experiment is that participants will have to look for differences between two consecutive simulated stall buffets. They will not have to judge whether the simulator model dynamics match the real aircraft dynamics.

The experiment will feature a within-subjects design where all four experiment conditions are evaluated for each participant. Therefore, the number of participants required for the experiments need to be an integer multiple of the amount of conditions being tested. Twelve participants are proposed for this experiment. Since human beings are involved in the experiments, some care needs to be taken

in the scheduling of the tested conditions. Computers are able to perform continuously with the same accuracy, but humans are not. Knowing that the accuracy of the human participants will decrease over time due to fatigue, two actions are proposed:

1. In-between the tested conditions, breaks will be provided to the participant in order to rest from the mental activities.
2. The four different experiment conditions will be tested in a different order for every participant. By randomising and balancing the experiment conditions over the participants, a fair comparison can be guaranteed. For this matter, the latin-square distribution will be applied, see table 4.1.

Table 4.1: Participant latin-square condition sequence for the experiment

Participant	Condition 1	Condition 2	Condition 3	Condition 4
1	ω_0^+	ω_0^-	X_{thres}^+	X_{thres}^-
2	X_{thres}^+	X_{thres}^-	ω_0^+	ω_0^-
3	ω_0^-	X_{thres}^+	X_{thres}^-	ω_0^+
4	X_{thres}^-	ω_0^+	ω_0^-	X_{thres}^+
5	X_{thres}^-	X_{thres}^+	ω_0^+	ω_0^-
6	ω_0^-	ω_0^+	X_{thres}^+	X_{thres}^-
7	ω_0^+	X_{thres}^-	ω_0^-	X_{thres}^+
8	X_{thres}^+	ω_0^-	X_{thres}^-	ω_0^+
9	ω_0^-	X_{thres}^+	ω_0^+	X_{thres}^-
10	ω_0^+	ω_0^-	X_{thres}^-	X_{thres}^+
11	X_{thres}^-	ω_0^+	X_{thres}^+	ω_0^-
12	X_{thres}^+	X_{thres}^-	ω_0^-	ω_0^+

4.3. Experiment Hypotheses

Based on the sensitivity analysis of the vertical stall buffet model (see chapter 3), some hypotheses about the JND thresholds for ω_0 and X_{thres} have been formulated. These will be tested during the experiment and either be retained or rejected based on the results.

1. The upper JND threshold for X_{thres} is larger than the lower JND threshold for X_{thres} .
2. The upper JND threshold for X_{thres} is unnoticeable to human pilots.
3. The upper and lower JND thresholds for ω_0 are symmetric with respect to the baseline value.

4.4. Experiment Procedures

In this section, the procedures for measuring the JND thresholds are explained. Both the procedures as experienced by the participants as well as the background procedures are elaborated.

4.4.1. Procedures Experienced by the Participants

Participants will get a briefing about the goal of the experiment, structure and their specific task before entering the simulator. Next, they will enter the SRS and be installed in the left-hand chair. Participants will have some time to visually inspect the cockpit layout of the SRS. When ready, participants will be given some training runs of the experiment such that they can familiarise themselves with the instrument panel, visual cues and vibratory feedback during the stall simulations in the SRS.

The actual experiment can then start once the participant is well trained. The experiment consists out of four cases/conditions and the task of the participant is the same for each one. Two consecutive stalls of about 15 seconds will be flown by an autopilot with only the vertical buffet vibrations active in the simulator. Participants will only be present as observers to fully focus on the buffet dynamics during the stalls. After each set of stalls, participants will be asked to answer a “yes/no” question: “Did you notice a difference between stall buffet 1 and stall buffet 2?”. They will not be required to justify their answers during the experiments. This procedure will be repeated until enough data points are gathered to determine the JND threshold for one condition. The procedure for the participants for one experiment condition is visualised in fig. 4.3.

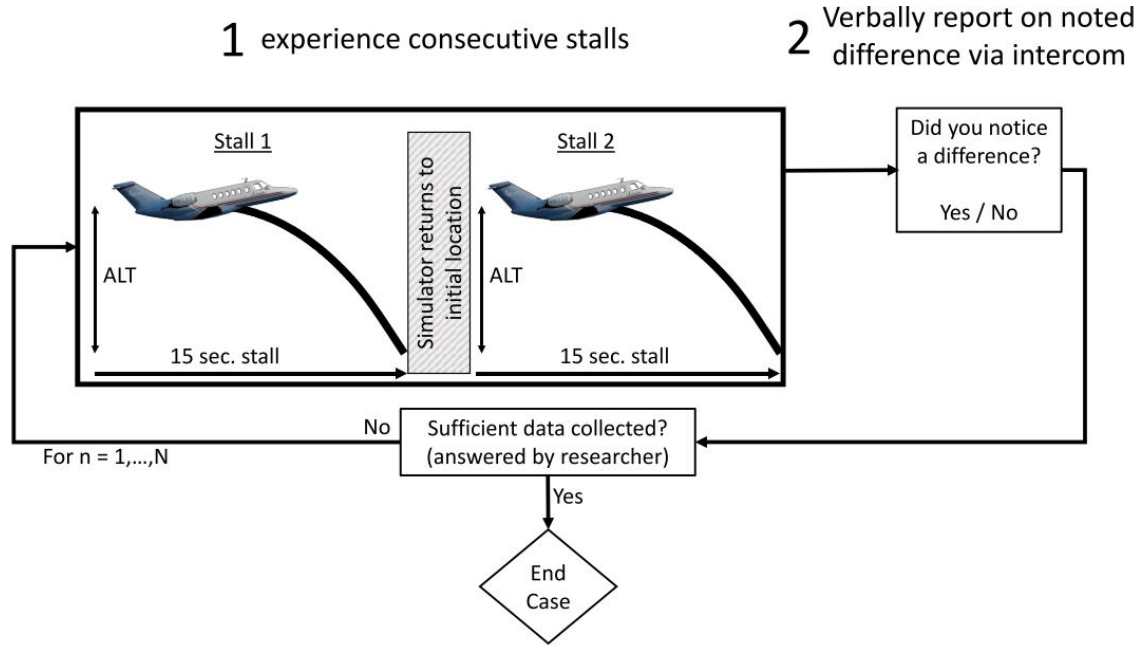


Figure 4.3: Experiment procedure for one JND threshold condition, adopted from [17]

4.4.2. Background Procedures

During the experiments the same paradigm also used by Smets et al. [17] is used by the researcher to determine the upper and lower JND thresholds for ω_0 and X_{thres} . Participants will experience two consecutive quasi-steady stall manoeuvres with the Cessna Citation II model in the SRS with vertical buffet vibrations active. One stall will be with the baseline parameter settings and the other one will be with a variation in either ω_0 or X_{thres} such that four experiment conditions will be tested in the experiment. The procedure is identical for all four cases, so only one (ω_0^+ for example) will be explained into detail.

To determine the JND threshold (ω_0^+), a staircase procedure will be applied. The starting position is an initial offset between the baseline stall and the tuned stall that is large enough such that the difference in ω_0 parameter is definitely noticeable for the human participant. Every time the participant notices the difference, the offset in the parameter is reduced with a fixed step size until the participant cannot distinguish any differences anymore between the buffet dynamics of the consecutive stalls and answers with “No”. In that case the offset in the parameter is enlarged again. From the second reversal in answers on wards, the step-size will be halved at every reversal. This makes the procedure oscillate around and converge to the JND threshold value, like fig. 4.2. The staircase procedure is ended in case one of the following conditions is met:

- The step-size equals 1/32th of the initial step-size
- A total of 30 stall buffet comparisons have taken place

The resulting JND threshold value for the individual participant will be the average of the three last reversal points in the staircase procedure. The applied staircase procedure is 1 Up/1 Down method

where the settings are altered at every comparison of stalls based on the answers of the previous trial. The resulting JND thresholds are the 50% level of correctness thresholds. Results of the experiment will be shown in individual participant's staircase plots for each experiment condition showing the individual JND thresholds of each participant. Combined results of all participants will be shown in a boxplot.

There is one issue that requires some attention. Using a staircase procedure with "yes/no" answers is prone to biases, because it is unclear if participants are giving honest answers or not. Therefore "Null Measures" will be performed with a frequency of three. A "Null Measurement" is a comparison of two baseline stalls where the participant is unknown of this situation. A "No" answer is expected, but a "Yes" answer is possible in case the human participant is to unsure. The answers to the "Null Measures" do not have any impact on the staircase procedure and are filtered out to determine the JND threshold value. The "Null Measures" are only used to get a better view on the consistency in the answers of participants.

Finally, the entire staircase measurement procedure for each condition will be automated in the simulator software. Only the answer of the participant will be required as an input by the researcher to automatically move to the next trial setup of the staircase. This is to minimise possible confounds that are the result of researcher mistakes.

Conclusion and Outlook

LOC-I remains one of the largest contributors to aviation accidents worldwide. In an effort to enhance the safety of aviation industry, new regulations have been implemented by the FAA and EASA in order to reduce the risk of LOC-I encounters. Since LOC-I accidents are generally the consequence of aircraft upsets and stall situations in particular, the regulations mandate that commercial pilots receive simulator-based training in prevention and recovery of upsets and stalls (UPRT), that is effective since 2019. As a result, there is a strong need for accurate, yet cost-effective, solutions for including accurate stall and post-stall dynamic models in flight simulators.

A key characteristic of a stall is the buffet, as buffeting is an initial cue for pilots which indicates entering of the unsafe part of the flight envelope. A common remaining deficiency in current FSTDs is the insufficient haptic and physical vibratory feedback of buffeting felt by pilots in simulated stalled conditions. This is usually done to limit FSTD maintenance, but a second reason is that it is, in fact, unknown what level of buffet model accuracy or fidelity is required for realistic and effective stall training. The available FSTD qualification standards reflect this uncertainty with quite lenient tolerances on simulated buffet characteristics.

Therefore, the goal of this thesis research is to provide additional quantitative guidance on the required accuracy for replicating stall buffets in flight simulators. The research will involve a human-in-the-loop experiment in the SIMONA Research Simulator at the TU Delft to measure JND thresholds for key buffet model parameters using a subjective staircase procedure, where about 12 pilots will be involved as observers during quasi-steady symmetric stall simulations. The experiment will utilise a Cessna Citation II stall model identified within earlier research at the TU Delft.

The key buffet model parameters were identified from the preliminary sensitivity analysis that has been performed in Matlab/Simulink using the stall autopilot for the simulations. The effects of varying the buffet model parameters (H_0 , ω_0 , Q_0 , K_z and X_{thres}) with fixed percentage wise offsets to their baseline value (-66%, -33%, +33%, +66%) have been investigated. Based on analysis of the sensitivity of the buffet model responses to variations in H_0 , ω_0 , Q_0 , K_z and X_{thres} , the human-in-the-loop experiment will only measure the JND thresholds for two key parameters that characterise the frequency content and temporal amplitude variations in the stall buffet vibrations: ω_0 and X_{thres} respectively. These parameters are also closely related to the following FSTD stall buffet requirements set by the FAA:

- Buffet threshold of perception should be based on 0.03g peak to peak normal acceleration above the background noise with a tolerance of $\pm 2.0^\circ$ angle of attack. In the specific case of quasi-steady stall simulations of the Cessna Citation II model, this translates in the following buffet onset threshold limits: X_{thres} lower limit: 0.551, X_{thres} upper limit: 0.982. This also implies a considerable time frame of around 26 seconds that falls within the ± 2.0 degrees AoA range around the nominal buffet onset threshold point ($X_{thres} = 0.89$).
- The appearance and trend of the buffet's power spectra should match flight data with at least three of the predominant frequency spikes being within ± 2 Hz of the flight data frequency spikes? The vertical buffet spectra of the Cessna Citation II only shows one peak at 12 Hz.

The acceptability of the above mentioned stall buffet simulation requirements will be verified from a pilot sensitivity point of view by comparing them to the measured JND thresholds from the human-in-the-loop experiment.

The main research question for this thesis project cannot be answered yet for the key stall buffet model parameters (ω_0 and X_{thres}). Further research is still required into the JND thresholds for these parameters and a series of steps will be discussed below that follow this preliminary thesis phase.

1. Modify the already existing DUECA software of the stall/buffet model (including the stall autopilot) such that the key buffet model parameters (ω_0 and X_{thres}) can be modified during the SIMONA experiment. DUECA is the middle-ware layer developed by the TU Delft to implement and deploy real-time simulations on different hardware, like the SIMONA research simulator.
2. Verify the motion cuing algorithm settings of the SIMONA such that optimal use is made of the available workspace during the stall buffet simulations without reaching the limits of the motion system.
3. The entire staircase procedure to measure the individual JND thresholds for participants will have to be automated in the DUECA software, with the only input being the answer of participants at every trial. This is to reduce the chances of human errors introduced by the researcher.
4. Once all the software is running in DUECA, the experiment will have to be tested in the SIMONA. If that all goes good, the experiments will have to be executed. Four conditions will be tested for each participant (ω_0^+ , ω_0^- , X_{thres}^+ and X_{thres}^-). A total of about 12 pilots will be invited for the experiments. It is chosen to work with pilots as they have experience with stall buffet vibrations.
5. With the individual JND threshold data collected from every pilot during the experiments, overall JND values for the key buffet model parameters will be determined, taking into account the participant's consistency by analysing their answers to the implemented null measures in the staircase procedures. The results will be combined and discussed in the final thesis paper.

Bibliography

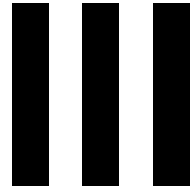
- [1] Boeing. *Statistical Summary of Commercial Jet Airplane Accidents, Worldwide Operations | 1959 – 2020*. 2021.
- [2] A A Lambregts et al. “Airplane upsets: Old problem, new issues”. In: *AIAA Modeling and Simulation Technologies Conference and Exhibit*. 2008. ISBN: 9781563479458. DOI: 10.2514/6.2008-6867.
- [3] Dennis A. Crider. “Accident lessons for stall upset recovery training”. In: *AIAA Guidance, Navigation, and Control Conference*. 2010. ISBN: 9781600869624. DOI: 10.2514/6.2010-8003.
- [4] John V. Foster et al. “Dynamics modeling and simulation of large transport airplanes in upset conditions”. In: *Collection of Technical Papers - AIAA Guidance, Navigation, and Control Conference*. Vol. 2. 2005, pp. 826–838. ISBN: 1563477378. DOI: 10.2514/6.2005-5933.
- [5] Sunjoo Advani, Jeffery Schroeder, and Bryan Burks. “What Really Can Be Done in Simulation to Improve Upset Training?” In: *AIAA Modeling and Simulation Technologies Conference*. Reston, Virginia: American Institute of Aeronautics and Astronautics, Aug. 2010. ISBN: 978-1-62410-152-6. DOI: 10.2514/6.2010-7791.
- [6] Sunjoo Advani and Joris Field. “Upset prevention and recovery training in flight simulators”. In: *AIAA Modeling and Simulation Technologies Conference 2011*. 2011, pp. 1137–1148. ISBN: 9781624101540. DOI: 10.2514/6.2011-6698.
- [7] Federal Aviation Administration (FAA). *Code of Federal Regulations, Title 14, Part 60: Flight Simulation Training Device Initial and Continuing Qualification and Use*. 2016.
- [8] Federal Aviation Administration. *Advisory Circular - Subject: Upset Prevention and Recovery Training (AC 120-111)*. Tech. rep. 2017.
- [9] Sunjoo K. Advani and Jeffery A. Schroeder. “Global implementation of upset prevention & recovery training”. In: *AIAA Modeling and Simulation Technologies Conference*. American Institute of Aeronautics and Astronautics Inc, AIAA, 2016. ISBN: 9781624103872. DOI: 10.2514/6.2016-1430.
- [10] C. LEMLEY and R. MULLANS. “Buffeting pressures on a swept wing in transonic flight - Comparison of model and full scale measurements”. In: American Institute of Aeronautics and Astronautics (AIAA), Mar. 1973. DOI: 10.2514/6.1973-311.
- [11] D. Caruana et al. “Buffet and buffeting control in transonic flow”. In: *Aerospace Science and Technology* 9.7 (Oct. 2005), pp. 605–616. ISSN: 12709638. DOI: 10.1016/j.ast.2004.12.005.
- [12] S.C.E. Marschall et al. “Stall Buffet Modeling using Swept Wing Flight Test Data”. In: *AIAA Scitech 2021 Forum*. January. American Institute of Aeronautics and Astronautics, 2021. DOI: 10.2514/6.2021-0286.
- [13] Jeffery A. Schroeder et al. “An evaluation of several stall models for commercial transport training”. In: *AIAA Modeling and Simulation Technologies Conference 2014*. American Institute of Aeronautics and Astronautics Inc., 2014. ISBN: 9781624102974. DOI: 10.2514/6.2014-1002.
- [14] L J Van Horssen, C. C. de Visser, and D. M. Pool. “Aerodynamic Stall and Buffet Modeling for the Cessna Citation II Based on Flight Test Data”. In: *2018 AIAA Modeling and Simulation Technologies Conference*. 2018. Kissimmee, Florida: American Institute of Aeronautics and Astronautics, Jan. 2018. ISBN: 978-1-62410-528-9. DOI: 10.2514/6.2018-1167.
- [15] J.B. Van Ingen, C C De Visser, and D. M. Pool. “Stall Model Identification of a Cessna Citation II from Flight Test Data Using Orthogonal Model Structure Selection”. In: *AIAA Modeling and Simulation Technologies Conference*. TU Delft. Nashville (TN): American Institute of Aeronautics and Astronautics, 2021, p. 145. DOI: 10.2514/6.2021-1725.

- [16] M A Van Den Hoek, C C De Visser, and D M Pool. "Identification of a Cessna Citation II Model Based on Flight Test Data". In: *4th CEAS Specialist Conference on Guidance, Navigation and Control*. Warsaw, 2017.
- [17] Stephan C.E. Smets, Coen C. de Visser, and Daan M. Pool. "Subjective Noticeability of Variations in Quasi-Steady Aerodynamic Stall Dynamics". In: *AIAA Modeling and Simulation Technologies conference*. San Diego (CA): American Institute of Aeronautics and Astronautics Inc, AIAA, Jan. 2019. ISBN: 9781624105784. DOI: 10.2514/6.2019-1485.
- [18] Jeffery Schroeder. "Research and Technology in Support of Upset Prevention and Recovery Training". In: *AIAA Modeling and Simulation Technologies Conference*. Reston, Virginia: American Institute of Aeronautics and Astronautics, Aug. 2012. ISBN: 978-1-62410-183-0. DOI: 10.2514/6.2012-4567.
- [19] John D. Anderson. *Introduction to flight*. 7th Editio. 1221 Avenue of the Americas, New York, NY 10020: McGraw Hill, 2012. ISBN: 9780071086059.
- [20] National Geographic Partners. *These 9 Airplanes Transformed Flight Over the Last Century*. 2017. URL: <https://www.nationalgeographic.com/environment/article/passenger-aircraft-milestones>.
- [21] John D Jr. Anderson. *Fundamentals of aerodynamics*. 5th editio. 2 Penn Plaza, New York NY 10121: McGraw-Hill, 2011. ISBN: 9781259010286.
- [22] Richard Shepherd. Shevell. *Fundamentals of flight*. 2nd Editio. Prentice Hall, 1989. ISBN: 978-0133390605.
- [23] SKYbrary Aviation Safety. *Stick Pusher*. URL: https://www.skybrary.aero/index.php/Stick_Pusher.
- [24] SKYbrary Aviation Safety. *Spin*. URL: <https://www.skybrary.aero/index.php/Spin>.
- [25] Andrew L. Reehorst, Harold E. Addy, and Renato O. Colantonio. "Examination of icing induced loss of control and its mitigations". In: *AIAA Guidance, Navigation, and Control Conference*. August. Toronto, Ontario Canada: AIAA, 2010. ISBN: 9781600869624. DOI: 10.2514/6.2010-8140.
- [26] Yiqiang Han and Jose Palacios. "Airfoil-Performance-Degradation Prediction Based on Nondimensional Icing Parameters". In: *AIAA Journal* 51.11 (Oct. 2013), pp. 2570–2581. DOI: 10.2514/1.J052207.
- [27] Konstantinos Stefanidis, Victor Klimenko, and Jimmy Krozel. "Impact Analysis for Volcanic Ash Hazards". In: *AIAA Guidance, Navigation, and Control Conference*. Portland, Oregon: American Institute of Aeronautics and Astronautics Inc., 2011. DOI: 10.2514/6.2011-6692.
- [28] Joseph R Chambers and Sue B Grafton. *Aerodynamic Characteristics of Airplanes at High Angles of Attack*. Tech. rep. NASA Langley Research Center, 1977. URL: <https://ntrs.nasa.gov/api/citations/19780005068/downloads/19780005068.pdf>.
- [29] John N. Ralston et al. "The application of potential data sources for simulator compliance with ICATEE recommended stall modeling requirements". In: *AIAA Modeling and Simulation Technologies Conference 2012*. American Institute of Aeronautics and Astronautics, 2012. ISBN: 9781624101830. DOI: 10.2514/6.2012-4568.
- [30] Salvatore Liguore and Dale Pitt. "Aircraft buffet prediction using unsteady aerodynamics wind tunnel model six-component balance data". In: *45th AIAA/ASME/ASCE/AHS/ASC Structures, Structural Dynamics & Materials Conference*. Palm Springs, California: American Institute of Aeronautics and Astronautics, 2004. DOI: 10.2514/6.2004-2045.
- [31] Adrien Bérard and Askin T. Isikveren. "Conceptual Design Prediction of the Buffet Envelope of Transport Aircraft". In: *Journal of Aircraft* 46.5 (May 2012), pp. 1593–1606. DOI: 10.2514/1.41367.
- [32] D. G. Mabey. "Buffeting criteria for a systematic series of wings". In: *Journal of Aircraft* 26.6 (May 1989), pp. 576–582. DOI: 10.2514/3.45805.

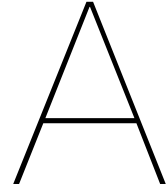
- [33] D. G. Mabey. "Some aspects of aircraft dynamic loads due to flow separation". In: *Progress in Aerospace Sciences* 26.2 (Jan. 1989), pp. 115–151. ISSN: 0376-0421. DOI: 10.1016/0376-0421(89)90006-7.
- [34] D. G. Mabey. "Review of the normal force fluctuations on aerofoils with separated flow". In: *Progress in Aerospace Sciences* 29.1 (Jan. 1992), pp. 43–80. ISSN: 0376-0421. DOI: 10.1016/0376-0421(92)90003-Z.
- [35] Jeffery A Schroeder and Robert H Burke. "Upset Prevention and Recovery Training-A Regulator Update". In: *AIAA Modeling and Simulation Technologies Conference*. San Diego, California: American Institute of Aeronautics and Astronautics, 2016. DOI: 10.2514/6.2016-1429.
- [36] SKYbrary Aviation Safety. *Stall Warning Systems*. 2020. URL: https://www.skybrary.aero/index.php/Stall_Warning_Systems.
- [37] Dennis A Crider. "The Need for Upset Recovery Training". In: *AIAA Modeling and Simulation Technologies Conference and Exhibit*. Honolulu, Hawaii: American Institute of Aeronautics and Astronautics, 2008. DOI: 10.2514/6.2008-6864.
- [38] ICAO. *Safety Report - 2020 Edition*. Tech. rep. 2020.
- [39] Boeing. *Statistical Summary of Commercial Jet Airplane Accidents Worldwide Operations | 1959 – 2019*. Tech. rep. 2020. URL: https://www.boeing.com/resources/boeingdotcom/company/about_bca/pdf/statsum.pdf.
- [40] European Aviation Safety Agency (EASA). *Loss of Control in General Aviation*. Tech. rep. 2016. URL: https://www.easa.europa.eu/sites/default/files/dfu/Loss%20of%20Control%20in%20General%20Aviation%20-%20update%2017112016-%20sourcedoc-final_0.pdf.
- [41] S. K. Advani et al. "Optimization of Six-Degrees-of-Freedom Motion Systems for Flight Simulators". In: *Journal of Aircraft* 36.5 (May 1999), pp. 819–826. DOI: 10.2514/2.2515.
- [42] B. CONRAD, S. SCHMIDT, and J. DOUVILLIER. "Washout circuit design for multi-degrees-of-freedom moving base simulators". In: *Visual and Motion Simulation Conference*. Palo Alto, CA, U.S.A.: American Institute of Aeronautics and Astronautics (AIAA), Sept. 1973. DOI: 10.2514/6.1973-929.
- [43] Daan M. Pool. "Objective Evaluation of Flight Simulator Motion Cueing Fidelity Through a Cybernetic Approach". PhD thesis. Delft University of Technology, 2012.
- [44] William W.Y. Chung. "A review of approaches to determine the effectiveness of ground-based flight simulation". In: *Modeling and Simulation Technologies Conference*. Denver, CO, U.S.A.: American Institute of Aeronautics and Astronautics Inc., 2000. DOI: 10.2514/6.2000-4298.
- [45] Peter R. Grant and Lloyd D. Reid. "Motion Washout Filter Tuning: Rules and Requirements". In: *Journal of Aircraft* 34.2 (Mar. 1997), pp. 145–151. ISSN: 0021-8669. DOI: 10.2514/2.2158. URL: <https://arc.aiaa.org/doi/10.2514/2.2158>.
- [46] Jeffery A Schroeder. *Helicopter Flight Simulation Motion Platform Requirements*. 1999. DOI: NASA/TP-1999-208766.
- [47] J. B. Sinacori. *The determination of some requirements for a helicopter flight research simulation facility*. 1977. DOI: NASACR152066.
- [48] Bas Gouverneur et al. "OPTIMISATION OF THE SIMONA RESEARCH SIMULATOR'S MOTION FILTER SETTINGS FOR HANDLING QUALITIES EXPERIMENTS". In: *AIAA Modeling and Simulation Technologies Conference and Exhibit*. Austin, Texas: AIAA, 2003. DOI: 10.2514/6.2003-5679.
- [49] INTERNATIONAL CIVIL AVIATION ORGANIZATION (ICAO). *Doc 9625 Manual of Criteria for the Qualification of Flight Simulation Training Devices*. Fourth Edi. Vol. 1 - Aeropl. Montréal, Quebec, 2015. ISBN: 9789292497613.
- [50] Ivan Koblen and Jana Kováčová. "Selected information on flight simulators-main requirements, categories and their development, production and using for flight crew training in the both Slovak Republic and Czech Republic conditions". In: *INCAS BULLETIN* 4.3 (2012), pp. 73–86. DOI: 10.13111/2066-8201.2012.4.3.7.

- [51] J N Field and D A Shikany. *Simulator fidelity requirements for upset prevention & recovery training*. Tech. rep. Nationaal Lucht-en Ruimtevaartlaboratorium, 2013.
- [52] Tommaso Sgobba et al. *Chapter 16 - Selection and training*. Butterworth-Heinemann, Jan. 2018, pp. 721–793. DOI: 10.1016/B978-0-08-101869-9.00016-9.
- [53] TU Delft. *The SIMONA Research Simulator*. URL: <https://cs.lr.tudelft.nl/simona/facility/>.
- [54] Olaf Stroosma, M. M. van Paassen, and Max Mulder. “USING THE SIMONA RESEARCH SIMULATOR FOR HUMAN-MACHINE INTERACTION RESEARCH”. In: *AIAA Modeling and Simulation Technologies Conference and Exhibit*. American Institute of Aeronautics and Astronautics, 2003. DOI: 10.2514/6.2003-5525.
- [55] Walter R Berkouwer et al. “Measuring the Performance of the SIMONA Research Simulator’s Motion System”. In: *AIAA Modeling and Simulation Technologies Conference and Exhibit*. San Francisco, California: American Institute of Aeronautics and Astronautics, 2005. DOI: 10.2514/6.2005-6504.
- [56] Lars Fucke et al. “FINAL RESULTS OF THE SUPRA PROJECT: IMPROVED SIMULATION OF UPSET RECOVERY”. In: *28TH INTERNATIONAL CONGRESS OF THE AERONAUTICAL SCIENCES*. 2012.
- [57] N B Abramov et al. “Pushing Ahead-SUPRA Airplane Model for Upset Recovery”. In: *AIAA Modeling and Simulation Technologies Conference*. Minneapolis, Minnesota: American Institute of Aeronautics and Astronautics, 2012. DOI: 10.2514/6.2012-4631.
- [58] NLR. *GRACE NLR Research Flight Simulator*. URL: <https://www.nlr.org/flyers/en/f381-grace-nlr-research-flight-simulator.pdf>.
- [59] Royal Netherlands Air Force. *Center for Man in Aviation*. URL: <https://english.defensie.nl/organisation/air-force/bases-and-units/centre-for-man-and-aviation>.
- [60] E.H.P. De Meester, Coen C. de Visser, and Daan M. Pool. *Towards an Asymmetric Stall Model for the Fokker 100*. Tech. rep. Technische Universiteit Delft, 2021.
- [61] M. Goman and A. Khrabrov. “State-space representation of aerodynamic characteristics of an aircraft at high angles of attack”. In: *AIAA Astrodynamics Conference*. Hilton Head (SC): American Institute of Aeronautics and Astronautics Inc, AIAA, 1992, pp. 759–766. DOI: 10.2514/6.1992-4651.
- [62] D Fischenberg and R V Jategaonkar. “Identification of Aircraft Stall Behavior from Flight Test Data”. In: *Proceedings of the RTO SCI Symposium on System Identification for Integrated Aircraft Development and Flight Testing, Madrid, Spain*. 1998, pp. 17–1.
- [63] Joaquim N. Dias. “Unsteady and Post-Stall Model Identification Using Dynamic Stall Maneuvers”. In: *Proceedings of the AIAA Atmospheric Flight Mechanics Conference, Dallas (TX)*. American Institute of Aeronautics and Astronautics (AIAA), June 2015. DOI: 10.2514/6.2015-2705.
- [64] Joaquim N. Dias. “High angle of attack model identification with compressibility effects”. In: *AIAA Atmospheric Flight Mechanics Conference, 2015*. Kissimmee, Florida: American Institute of Aeronautics and Astronautics Inc., 2015. ISBN: 9781624101328. DOI: 10.2514/6.2015-1477.
- [65] C A A M Van Der Linden. *DASMAT-Delft University Aircraft Simulation Model and Analysis Tool: A Matlab/Simulink Environment for Flight Dynamics and Control Analysis*. Delft University Press, 1998. ISBN: 90-407-1582-3.
- [66] European Aviation Safety Agency (EASA). *Certification Specifications for Aeroplane Flight Simulation Training Devices (CS-FSTD(A))*. 2018.
- [67] W. J. Dixon and A. M. Mood. “A Method for Obtaining and Analyzing Sensitivity Data”. In: *Journal of the American Statistical Association* 43.241 (1948), pp. 109–126. ISSN: 1537274X. DOI: 10.1080/01621459.1948.10483254.
- [68] G. B. Wetherill and H. Levitt. “SEQUENTIAL ESTIMATION OF POINTS ON A PSYCHOMETRIC FUNCTION”. In: *British Journal of Mathematical and Statistical Psychology* 18.1 (May 1965), pp. 1–10. ISSN: 20448317. DOI: 10.1111/j.2044-8317.1965.tb00689.x.

- [69] Christian Kaernbach. "Simple adaptive testing with the weighted up-down method". In: *Perception & Psychophysics* 49.3 (May 1991), pp. 227–229. ISSN: 00315117. DOI: 10.3758/BF03214307.
- [70] Miguel A. García-Pérez. "Forced-choice staircases with fixed step sizes: Asymptotic and small-sample properties". In: *Vision Research* 38.12 (June 1998), pp. 1861–1881. ISSN: 00426989. DOI: 10.1016/S0042-6989(97)00340-4. URL: <https://pubmed.ncbi.nlm.nih.gov/9797963/>.
- [71] Frederick Kingdom and Nicolaas Prins. *Psychophysics - A Practical Introduction*. 2nd Editio. 32 Jamestown Road, London NW1 7BY, UK: Academic Press, 2016. ISBN: 9780124071568.
- [72] Jason J Jerald. "Scene-Motion-and Latency-Perception Thresholds for Head-Mounted Displays". PhD thesis. Chapel Hill: University of North Carolina, 2010.
- [73] N. W.M. Beckers et al. "Perception and behavioral phase coherence zones in passive and active control tasks in yaw". In: *AIAA Modeling and Simulation Technologies Conference 2012*. 2012. ISBN: 9781624101830. DOI: 10.2514/6.2012-4794.



Appendix to Preliminary Thesis Report



Vertical Stall Buffet Model Time Domain Sensitivity Analysis Results

This appendix includes the results of the preliminary sensitivity analysis of the vertical Cessna Citation II buffet model in the time domain. Quasi-steady symmetric stall simulation flights of 90 seconds have been performed using the Cessna Citation II stall Simulink model that was developed at the TU Delft. The time responses of those simulations for the vertical buffet acceleration only (A_z) can be seen in fig. A.1, zoomed in on the complete stalled portion of the 90 seconds simulation flights. The vertical buffet model parameters (H_0 , ω_0 , Q_0 , K_z and X_{thres}) have been varied respectively with -66%, -33%, 0%, +33% and +66% offsets with respect to the baseline settings for the sensitivity analysis results shown. The effects of varying the buffet model parameters on the simulated vertical buffet accelerations is better visualised in fig. A.2, which shows only a few seconds of the stall for each varying parameter.

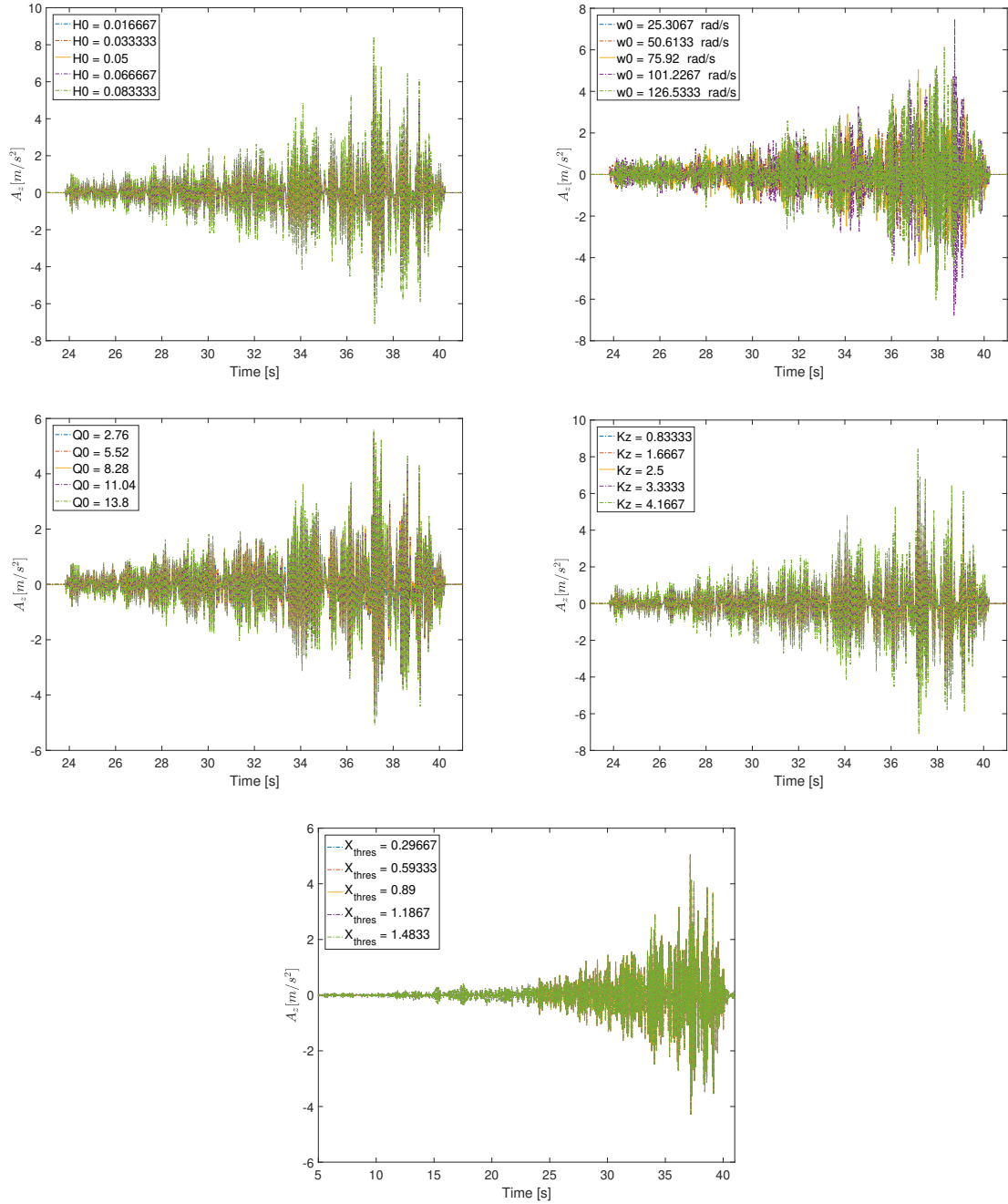


Figure A.1: Example symmetrical quasi-steady vertical stall buffet model simulation results showing A_z in the time domain under variation of the buffet model parameters, zoomed in on the stalled portion of the 90 seconds Cessna Citation II model simulations

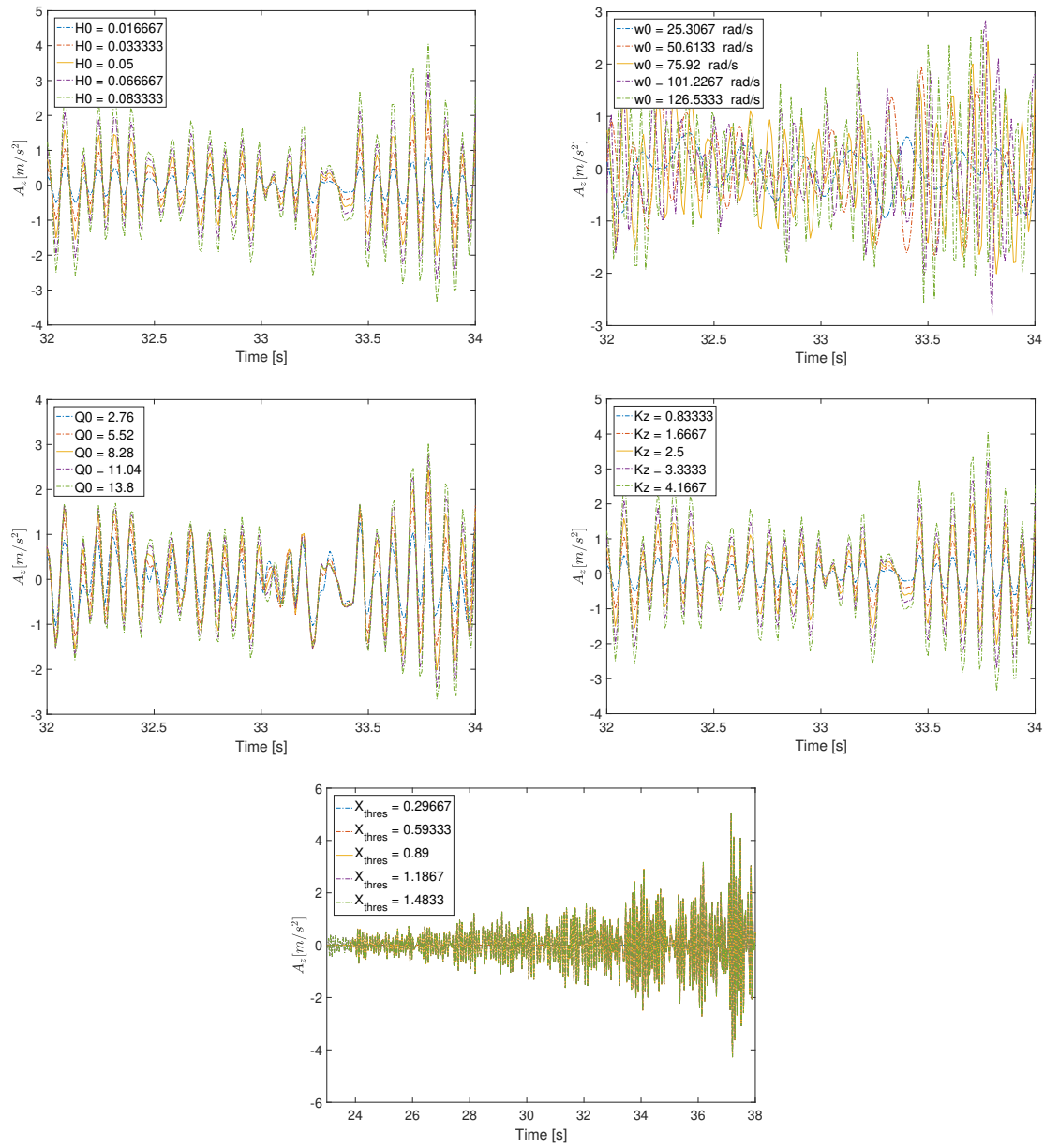
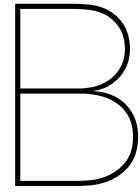


Figure A.2: Example symmetrical quasi-steady vertical stall buffet model simulation results showing A_z in the time domain under variation of the buffet model parameters, zoomed in on a smaller portion of the stalled parts of the 90 seconds Cessna Citation II model simulations showing more details on the effect of the variations in buffet model parameters

IV

Appendix to Final Report



Experiment Briefing and Consent Form

Before the start of the experiment, participants were briefed on the safety and experiment procedures. For this a document was created that participants received together with the invitation to the experiment. The researcher discussed this document together with the participant and answered any remaining questions before entering the simulator. The composed briefing document can be found on the next pages.

All participants were required to fill out and sign a consent form stating that they are participating voluntarily and understand the experiment tasks and safety procedures. Furthermore, the participants also gave permission to use their data anonymously for reports and scientific papers. An empty example of the used consent form is shown after the experiment briefing.

Briefing: Pilot Noticeability of Stall Buffet Simulation Settings

Written at the Faculty of Aerospace Engineering of the TU Delft on September 21, 2021.

Within the Control & Simulation section at the Faculty of Aerospace Engineering, a stall task force group is working hard to develop an accurate model of the Cessna Citation II which can be used for stall recovery training. With this human-in-the-loop experiment we want to get a better understanding of the required accuracy of the critical stall buffet model parameters.

The experiment will be performed in the SIMONA Research Simulator (SRS) at the Faculty of Aerospace Engineering at TU Delft, see Figure 1. You, as a participant, will be seated in the left hand seat of the simulator and be provided with motion, an outside visual environment representation, an instrument panel where you can read airspeed, altitude, vertical speed, heading, etc. and an additional display with the engine settings. Figure 1 shows the pilot station and simulator cabin. You will wear a noise-cancellation headset to cancel out false cues caused by the noise coming from the actuators when moving you around in space.

In this experiment we will investigate three different cases. For all three, we follow a procedure where we ask you to detect whether two consecutive simulated stall manoeuvres differ from each other. The procedure of each case will be as follows:

1. You will experience two consecutive simulated stalls (each one takes approx. 15 seconds)
2. You inform the researcher whether you detected a difference or not between the stall buffets. During the experiment there may or may not be a difference between the two consecutive stalls. It is important that you answer "Yes" only if you are sure there was a difference!
3. The researcher will define when sufficient data is collected. If this is not the case, a new trial will be performed where all the steps mentioned above will be repeated for a new comparison of two stalls.

Figure 2 illustrates the procedure. The stalls will be flown by a pre-programmed autopilot and you will experience them as a "passenger". In this way, the stall is always performed in the same way, allowing you to fully focus on detecting differences (if any).

Before the experiment starts we will do some familiarization runs where the researcher will help to detect the differences. After this initial training the experiment will start. We will investigate the three test cases one by one.

The structure of the experiment will be as follows:

1. Familiarization/training runs (+/- 15 min.)
2. Case 1 (+/- 30 min.)
3. Break (+/- 10 min.)
4. Case 2 (+/- 30 min.)
5. Break (+/- 10 min.)
6. Case 3 (+/- 30 min.)
7. End of the experiment + debriefing

The entire experiment will take around two hours, including the breaks. Note that your participation in the experiment is completely voluntary.



Figure 1: The experiment setup in the SIMONA Research Simulator (SRS) used for the experiment.

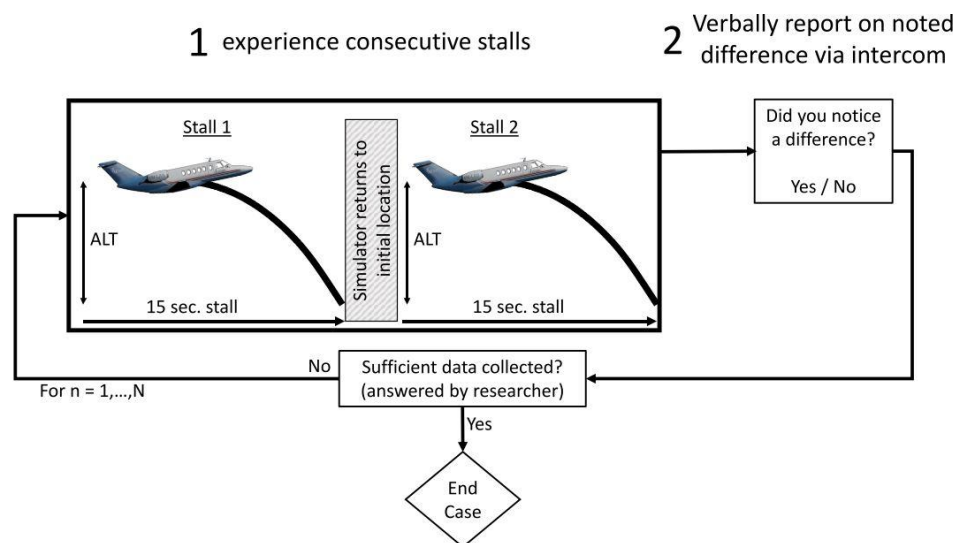


Figure 2: Experiment structure for one case

Experiment Consent Form

Just Noticeable Differences for Variations in Quasi-Steady Stall Buffet Model Parameters

I hereby confirm, by ticking the box, that:

1. I volunteer to participate in the experiment conducted by the researcher (**Arne Imbrechts**) under supervision of **dr.ir. Daan Pool** from the Faculty of Aerospace Engineering of TU Delft. I understand that my participation in this experiment is voluntary and that I may withdraw from the study at any time, for any reason. ☐
2. I have read the briefing document and I understand the experiment instructions and have had all remaining questions answered to my satisfaction. ☐
3. I understand that taking part in the experiment involves performing an observation task in the SIMONA Research Simulator, where I will inform the researcher whether I detect a difference between two consecutive simulation runs with physical motion. Only the simulation settings and the answers that I give regarding the noticeability of a certain difference between runs are saved. ☐
4. I confirm that the researcher has provided me with detailed safety and operational instructions for the SIMONA Research Simulator (simulator setup, flight instrumentation, fire escape ladder) used in the experiment. Furthermore, I confirm that I have understood the researcher's instructions for guaranteeing that the experiment will be performed in line with current RIVM COVID-19 guidelines and that this experiment shall at all times follow these RIVM guidelines. ☐
5. I confirm that (tick the appropriate box):
 - I am a student or staff member at TU Delft and am aware of the requirements for self-testing for COVID-19 for on-campus activities. ☐
 - I am not a student or employee at TU Delft and have presented the researcher with a valid 'CoronaCheck' QR code upon my arrival for the experiment. ☐
6. I understand that the researcher will not identify me by name in any reports or publications that will result from this experiment, and that my confidentiality as a participant in this study will remain secure. Specifically, I understand that any demographic information I provide (age, pilot license type, flight hours, etc.) will only be used for reference and always presented in aggregate form in scientific publications. ☐
7. I understand that this research study has been reviewed and approved by the TU Delft Human Research Ethics Committee (HREC). To report any problems regarding my participation in the experiment, I know I can contact the researchers using the contact information below. ☐

My Signature

Date

My Printed Name

Signature of researcher

Contact information researcher:

Arne Imbrechts

a.imbrechts@student.tudelft.nl

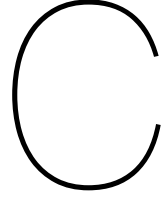
+32 473 28 60 54

Contact information research supervisor:

dr. ir. Daan Pool

d.m.pool@tudelft.nl

+31 15 2789611



Individual Experiment Results

This appendix shows the individual experiment results of each participant. Figures C.1 till C.15 show the results of the normal pilot group that includes a combination of glider, private and commercial pilots. The results of the Cessna Citation II pilots can be found in Figures C.16 till C.21.

Each figure contains nine subfigures (i.e., plots (a)-(i)). Each row presents the results of a different experiment condition, X_{thres}^- (plots (a)-(c)), ω_0^+ (plots (d)-(f)) and ω_0^- (plots (g)-(i)). The first column (plots (a), (d) and (g)) shows the staircase results with null measures for each experiment condition. In the second column (plots (b), (e) and (h)) the staircase results without null measures are shown. The last column (plots (c), (f) and (i)) presents the best cumulative density function fit through all the staircase data points, as well as through the staircase data points excluding null measures.

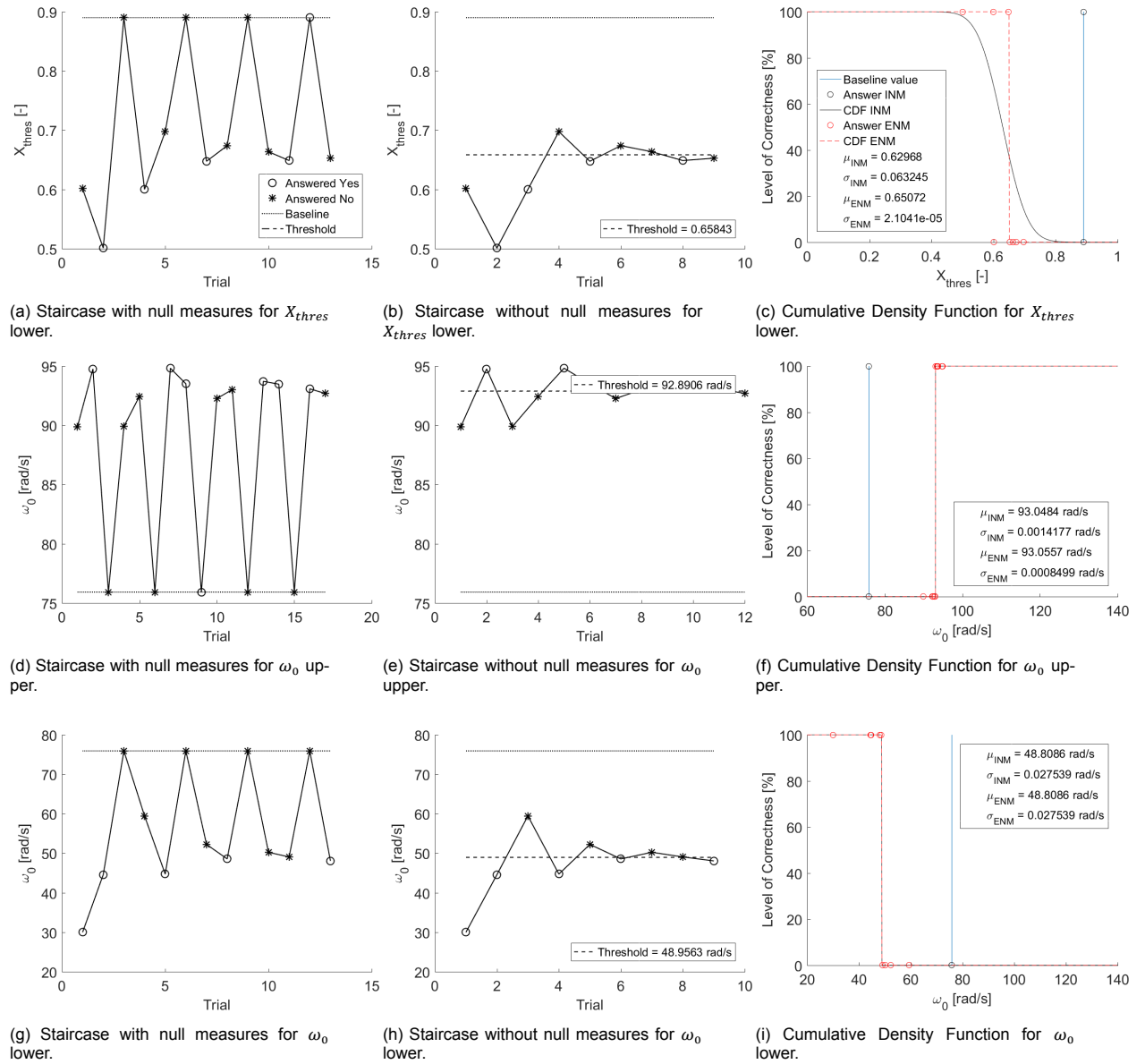


Figure C.1: Staircase- and Cumulative Density Function plots of participant 1.

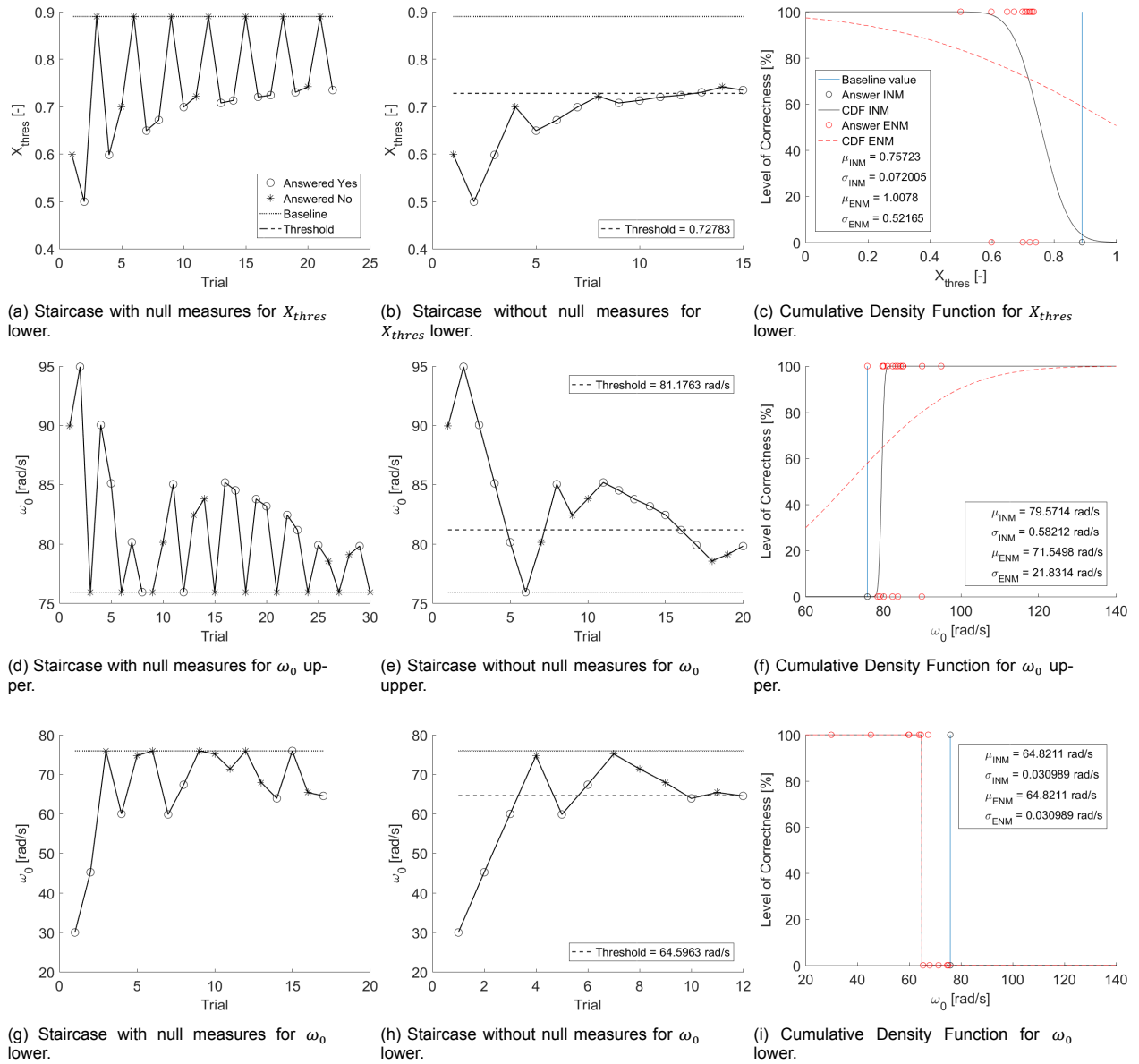


Figure C.2: Staircase- and Cumulative Density Function plots of participant 2.

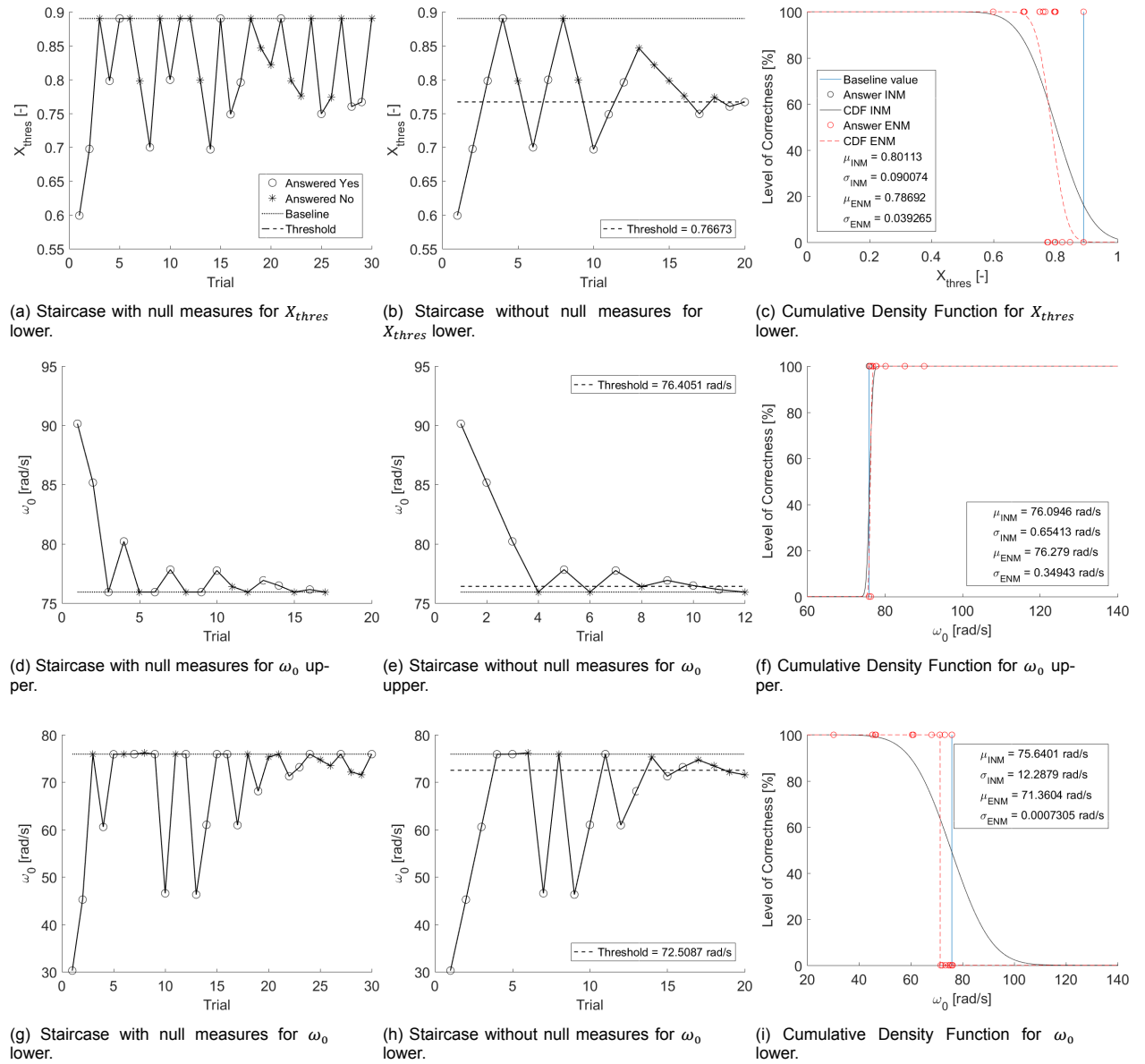


Figure C.3: Staircase- and Cumulative Density Function plots of participant 3.

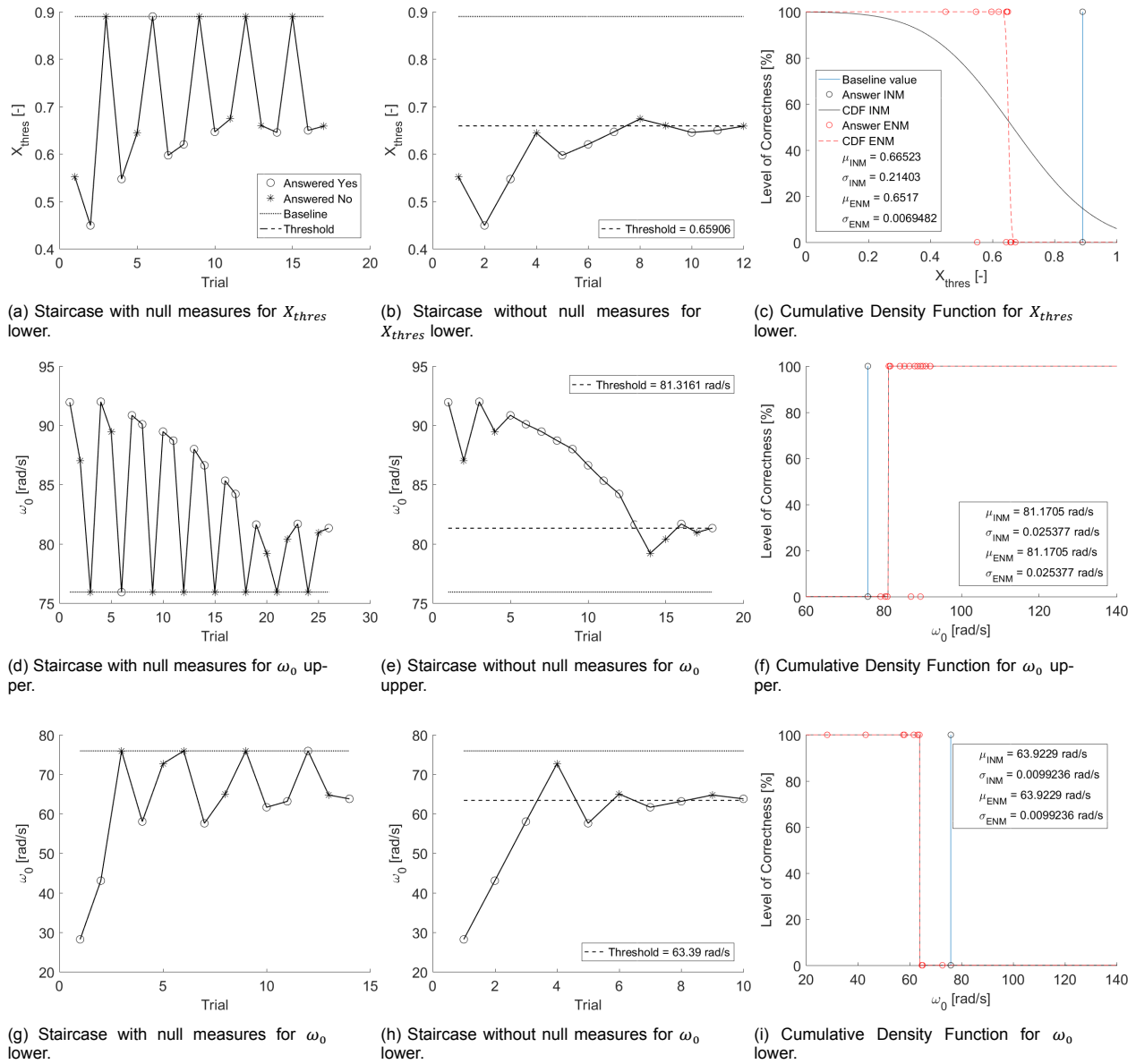


Figure C.4: Staircase- and Cumulative Density Function plots of participant 4.

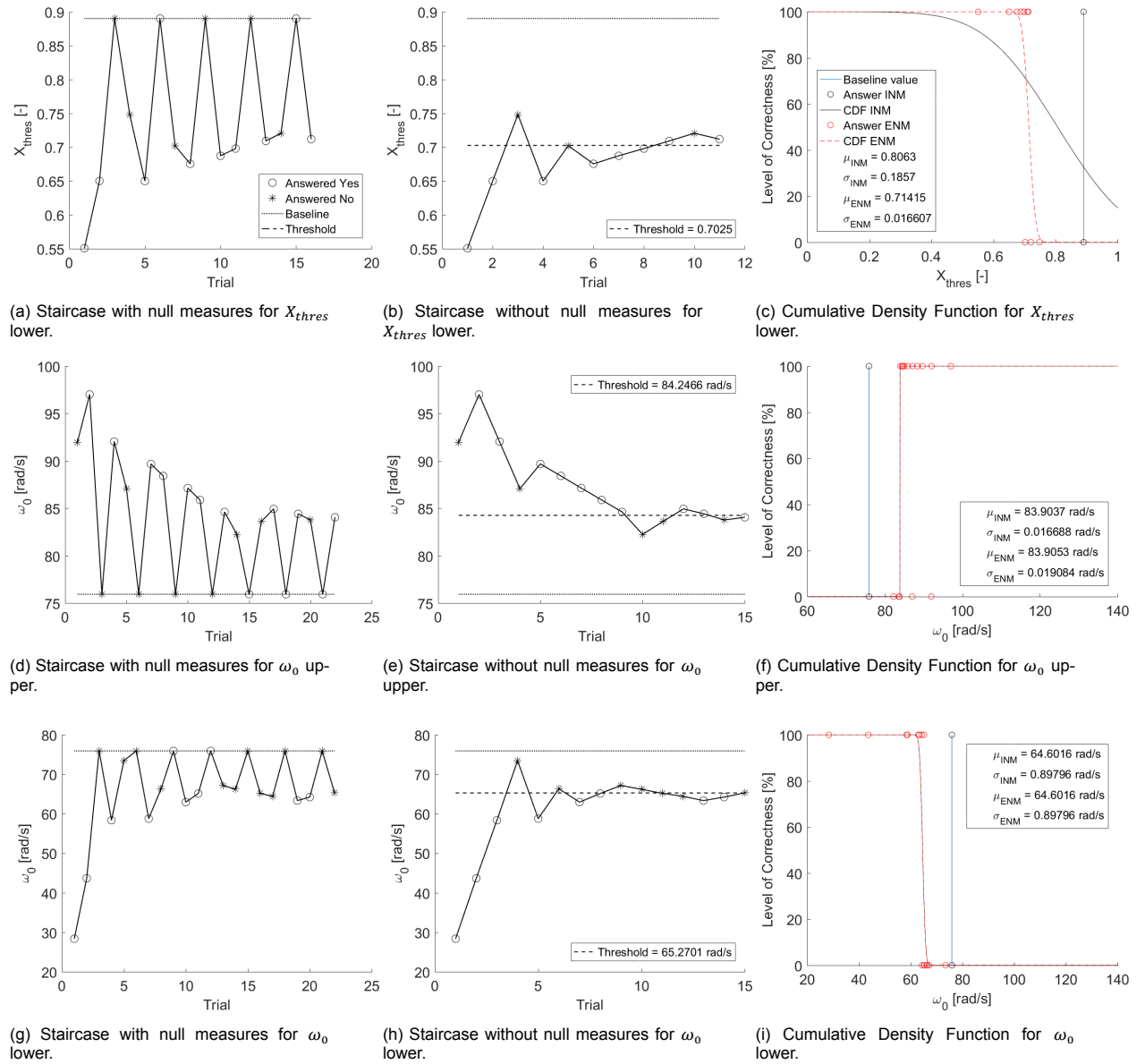


Figure C.5: Staircase- and Cumulative Density Function plots of participant 5.

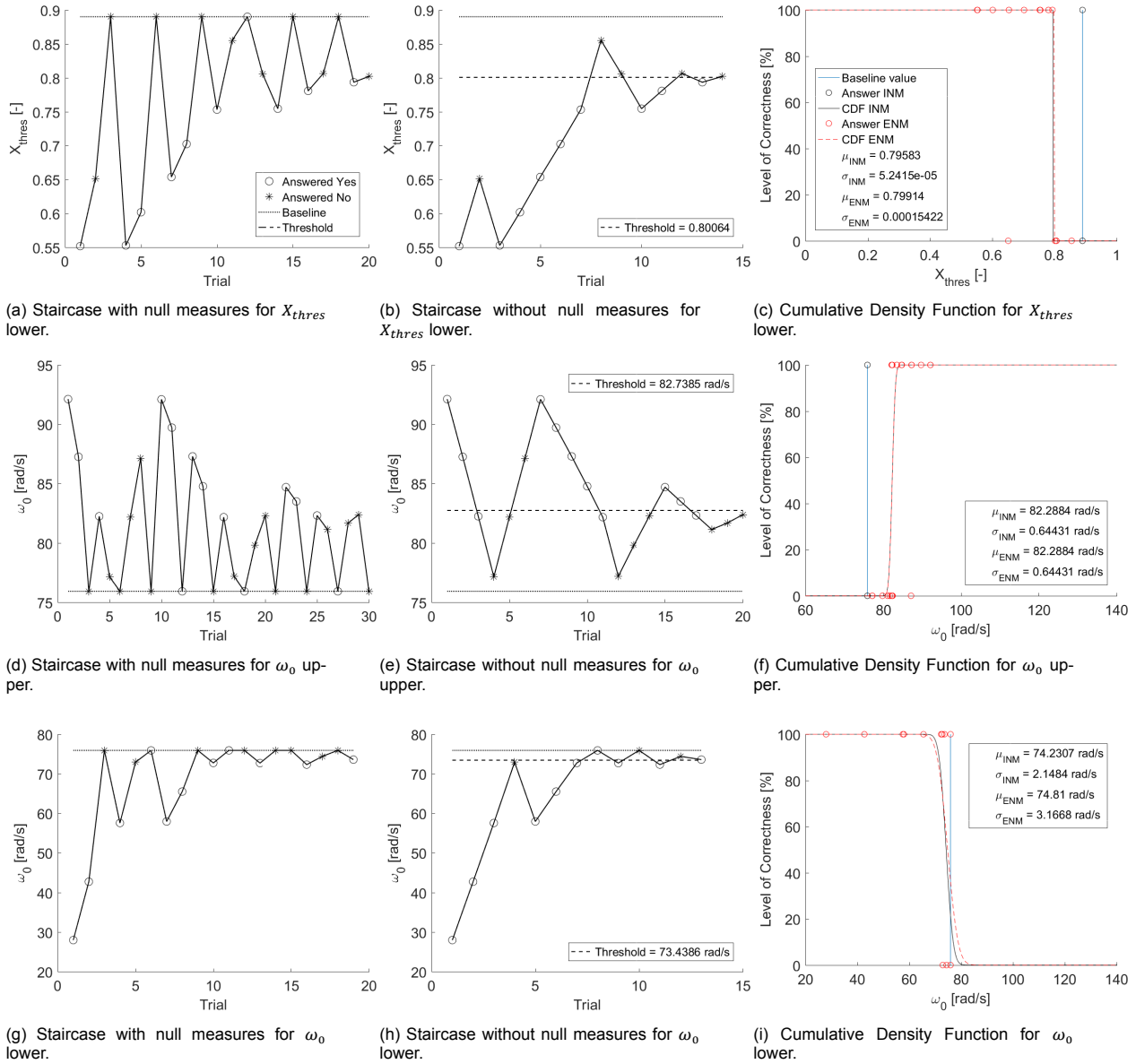


Figure C.6: Staircase- and Cumulative Density Function plots of participant 6.

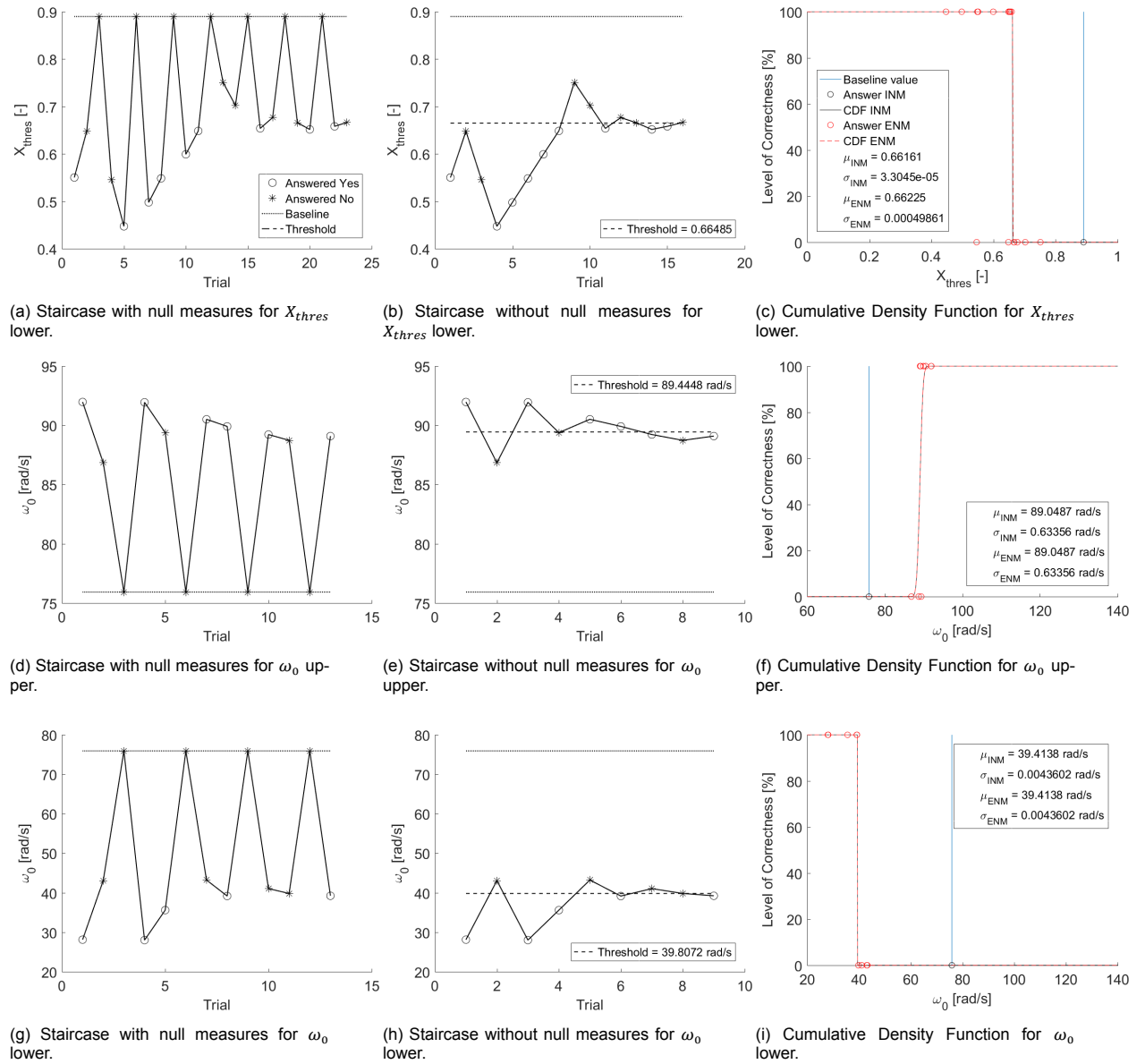


Figure C.7: Staircase- and Cumulative Density Function plots of participant 7.

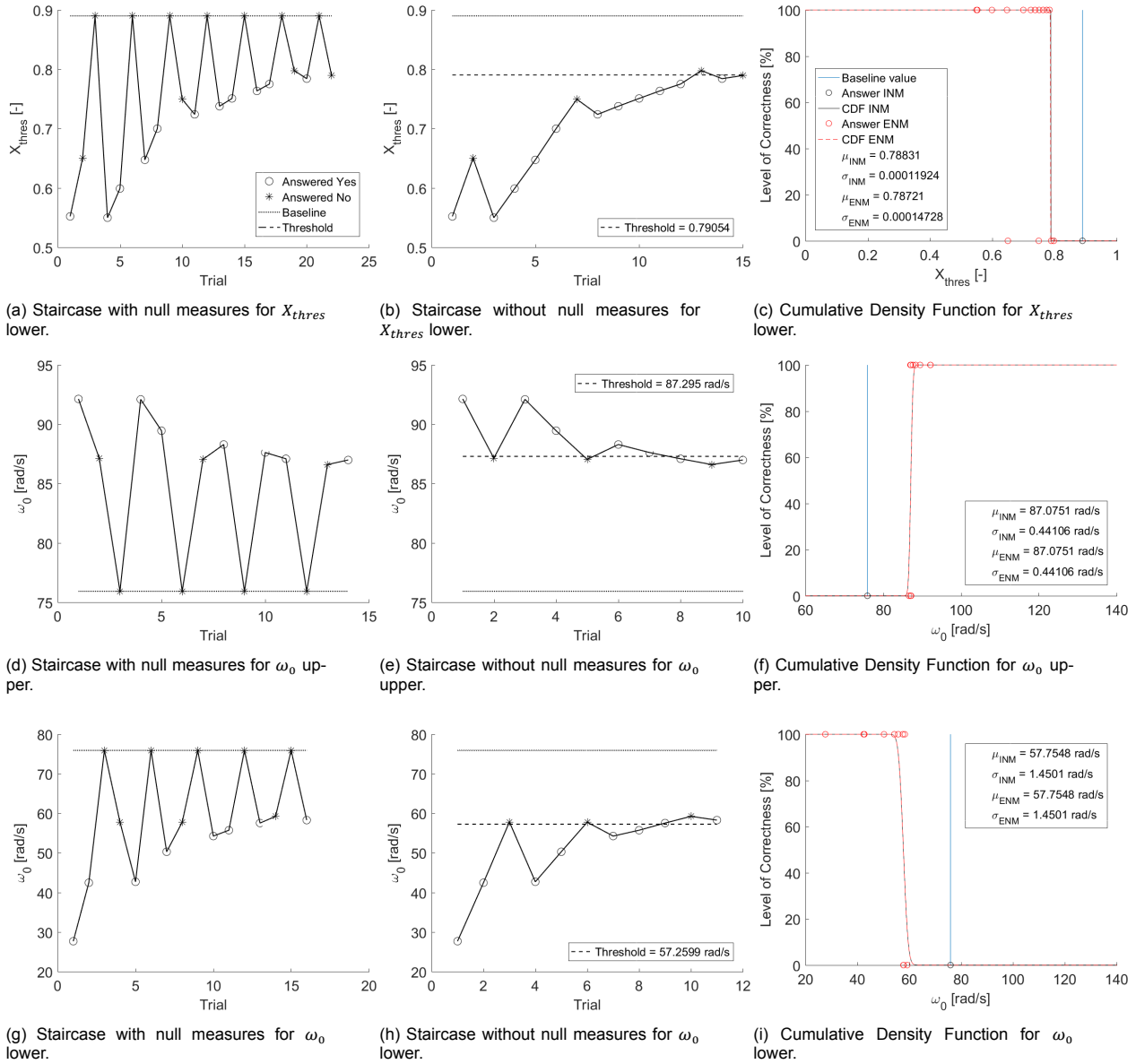


Figure C.8: Staircase- and Cumulative Density Function plots of participant 8.

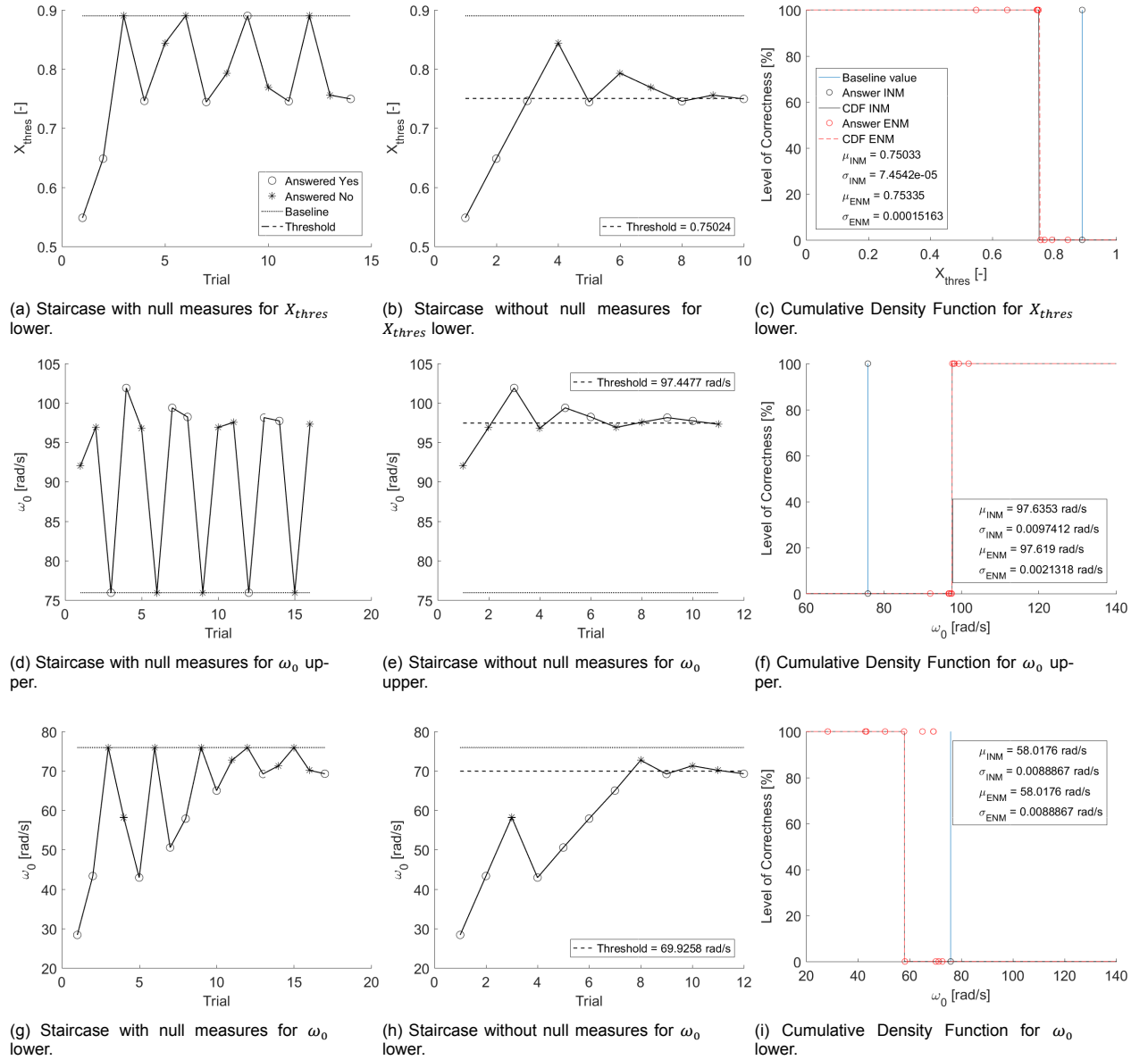


Figure C.9: Staircase- and Cumulative Density Function plots of participant 9.

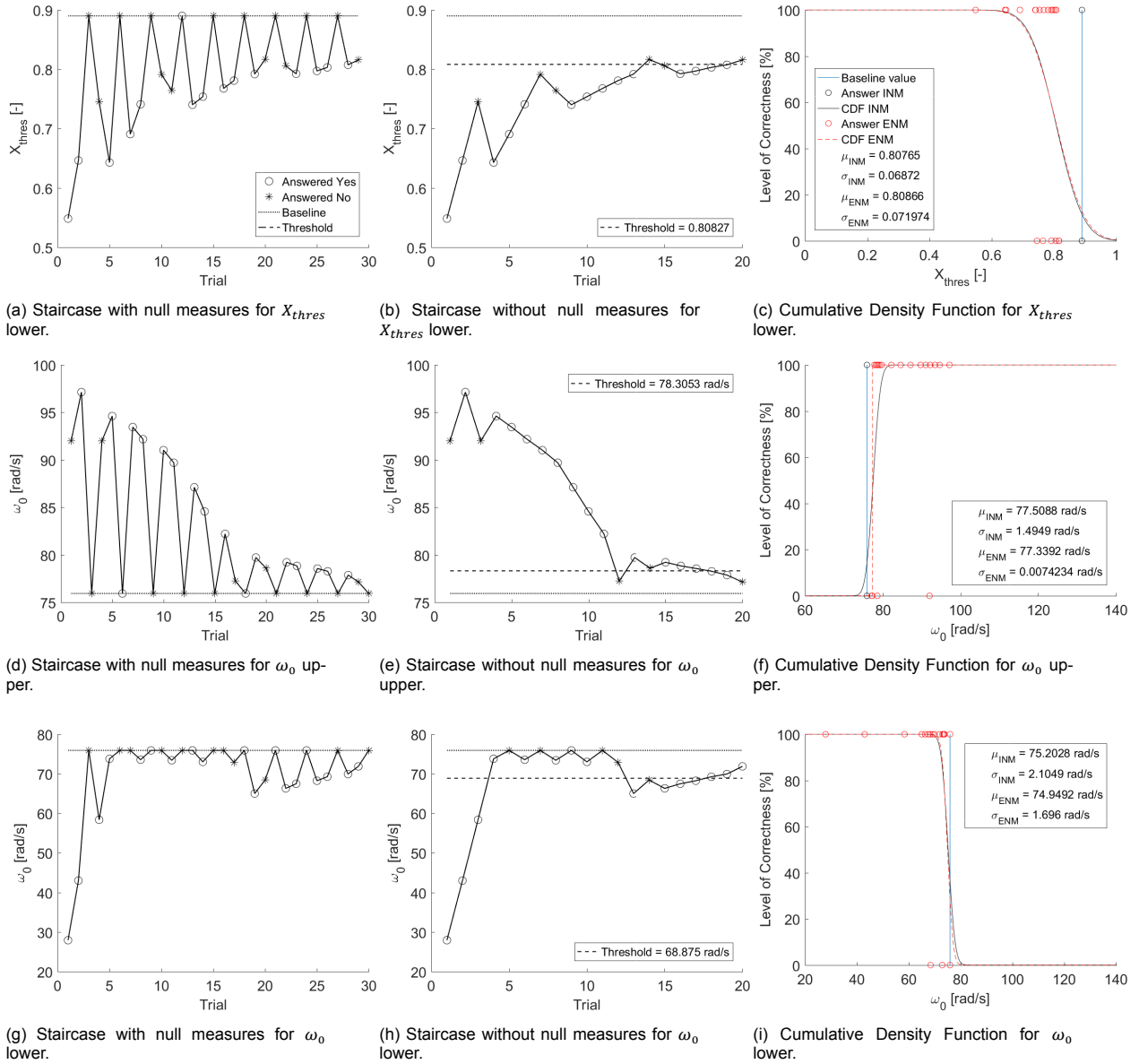


Figure C.10: Staircase- and Cumulative Density Function plots of participant 10.

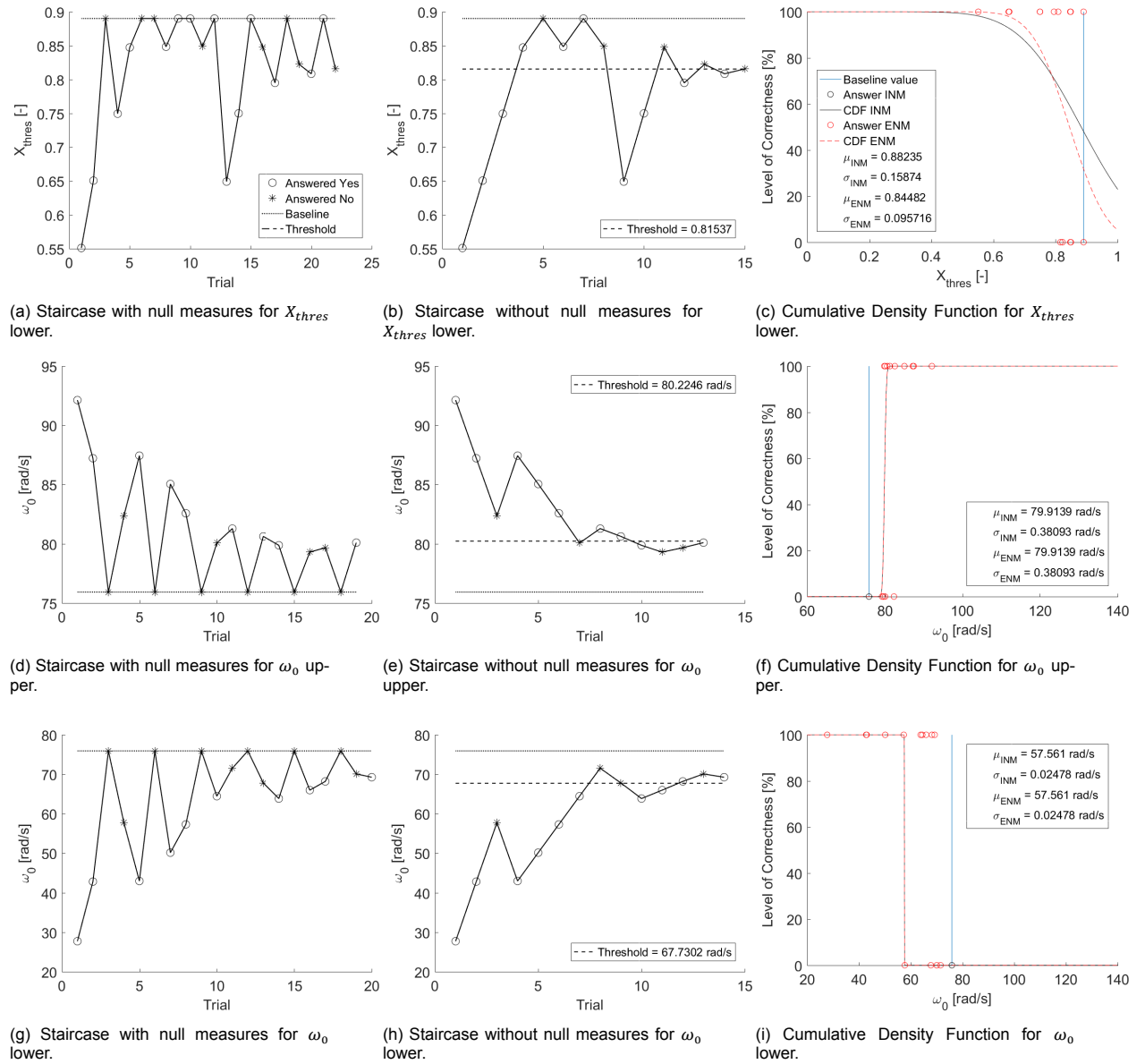


Figure C.11: Staircase- and Cumulative Density Function plots of participant 11.

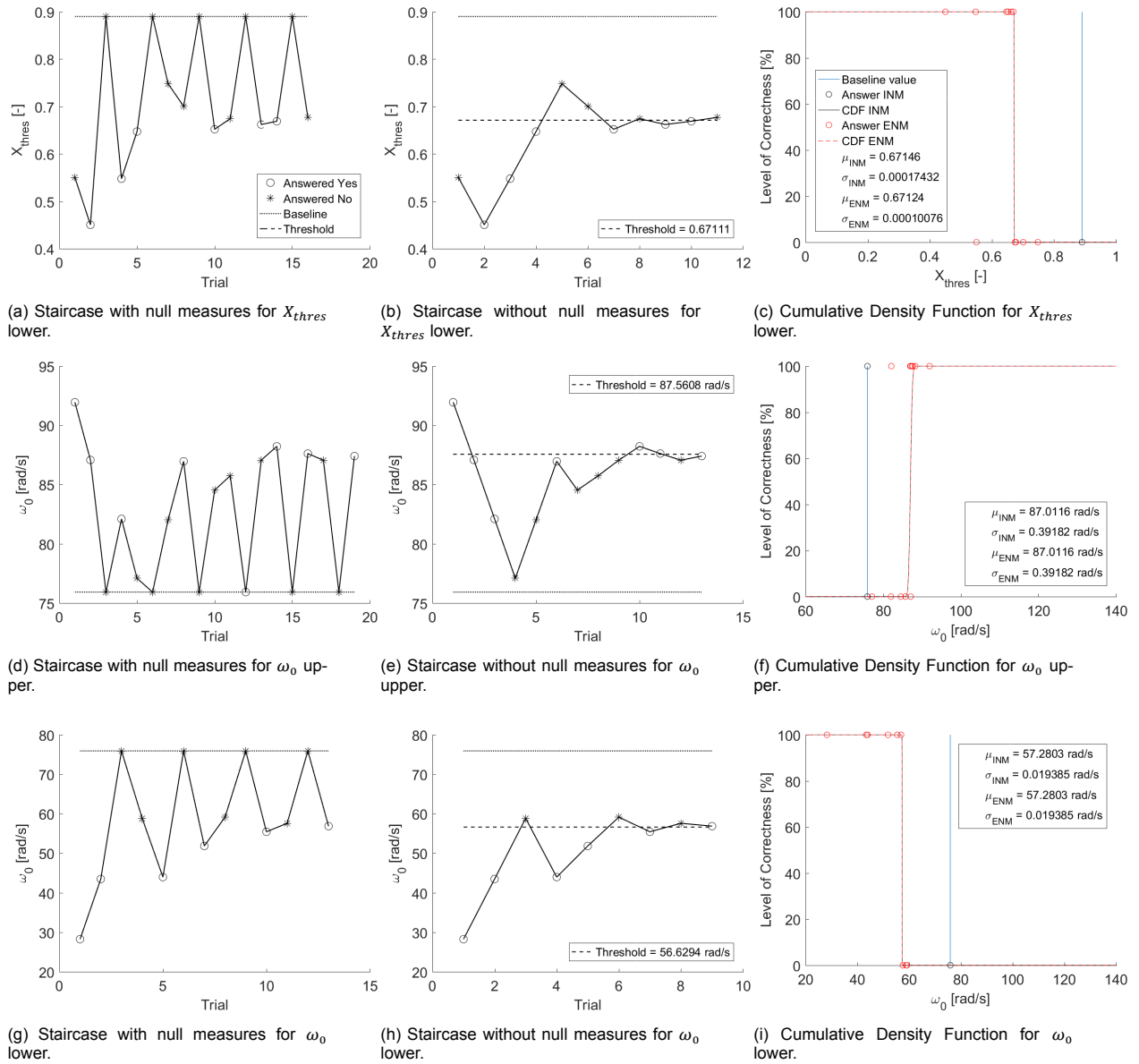


Figure C.12: Staircase- and Cumulative Density Function plots of participant 12.

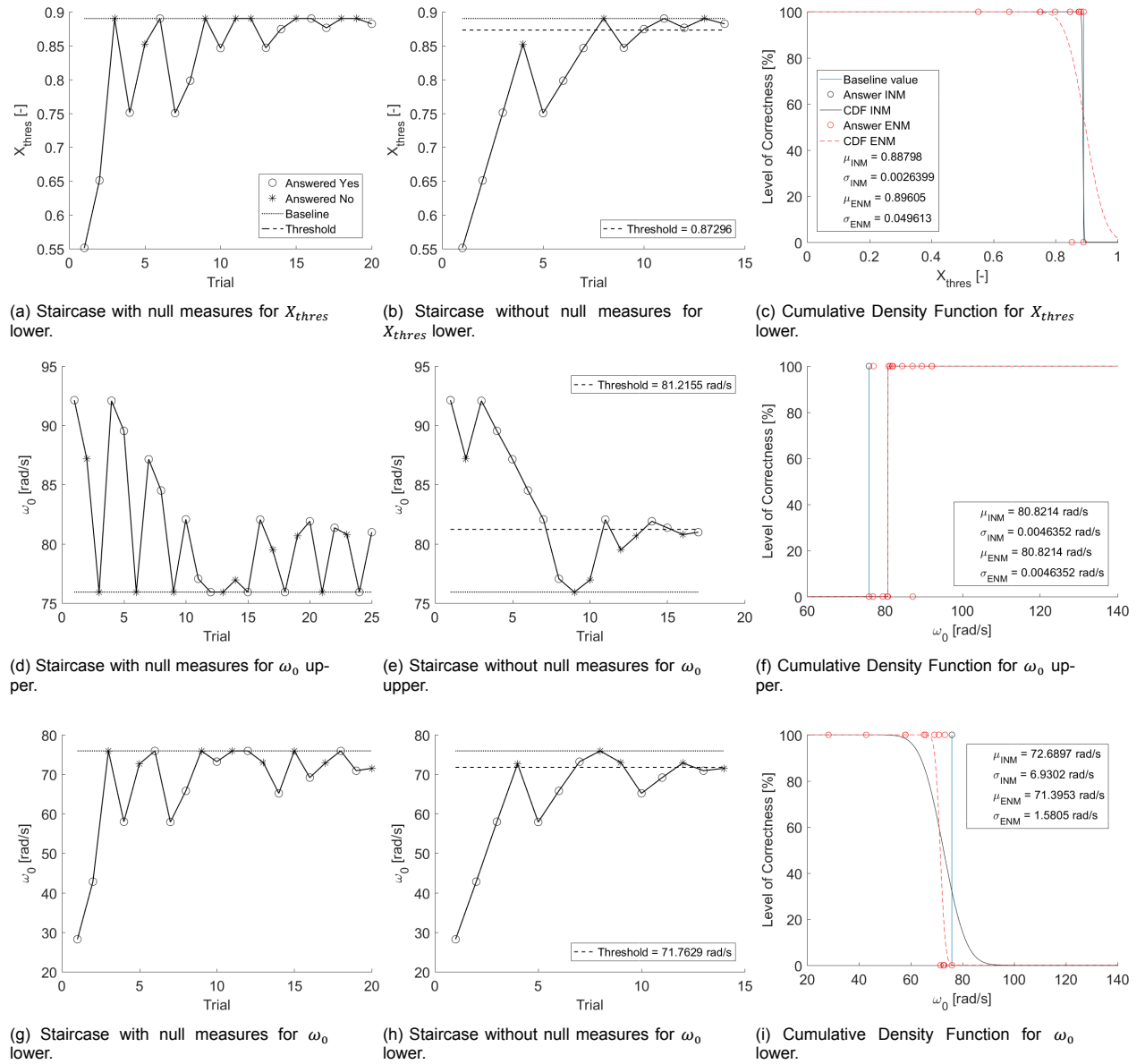


Figure C.13: Staircase- and Cumulative Density Function plots of participant 13.

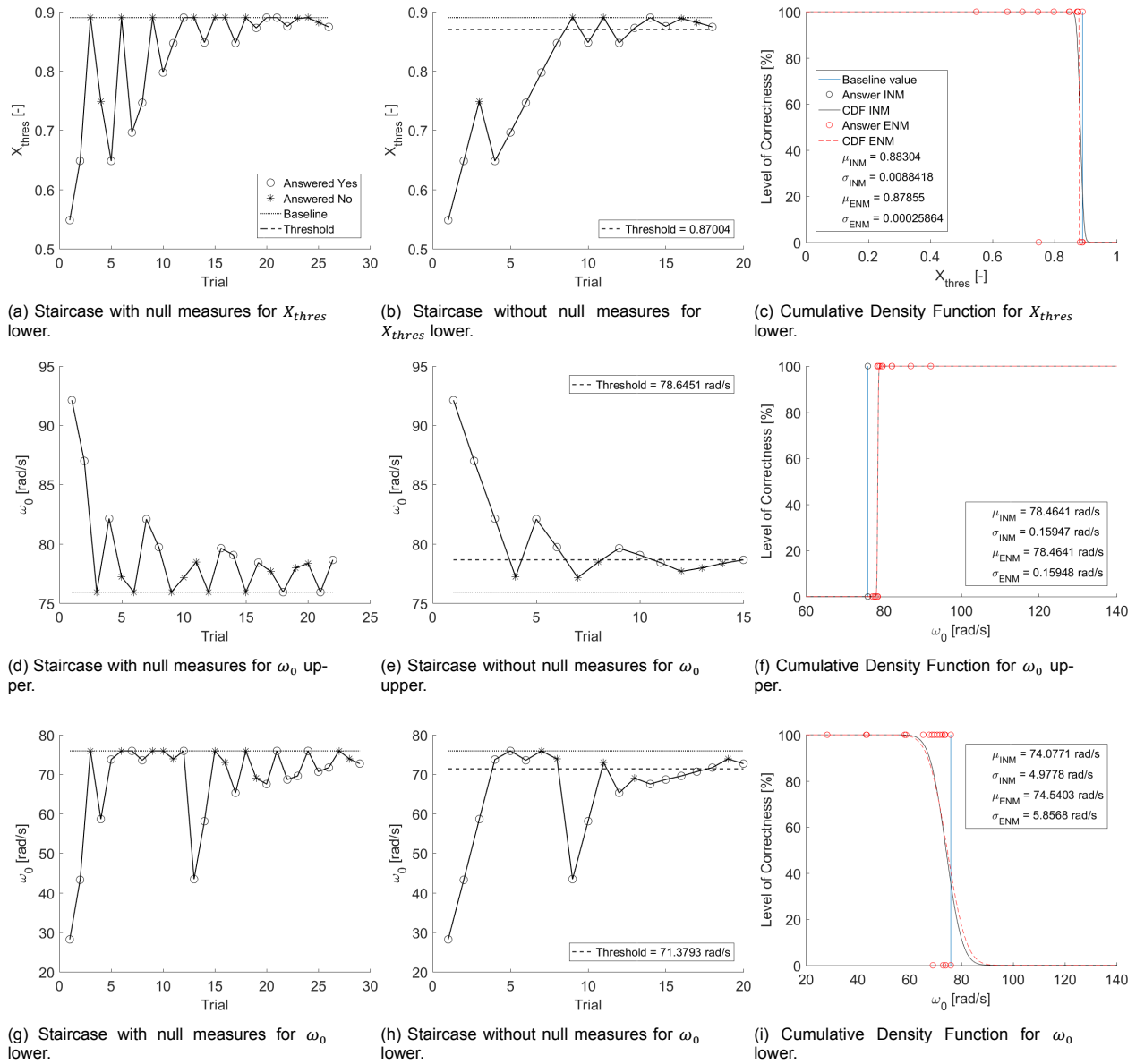


Figure C.14: Staircase- and Cumulative Density Function plots of participant 14.

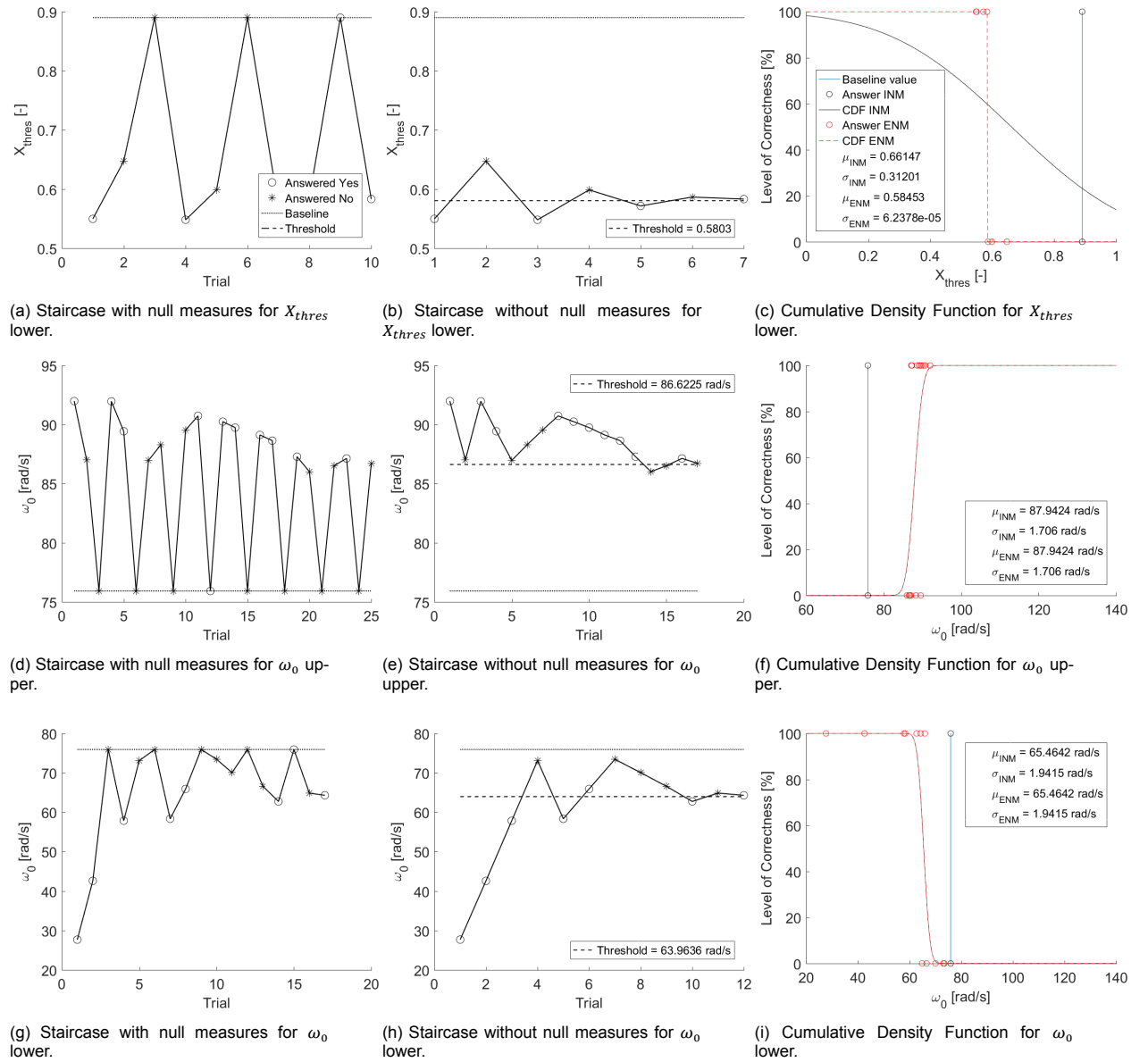


Figure C.15: Staircase- and Cumulative Density Function plots of participant 15.

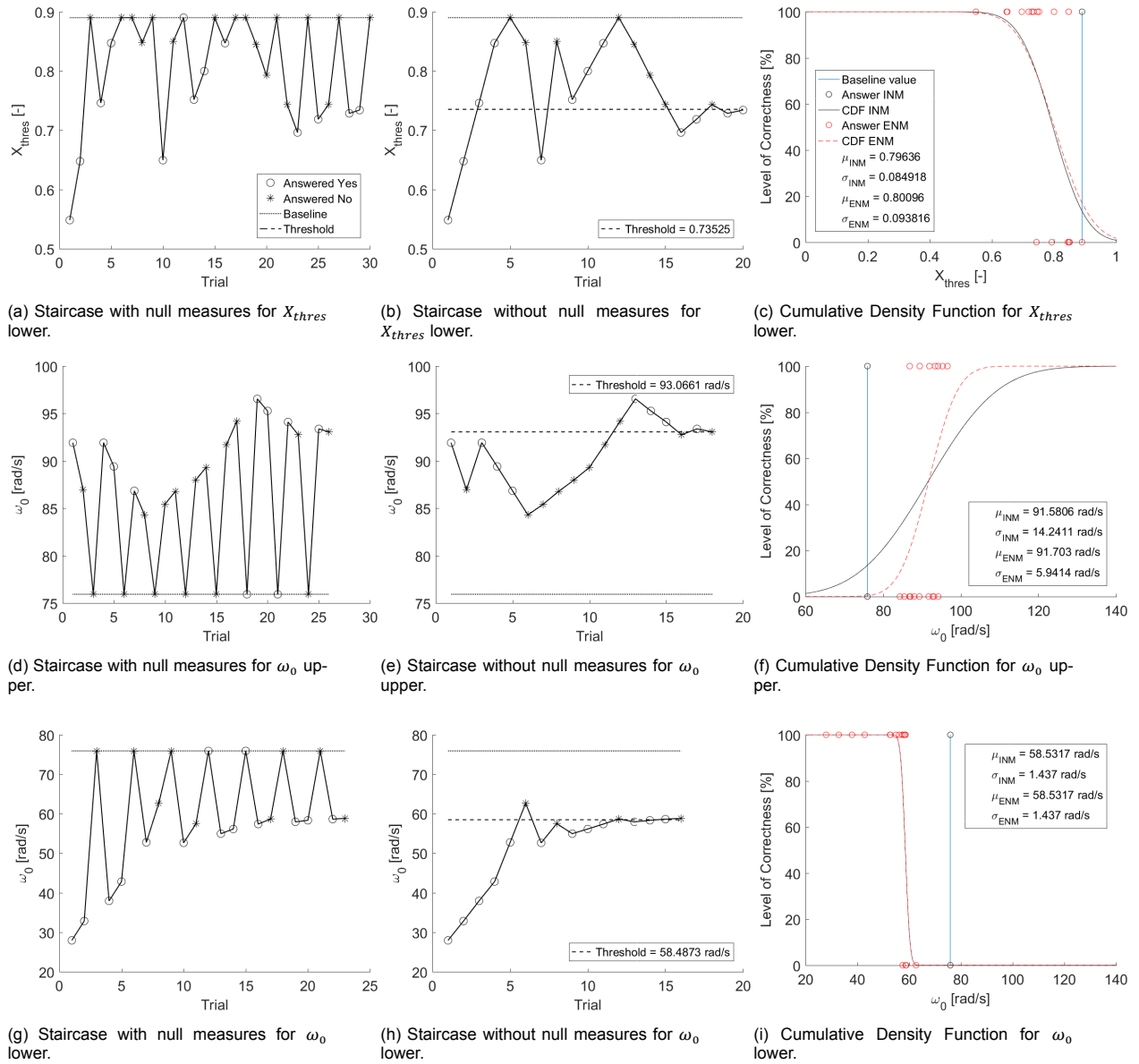


Figure C.16: Staircase- and Cumulative Density Function plots of participant C1.

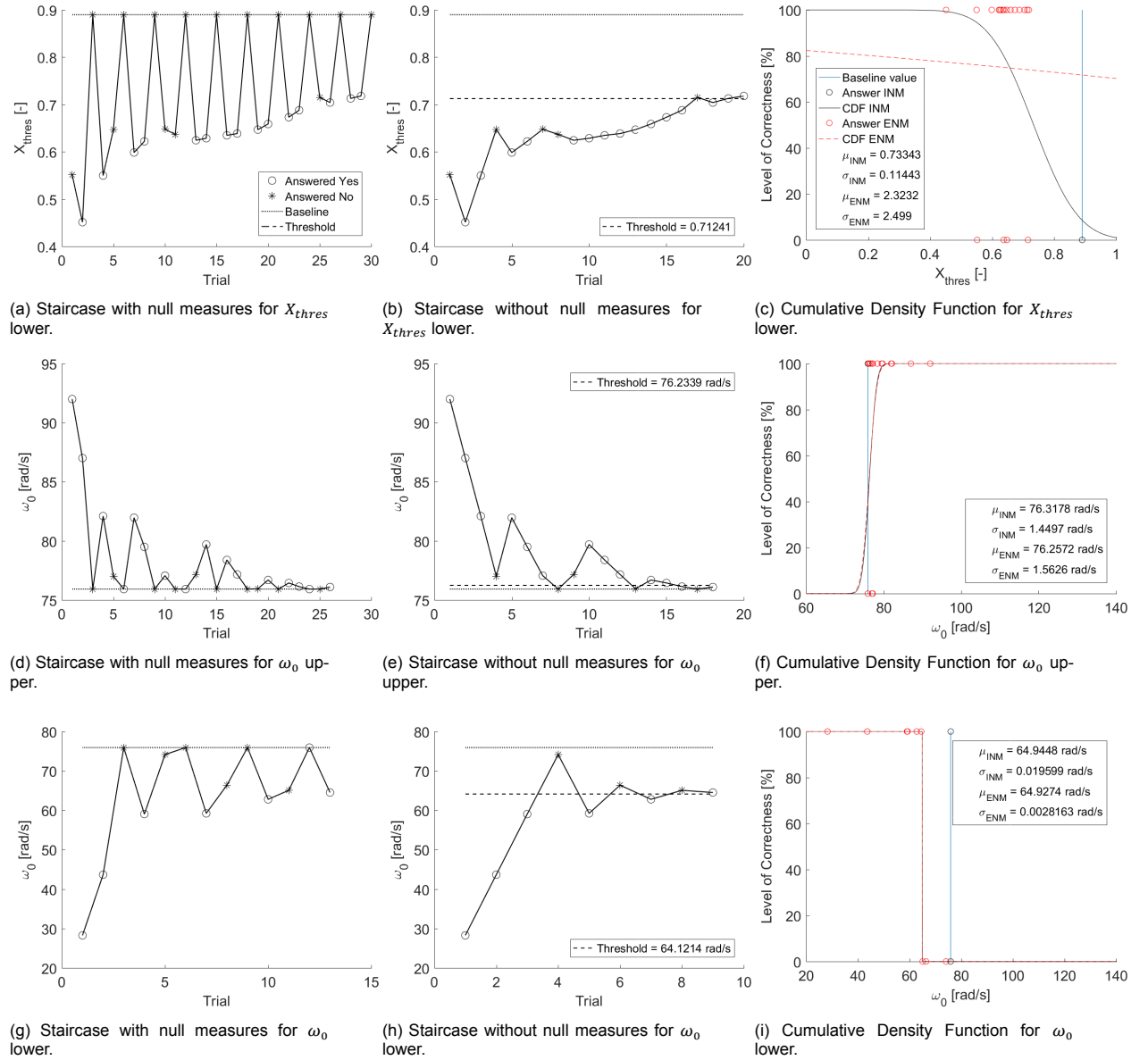


Figure C.17: Staircase- and Cumulative Density Function plots of participant C2.

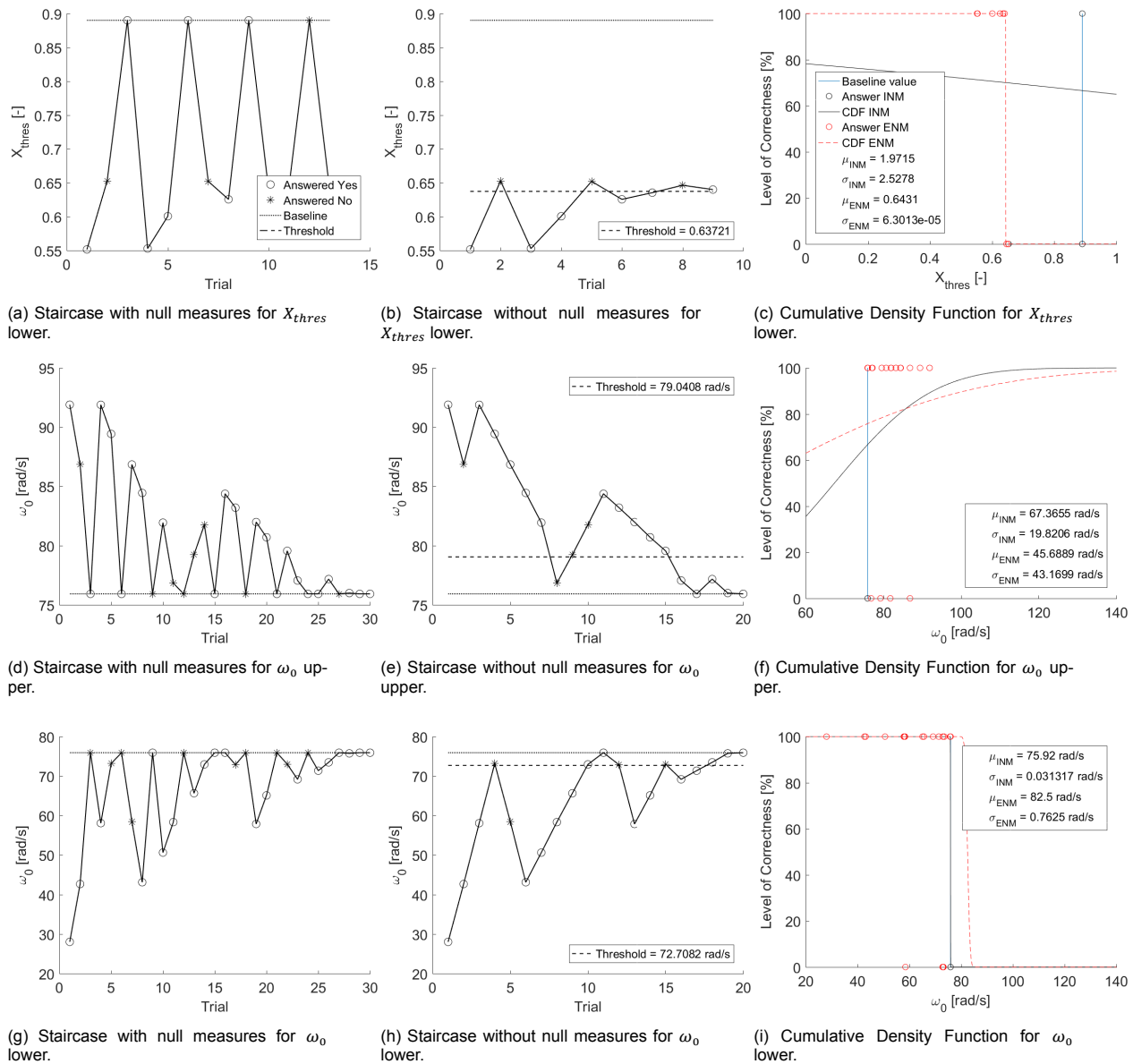


Figure C.18: Staircase- and Cumulative Density Function plots of participant C3.

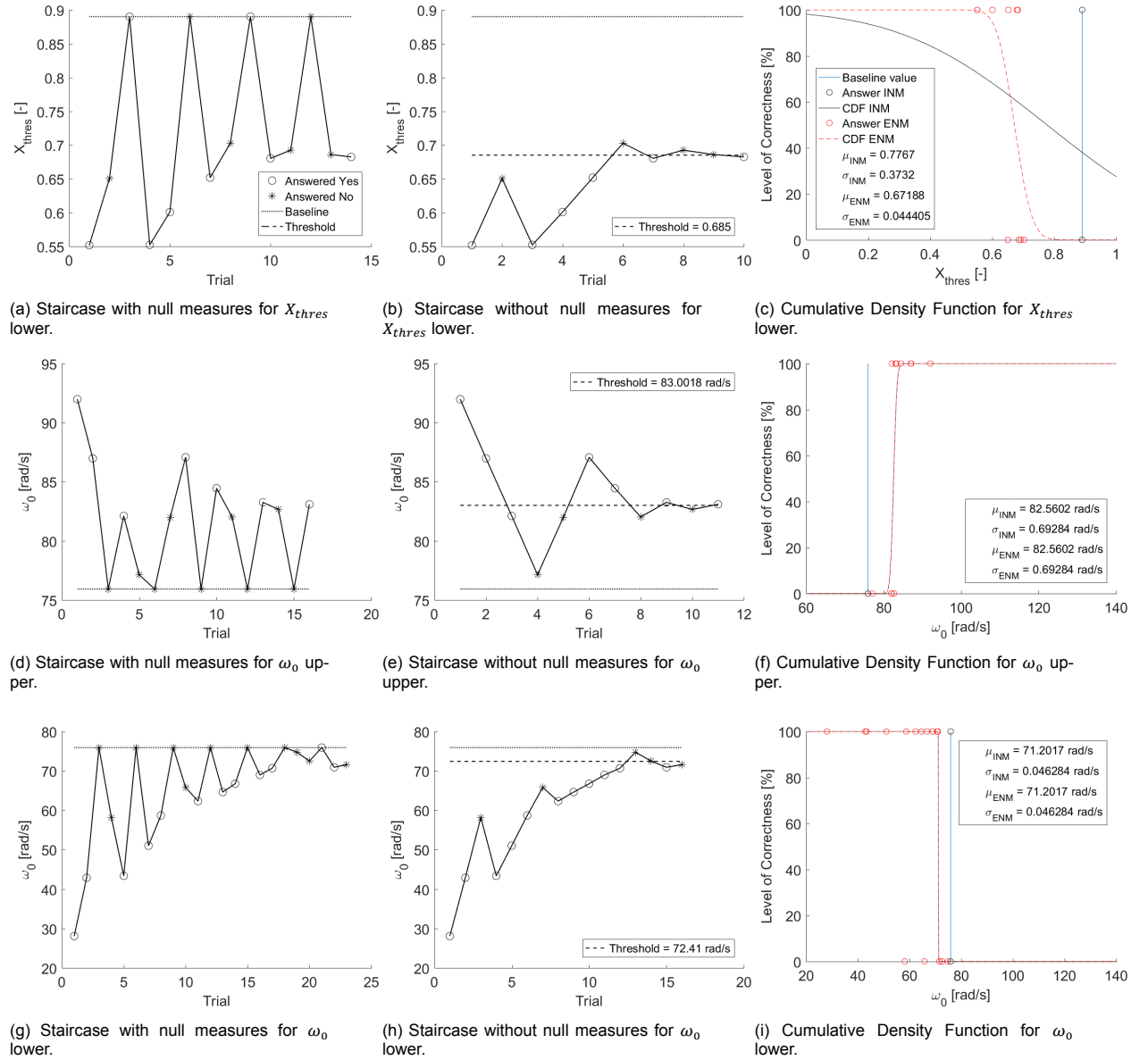


Figure C.19: Staircase- and Cumulative Density Function plots of participant C4.

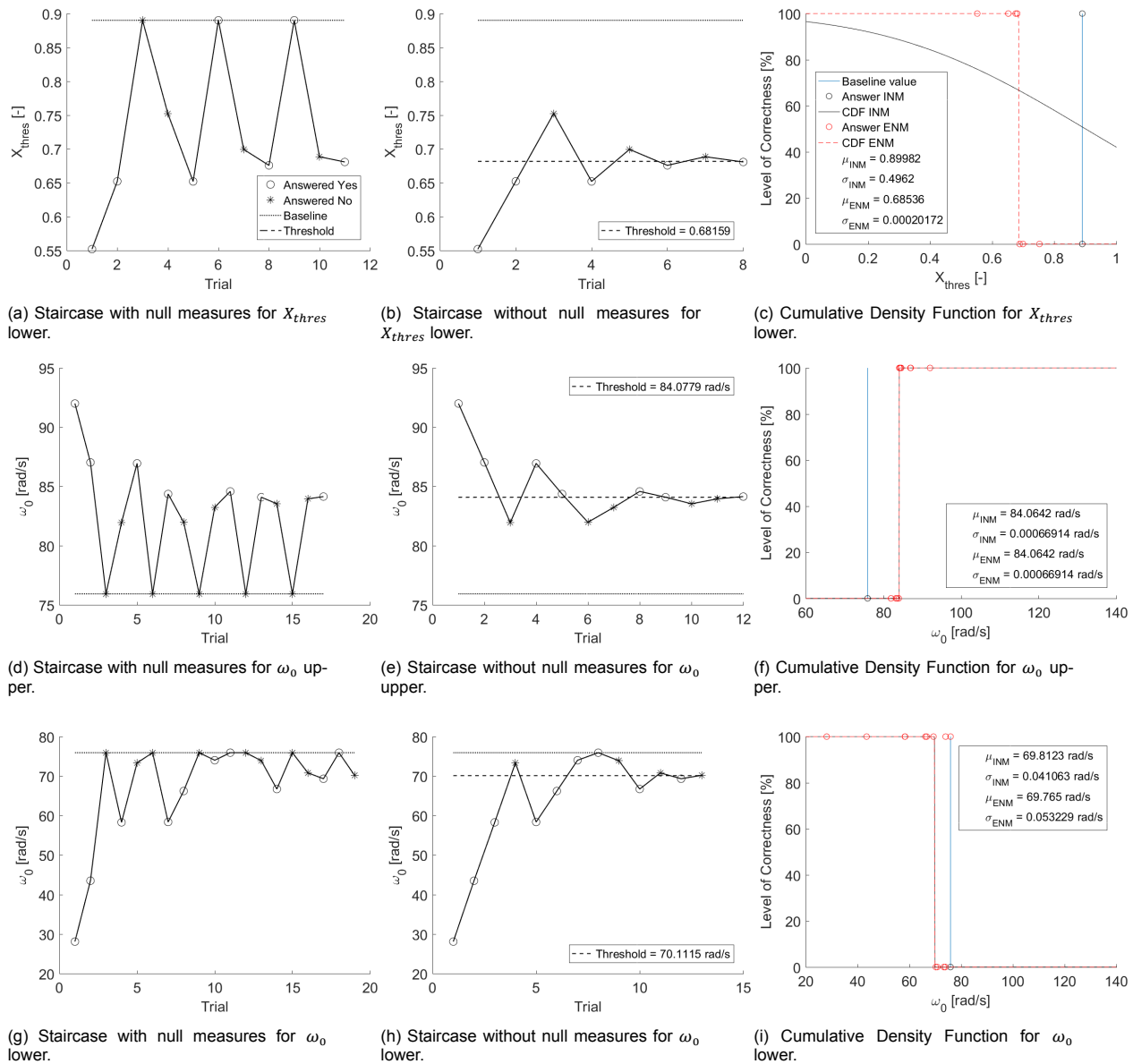


Figure C.20: Staircase- and Cumulative Density Function plots of participant C5.

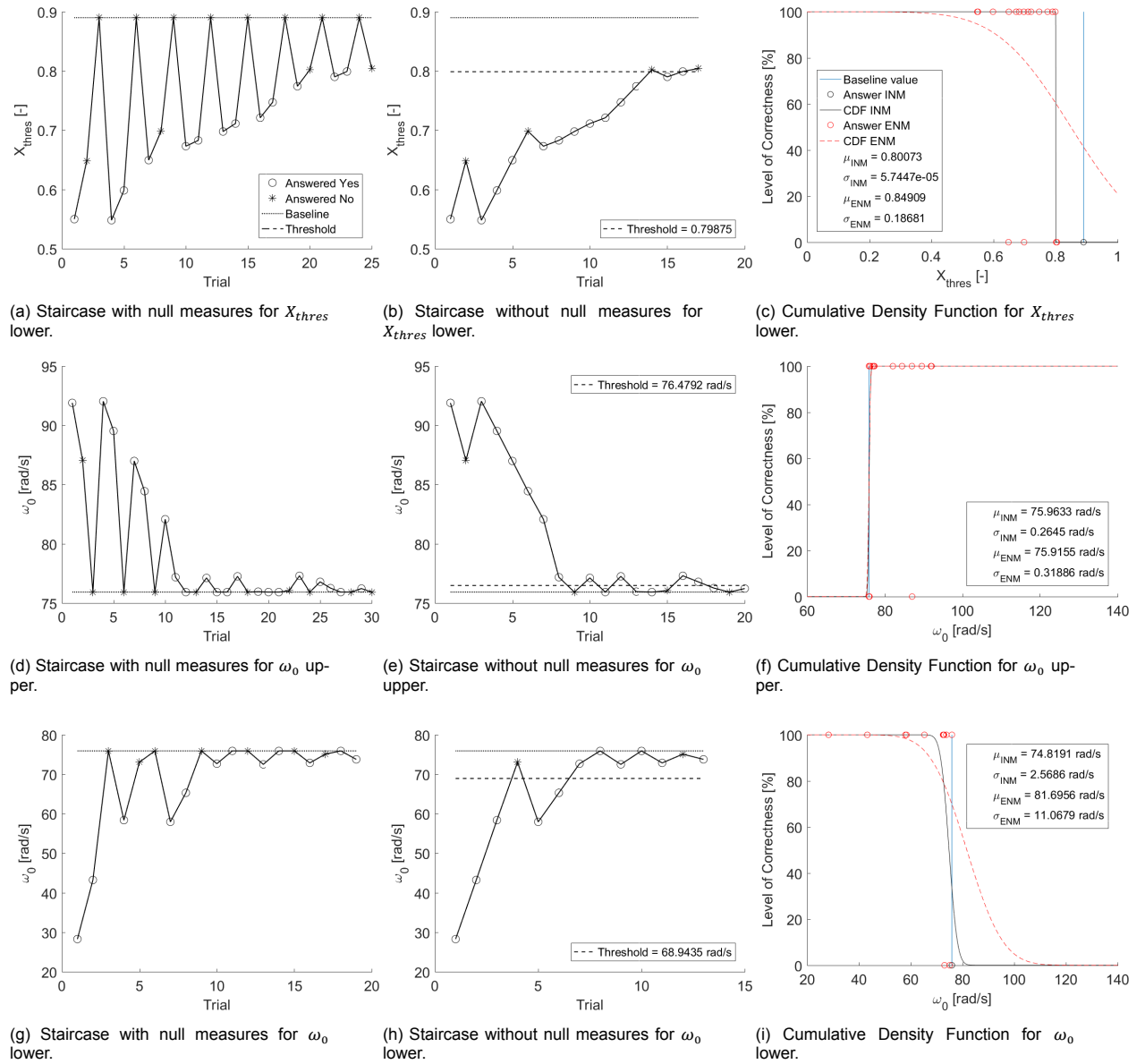


Figure C.21: Staircase- and Cumulative Density Function plots of participant C6.